NITRATE TRANSPORT TO COASTAL MONTEREY BAY: INVESTIGATING SOURCE INPUTS FROM ELKHORN SLOUGH

A Thesis

Presented to the

Faculty of the

Moss Landing Marine Laboratories

California State University Monterey Bay

In Partial Fulfillment

of the Requirements for the Degree

Master of Science

in

Marine Science

---

by

Tanya Novak

Fall, 2011

CALIFORNIA STATE UNIVERSITY MONTEREY BAY

The Undersigned Faculty Committee Approves the

Thesis of Tanya Novak:

NITRATE TRANSPORT TO COASTAL MONTEREY BAY:

INVESTIGATING SOURCE INPUTS FROM ELKHORN SLOUGH

_____

Erika McPhee-Shaw, Chair
Moss Landing Marine Laboratories

_____

Nick Welschmeyer
Moss Landing Marine Laboratories

_____

Ken Johnson
Monterey Bay Aquarium Research Institute, Moss Landing

_____

Marsha Moroh, Dean
College of Science, Media Arts, and Technology

_____

Approval Date

ABSTRACT

Nitrate Transport to Coastal Monterey Bay: Investigating
Source Inputs from Elkhorn Slough
by
Tanya Novak
Master of Science, Marine Science
California State University Monterey Bay, 2011

Nitrate transport from Elkhorn Slough (ES) to the nearshore surface waters of Monterey Bay is examined using two years of time-series data from the Land-Ocean Biogeochemical Observatory (LOBO). Hourly nitrate, temperature and salinity measurements from nearshore moorings 2.5 km north (summer, 2008) and 2.5 km south (summer– fall, 2009, winter 2010) of the Moss Landing Harbor entrance at 20-m depth were monitored with the objective of observing high nitrate events associated with terrestrial-sourced waters. Nearshore nitrate supply from ES was quantified in comparison to upwelling and internal waves based on estimates of volume transport and average nitrate concentrations observed at LOBO moorings. One distinct runoff event, October 13-14, 2009, was observed during the two-year study period. Data from the LOBO mooring array was used to assess the impact of this winter-type event in comparison to the longer time-series of summer conditions. Despite intensive agricultural-based nitrate loading within Old Salinas River, the summer contribution to the nearshore nitrate budget from the Elkhorn Slough system was over an order of magnitude less than upwelling and 4 to 13-fold less than internal waves. While rates of nitrate transport vary seasonally, assessment of nitrate transport mechanisms to coastal Monterey Bay in the summer to early fall is essential to understanding the dynamics of extreme algal blooms that typically occur during these months.

TABLE OF CONTENTS

PAGE

ABSTRACT ii
LIST OF TABLES v
LIST OF FIGURES vi
ACKNOWLEDGEMENTS x
CHAPTER
1. INTRODUCTION AND BACKGROUND 1
1.1 Overview 1
1.2 Monterey Bay 2
1.2.1 Physical Oceanography 2
1.2.2 Monterey Submarine Canyon 5
1.2.3 Freshwater Sources to Monterey Bay 5
1.3 Elkhorn Slough 7
1.4 Bloom Dynamics in Monterey Bay and the Land-Sea Link 13
1.5 Scope of Project 16
2. METHODS 17
2.1 Datasets 17
2.1.1 Land-Ocean Biogeochemical Observatory 17
2.1.2 Hydrologic Data 22
2.1.3 Meteorological Data 25
2.1.4 Portable Underway Data Acquisition System (UDAS) 26
2.2 Data Summary 26
2.3 Nitrate Transport Calculations 27
2.4 Time Series Analysis 30
3. RESULTS 31
3.1 Terrestrial Nitrate Transport out of Elkhorn Slough 31
3.1.1 Seasonal Hydrology in Elkhorn Slough 31
3.1.2 Summer Nitrate Loads from Elkhorn Slough 34
3.1.3 Winter Nitrate Loads from Elkhorn Slough 37
3.2 Coastal Nitrate Transport from Oceanographic Sources 40
3.2.1 Spectral Analysis 40

3.2.2 Seasonal Upwelling Dynamics in Monterey Bay 42
3.3.2 Coastal Upwelling Conditions during the Summer Study Period 46
3.2.3 Nitrate Loads from Coastal Upwelling 47
3.2.4 Nitrate Transport from Internal Waves 53
3.3 Nearshore Monterey Bay Surface Nitrate Variability 58
3.3.1 Nearshore Mixing Model 58
3.3.2 Nearshore Mooring Observations 62
3.3.3 Identification of Terrestrial Signals 67
3.3.4 Surface Mapping of the Elkhorn Slough Summer Discharge Plume 70
3.3.5 Terrestrial Runoff Event – "First flush, 2009" 76
4. DISCUSSION & CONCLUSION 87
4.1 Characterization of Coastal Ocean Surface Nitrate Variability 87
4.2 The Significance of Nitrate Loads in Elkhorn Slough 88
4.2.1 Biological Uptake in Elkhorn Slough 88
4.2.2 Seasonal Context 90
4.3 Comparing Terrestrial (ES) and Oceanographic Source Inputs 91
4.5 Detection of Terrestrial (ES) Nitrate Signals in Nearshore Monterey Bay 98
4.6 Harmful Algal Blooms in Monterey Bay and the Land-Sea Link 99
REFERENCES 101

LIST OF TABLES

Table 1 : Average annual discharge from major freshwater sources to Monterey Bay (USGS, PVWMA) 7

Table 2: LOBO mooring specifications 1

Table 3: LOBO nitrate data offsets 20

Table 4: Matrix of possible mixing volumes (in m3) 61

Table 5: Matrix of minimum daily transport required for detection at LOBO nearshore moorings, assuming 2μM/hr detection limit and possible mixing dimensions outlined above in Table 4. Units are in kmol/d. 62

Table 6: Parameter statistics for nearshore mooring L20 (June – November, 2008), surface array. 65

Table 7: Parameter statistics for nearshore mooring L20-2 (June – November, 2009), surface array. 66

Table 8: Parameter statistics for nearshore mooring L20 (June – November, 2008), deep array. 66

Table 9: Parameter statistics for nearshore mooring L20-2 (June – November, 2009), deep array. 66

Table 10: Comparison of summer (left column) and winter (right column) Nitrate Loads out of Elkhorn Slough. 91

Table 11: Comparative summary of nitrate transport results for terrestrial, upwelling and internal wave supply mechanisms. Units of average daily flux and integrated flux are kmol/d and kmol, respectively, unless otherwise indicated. 92

Table 12: Comparative summary of nitrate transport results for terrestrial, upwelling and internal wave supply mechanisms. Units of average daily flux and integrated flux are kmol $d^{-1}km^{-1}$ and kmol/km, respectively. 94

LIST OF FIGURES

Figure 1: Geographic location of Monterey Bay depicting major bathymetric features of the Monterey Bay Submarine Canyon (Google Earth)..... 4

Figure 2: Central California sea surface temperature during upwelling (NASA) 4

Figure 3: Location of major freshwater sources to Monterey Bay (See Table 1 for number references; USGS, PVWMA) 6

Figure 4: Map of Elkhorn Slough (ESTWPT, 2007)..... 8

Figure 5: Map of major watersheds surrounding Monterey Bay. The three watersheds that drain into the Elkhorn Slough system are outlined in yellow. The white dot represents the location of drainage into Old Salinas River (ESTWPT, 2007)..... 10

Figure 6: Nitrate concentrations in Old Salinas River Channel (OSR) (top) and coastal Monterey Bay, 3km north (bottom left) and 3km south (bottom right) of the harbor. Horizontal line depicts 25 μM for reference between plots. 11

Figure 7: Ariel "KiteCam" photo depicting the pulse of high-nitrate OSR water entering Elkhorn Slough on a rising tide (courtesy of Gary Thurmond, MBARI). 12

Figure 8: Chlorophyll (a), colored dissolved organic matter (CDOM) (b), turbidity (c) and phycocyanin (d) fluorescence gradients within the main channel of Elkhorn Slough. Phycocyanin is an accessory pigment found in cyanobacteria. Data collected September, 20 using a Turner CFINS fluorometry package. 13

Figure 9: Satellite image of November, 2007 harmful algal bloom in Monterey Bay (NOAA) 15

Figure 10: LOBO mooring locations. 21

Figure 11: Typical LOBO mooring instrument configuration. 21

Figure 12: Location of Old Salinas River tide gates and Sontek Argonaut current meter. (images: google maps, http://www.sontek.com/argonautsw.php) 23

Figure 13: Regression relationship between flow data from USGS station 11152650 and flow data derived from the Argonaut current meter. 23

Figure 14: Map depicting channel classification in the Tembladero watershed and location of pertinent discharge stations (CCoWS, 2004)..... 24

Figure 15: Date ranges for time-series datasets used in this project. 27

Figure 16: Five-year precipitation record from Moss Landing Marine Laboratories weather station (a), stream flow in Old Salinas River (b), surface nitrate concentration at LOBO mooring L03 (in Old Salinas River) (c) and surface nitrate concentrations at LOBO moorings L01 (ES main channel) and L02 (Kirby Park) (d). 30

Figure 17: Surface nitrate concentrations at LOBO mooring L02 in Kirby Park from June – November, 2008 and 2009, surface and deep. 34

Figure 18: Stream flow (m^3s^{-1}) (a), calculated freshwater nitrate concentration (μM) (b), and total nitrate load (kmol/d) (c) in Old Salinas River from June – November, 2008 (blue) and 2009 (black). 36

Figure 19: Stream flow (m3s-1) (a), calculated freshwater nitrate concentration (μM) (b), and total nitrate load (kmol/d) (c) in Old Salinas River from November – March, 2008 (blue) and 2009 (black). 39

Figure 20: Power spectral density of surface and deep (20m) temperature records at LOBO moorings L20 (left panel) and L20-2 (right panel). Bold black lines depict 95% confidence interval. Spectral peaks at diurnal (K1, left) and semidiurnal (M2, right) tidal frequencies are indicated. 41

Figure 21: Power spectral density of surface and deep (20m) nitrate records at LOBO moorings L20 (left panel) and L20-2 (right panel). Bold black lines depict 95% confidence interval. Spectral peaks at diurnal (K1, left) and semidiurnal (M2, right) tidal frequencies are indicated. 41

Figure 22: M1 winds (a), and NOAA PFEL upwelling index (b) from January, 2005 – January, 2010. 40

Figure 23: Daily average temperature (a), and salinity (b) data from the MBARI M1 mooring from January, 2005 – January, 2010. 45

Figure 24: M1 winds (a), NOAA PFEL upwelling index (b), M1 temperature (surface and deep) (c), and M1 salinity (surface and deep) (d) from June – November, 2008. 48

Figure 25: M1 winds (a), NOAA PFEL upwelling index (b), M1 temperature (surface and deep) (c), and M1 salinity (surface and deep) (d) from June – November, 2009. 49

Figure 26: a) Summer temperature at mooring L20, surface and deep. b) Daily averaged temperature at mooring L20, surface and deep. Red line depicts temperature threshold for defining upwelling days. c) Vertical temperature difference between surface and deep nodes at mooring L20. Red line depicts threshold for defining upwelling days. d) Daily averaged nitrate concentration at depth, mooring L20. Red circles denote upwelling days, as defined by the two threshold conditions.. 50

Figure 27: a) Summer temperature at mooring L20-2, surface and deep. b) Daily averaged temperature at mooring L20-2, surface and deep. Red line depicts temperature threshold for defining upwelling days. c) Vertical temperature difference between surface and deep nodes at mooring L20-2. Red line depicts threshold for defining upwelling days. d) Daily averaged nitrate concentration at depth, mooring L20-2. Red circles denote upwelling days, as defined by the two threshold conditions. 51

Figure 28: Nitrate transport to Monterey Bay from coastal upwelling during June - November, 2008 (top panel) and 2009 (bottom panel). 52

Figure 29: Nitrate concentration (a) and temperature (b) at mooring L20, surface and deep, from June 24 – July 1, 2008. 54

Figure 30: Nitrate concentration (a) and temperature (b) at mooring L20, surface and deep, from August 2 -9, 2009. 55

Figure 31: Unfiltered temperature data (a) and daily temperature variance within the 0.45 – 1.1 d frequency band (b) at mooring L20, deep node. Red line denotes threshold for defining internal wave days. 56

Figure 32: Unfiltered temperature data (a) and daily temperature variance within the 0.45 – 1.1 d frequency band (b) at mooring L20-2, deep node. Red line denotes threshold for defining internal wave days. 57

Figure 33: Possible areal mixing scenarios for nearshore surface waters and the Elkhorn Slough discharge plume. 61

Figure 34: Nitrate (a), temperature (b), and salinity(c) at LOBO nearshore mooring L20 (3km north of Moss Landing Harbor, and 1.5 km offshore), surface (blue) and 16 m depth (red). 64

Figure 35: Nitrate (a), temperature (b), and salinity(c) at LOBO nearshore mooring L20-2 (3km south of Moss Landing Harbor, and 1.5 km offshore), surface (blue) and 16 m depth (red). 65

Figure 36: Temperature-salinity plot for select moorings in Elkhorn Slough and Monterey Bay from June - November, 2008 (a) and 2009 (b). 68

Figure 37: Temperature-salinity plot for select moorings in Elkhorn Slough and Monterey Bay from November, 2009 - March, 2010. 69

Figure 38: Temperature-salinity (a) and salinity-nitrate (b) time-progressive scatter plots for LOBO surface mooring L20-2 (June, 2009 – May, 2010). 70

Figure 39: Surface nitrate at mooring L20-2 (a) and Moss Landing tidal stage (b) during the early summer, 2009. 71

Figure 40: Fluorescence (a), turbidity (b), transmission (c), salinity (d), temperature (e), and nitrate (f) measurements taken during the July 27, 2009 UDAS field program. Strepresents the location of mooring L20-2 73

Figure 41: Nitrate (a), salinity (b), temperature (c), and chlorophyll (d) at mooring L20-2 from July 26 – July 29, 2009. Red fill denotes period of UDAS deployment. Times are in GMT. 74

Figure 42: Temperature-salinity (left) and temperature-nitrate (right) property plots for water masses within ES and coastal Monterey bay (SU stands for surface, DP, deep). Yellow dots represent measurements taken during the UDAS deployment. 75

Figure 43: Daily precipitation (a), and stream flow (b), nitrate concentration (c), and nitrate load (d) in OSR. 77

Figure 44: Temperature (a), salinity (b), nitrate concentration (c), and calculated density (d) at LOBO inner-shelf mooring L20-2 surface and deep (20m) during the period surrounding the 2009 "first-flush" precipitation event. Gray fill denotes period of precipitation. 78

Figure 45: Salinity difference from pre-storm at L20-2 (a), and hourly freshwater fraction relative to pre-storm at L20-2 (b) from October 4 –20, 2009. 79

Figure 46: Predicted and observed (black) surface nitrate concentration at LOBO mooring L20-2, based on terrestrial freshwater fraction. 81

Figure 47: Salinity-temperature (a), nitrate-temperature (b), salinity-nitrate (c) and density-nitrate (d) characteristics for surface and deep waters preceding the storm (October 8 – October 12), during the storm (October 13 – midday October 14), and after the storm (October 14 midday – October 17). 85

Figure 48: Equatorward winds (a), temperature (b), salinity (c), nitrate concentration (d), and calculated density (e) at MBARI offshore mooring M1, surface and deep (20m, when available) during the period surrounding the 2009 "first-flush" precipitation event. Positive wind vectors denote downwelling-favorable conditions. Gray fill denotes period of precipitation. 86

Figure 49: Water depth (m) (a), nitrate concentration (μM) (b), and salinity (c) at LOBO mooring L03 (left panel) and L01 (right panel). 89

Figure 50: Percentage of total integrated nitrate suply to the nearshore from Elkhorn Slough (ES), upwelling and internal waves (IW). Upwelling represents an average of the two approaches used for calculating transport from upwelling. ... 95

Figure 51: Nitrate transport from Elkhorn Slough, upwelling (PFEL and LOBO methods) and internal waves over the two-summer study period. Circles represent days where each supply mechanism was active, as defined by threshold conditions for those methods..... 97

ACKNOWLEDGEMENTS

I would like to thank my thesis committee members, Dr. Erika McPhee-Shaw, Dr. Ken Johnson, and Dr. Nick Welschmeyer, for their valuable guidance, insight and support throughout this study. I am also deeply indebted to Craig Hunter for his field expertise and continuous enthusiasm for this project. I would also like to acknowledge the LOBO group and MBARI for their invaluable scientific, technical, and mechanical knowledge, all of which has assisted me throughout the completion of this project. In addition, special thanks to John Douglas, Scott Hansen and Lee Bradford at Moss Landing Marine Laboratories (MLML) small boats facility for their assistance with boating operations, along with the MLML community as a whole for providing a wonderful graduate experience. Lastly, I would like to dedicate this project to the late Steve Fitzwater, whose positive outlook on work and play has forever influenced my life as a scientist.

1. INTRODUCTION AND BACKGROUND

1.1 Overview

Nitrate levels within coastal hydrologic systems are steadily increasing due to population growth and intensified agriculture in adjacent watersheds (Vitousek et al, 1997). Nitrate from fertilizers as well as human and animal waste gets transported to the coastal ocean through storm-drains, irrigation channels, rivers and coastal streams. The net effect of terrestrial nitrate loading on coastal ocean ecosystems depends on a variety of factors, including local residence times, degree of tidal pumping between ocean and freshwater and seasonal cycles in oceanic and estuarine hydrodynamics. Shallow, semi-enclosed basins, such as coastal bays and gulfs, are often particularly susceptible to the effects of terrestrial nitrate pollution because they remain somewhat geographically isolated from the open ocean. For example, nitrate-rich runoff from adjacent agriculture in the Yaqui Valley has been shown to stimulate production in the Gulf of California (Beman et al, 2005). Additionally, in a 2007 publication, Rabalais et al documented the strengthening relationship between the nitrate-load of the Mississippi River and the extent of hypoxia in the northern Gulf of Mexico.

In Monterey Bay, the link between terrestrial-sourced nitrate and coastal ocean productivity remains poorly constrained. More specifically, the significance of nitrate transport out of Elkhorn Slough (ES), a highly eutrophic estuarine system in Moss Landing, California, to coastal Monterey Bay has not been thoroughly examined. Persistent loading from surrounding agriculture in the Salinas Valley and high nitrate levels mark ES as a potentially important source of nitrate to the inner-shelf. However,

nearshore surface waters in Monterey Bay are also influenced by physical oceanographic processes that force the delivery of nitrate to surface waters. Wind-driven upwelling, for example, is a dominant process along the California margin leading to the vertical transport of deep, nutrient-rich water to the euphotic zone. Internal waves have also been identified as important mechanisms for transporting nitrate to the California inner-shelf (McPhee-Shaw et al, 2007). Such processes and associated ecosystem response have been well documented in the Monterey Bay area (Rosenfeld et al, 1994) (Carroll, 2009).

While it is well known that upwelling supplies the majority of nutrients to California coastal ecosystems over annual timescales, the disconnect between the timing of maximum upwelling intensities and extreme algal blooms in Monterey Bay implies that alternative processes may play a key role in bloom dynamics. Ryan (2008) suggests that constituents from terrestrial drainage could trigger bloom events during periods of relaxed upwelling and intensified coastal stratification.

In this study, nitrate delivery to Monterey Bay from Elkhorn Slough and the adjacent Old Salinas River (OSR) is quantified and compared to relative contributions from oceanographic processes during the transitional, summer season. The main objective is to further characterize the role of local terrestrial-sourced nitrate in the nearshore nitrate variability of Monterey Bay.

1.2 Monterey Bay

1.2.1 Physical Oceanography

With an approximate area of 800 km^2, Monterey Bay is the largest open embayment on the west coast of the United States and maintains open communication

with the Pacific Ocean (Figure 1) (Rosenfeld et al, 1994). The physical oceanography that drives nutrient distributions within coastal Monterey Bay is influenced primarily by the presence of the California Current System (CCS) and seasonal shifts in wind patterns. Three distinct oceanographic periods within Monterey Bay were defined by Skogsberg and Phelps (1946), further described by Pennington and Chavez (2000): the spring/summer 'upwelling season', the summer/fall 'oceanic season', and the winter 'Davidson Current' season. Characterized by intense, northwest winds, the upwelling season occurs from February to early June and results in the vertical transport of cold (10 – 12 °C), nutrient-rich (15-20 μM NO_3^-) waters to the surface.

From June to November, equatorward winds weaken and upwelling relaxes, leading to the onshore movement of lower salinity California Current water (Pennington & Chavez, 2000; Rosenfeld et al, 1994). This 'oceanic season' is somewhat indistinct and can be thought of as a transitional phase, exhibiting variable winds and intermittent periods of upwelling between long relaxation events and associated increases in stratification (Breaker & Broenkow, 1994).

As equatorward winds continue to weaken, winter conditions develop resulting in northward surface flow (Davidson Current) and low vertical surface gradients (salinity, temperature and nitrate) from increased storm activity and mixing. Nitrate concentrations during this time are relatively low compared to the upwelling season (< 5 μM) although episodic mixing events may periodically elevate surface nutrient concentrations (Pennington & Chavez, 2000).

Figure 1: Geographic location of Monterey Bay depicting major bathymetric features of the Monterey Bay Submarine Canyon (Google Earth)

Figure 2: Central California sea surface temperature during coastal upwelling (NASA)

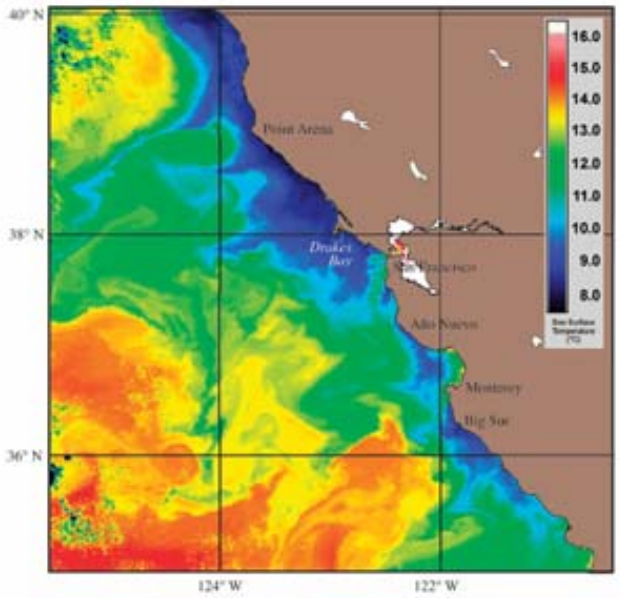

1.2.2 Monterey Submarine Canyon

The presence of the Monterey Submarine Canyon, one of the deepest submarine canyon systems in the world (Shepard, 1973), also affects the hydrography and nutrient dynamics in coastal Monterey Bay (Figure 1). Early ideas that the canyon was a major source of local upwelled water (Bigelow & Leslie, 1930; Bolin & Abbot, 1963) have since been refuted (Rosenfeld et al, 1993); however, complex canyon bathymetry enhances baroclinic motion, providing alternative mechanisms for nutrient enrichment. Shea and Broenkow (1982) describe how internal wave oscillation and isotherm displacement above the canyon rim can result in lateral flow and mixing along the shelf. Also, shoaling at the canyon head can induce breaking internal waves, generating a source of enhanced turbulence and mixing. Kunze et al (2001) showed that turbulent diffusivities resulting from internal wave energy flux convergences within Monterey Canyon are three orders of magnitude stronger than values characteristic of the open ocean. Such mechanisms provide important pathways for nutrient fluxes to the euphotic zone of the inner-shelf, at time-scales distinguishable from upwelling.

1.2.3 Freshwater Sources to Monterey Bay

Monterey Bay receives freshwater input from three rivers and numerous coastal streams. Each tributary is responsible for transporting dissolved constituents, including chemical pollutants, nitrate and other nutrients, to the nearshore environment. Nitrate transport rates are controlled by flow volume and nitrate concentration. Combined outflow from Carneros Creek and Old Salinas River (OSR), the two tributaries draining

into Elkhorn Slough, is less than 5% of total fluvial discharge to Monterey Bay (Figure 3, Table 1). However, extreme nutrient concentrations in Old Salinas River heighten the significance of nitrate transport out of the Elkhorn Slough system to coastal Monterey Bay.

Figure 3: Location of major freshwater sources to Monterey Bay (See Table 1 for number references; USGS, PVWMA)

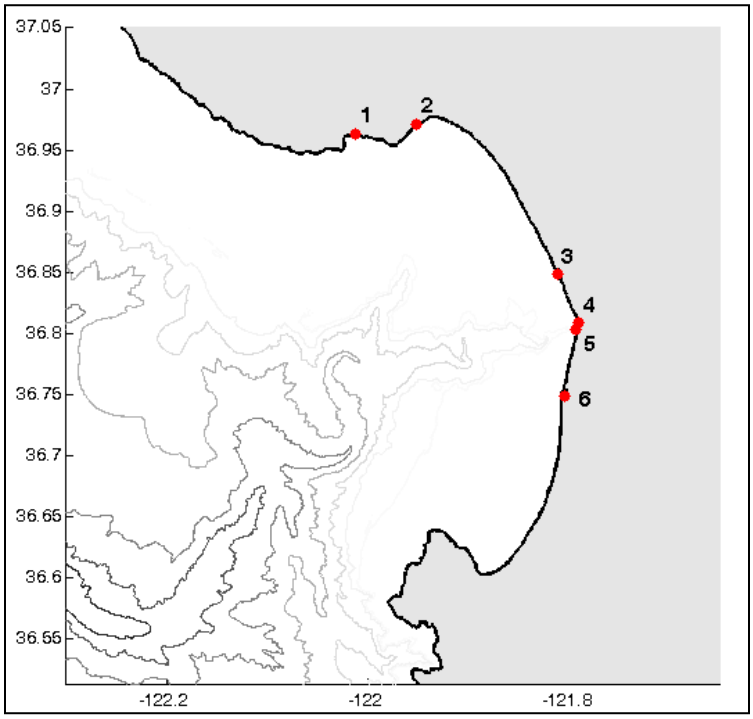

Table 1 : Average annual discharge from major freshwater sources to Monterey Bay (USGS, PVWMA)

Name	USGS Station #	Average Annual Discharge (m^3/d)
San Lorenzo River [1]	11160500	269,960
Soquel Crk [2]	11160000	91,650
Pajaro River [3]	11159000	284,830
Carneros Creek [4]	--	10,000
Old Salinas River Channel [5]	11152650	28,530
Salinas River [6]	11152500	636,450

1.3 Elkhorn Slough

Elkhorn Slough (ES) is a shallow (< 3 m average depth), seasonal estuary in Moss Landing, CA with direct drainage into Monterey Bay. The slough's 9.1 km^2 surface area (Chapin et al, 2004), including numerous tidal creeks, mudflats, and marshland, has been designated the Elkhorn Slough National Estuarine Research Reserve (ESNERR) by the National Oceanographic and Atmospheric Administration (NOAA) (Elkhorn Slough Tidal Wetland Project Team (ESTWPT), 2007). The main channel extends 11.4 km inland from Monterey Bay and is part of the Monterey Bay National Marine Sanctuary (Chapin et al, 2004). Old Salinas River Channel (OSR) extends approximately 2 km south, from Moss Landing harbor to the outflow and tide-gate at Potrero Rd (Figure 4).

Figure 4: Map of Elkhorn Slough (ESTWPT, 2007)

ES is a tidally-forced estuary with an average tidal prism of 5.7×10^6 m^3 (excluding OSR) (Broenkow & Breaker, 2005). Tides within the slough are mainly semidiurnal with maximum tidal currents occurring on the ebbing tides that can reach up to 1.5 ms^{-1} (Broenkow & Breaker, 2005). ES is often divided geographically into a "lower slough", extending from Moss Landing Harbor to Parson's Slough, and an "upper slough", consisting of the area between Parson's Slough and Hudson's Landing (Breaker et al, 2008). The lower slough experiences daily tidal flushing, resulting in short residence times and a water column that is well-mixed (Breaker et al, 2008). Due to angled channel morphology, the upper slough is somewhat isolated geographically from the lower slough and is less influenced by tidal action. Residence times in the upper

slough can approach a month, often resulting in thermal stratification and hypersalinity, especially during the summer season (Largier et al, 1997).

Three separate watersheds drain into the Elkhorn Slough system, containing approximately 200 km^2 of heavily-fertilized cropland (Figure 5) (ESTWPT, 2007) (Monterey County Water Resources Agency (MCWRA), 2008). 79% of adjacent agricultural land exists within the Tembladero watershed which drains directly into OSR (ESTWPT, 2007). Freshwater input into ES occurs through two major headwaters, Carneros Creek at the northern head of the main channel, and OSR in the southern channel (Figure 5). Freshwater input is seasonal, with maximum flow rates occurring during winter storm events. During the summer months freshwater input is minimal (< 1 m^3s^{-1}), consisting primarily of irrigation runoff that enters OSR.

Due to surrounding agriculture, the nitrate concentration of freshwater entering OSR is on the order of 10^3 μM, especially during months when precipitation is minimal and there is no dilution by heavy rains. As a result, nutrient levels within the ES system are amongst the highest on record for United States estuaries (Caffrey et al, 2002). Such loading causes nitrate concentrations within OSR to exceed 1000 μM daily, which is over 100 times the typical nitrate concentrations found in ocean surface water (Figure 6).

Figure 5: Map of major watersheds surrounding Monterey Bay. The three watersheds that drain into the Elkhorn Slough system are outlined in yellow. The white dot represents the location of drainage into Old Salinas River (ESTWPT, 2007)

Figure 6: Nitrate concentrations in Old Salinas River Channel (OSR) (top) and coastal Monterey Bay, 3km north (bottom left) and 3km south (bottom right) of the harbor. Horizontal line depicts 25 µM for reference between plots.

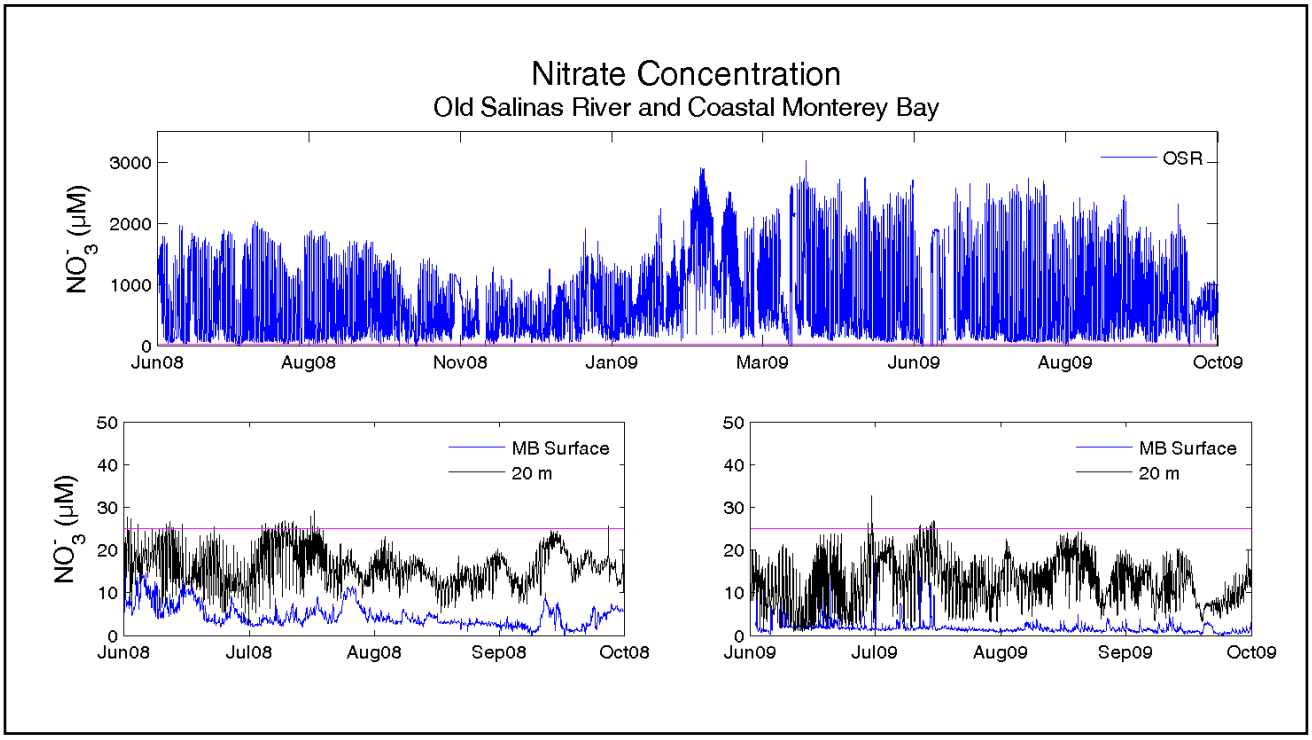

The fate of nitrate entering OSR and ES is ultimately determined by physical transport processes and the degree of biological cycling occurring in the slough. Transport in the slough is largely affected by tidal forcing. Ebb flow draws OSR water through the tide gates at Potrero Rd and out the harbor entrance. A proportion of OSR water remaining in the harbor at minimum low tide is then pushed up the main channel of the slough on the flooding tide, creating a source of nitrate for planktonic and benthic organisms in the slough's main channel (Figure 7).

Elkhorn Slough is highly productive, with chlorophyll concentrations exceeding 100 mg m^{-3} at the head of the estuary at times (Caffrey et al, 2007). The phytoplankton community in Elkhorn Slough is best exemplified by the distinct along-channel gradient in species composition. The slough's lower reaches, influenced by exchange with Monterey Bay, house mainly diatom taxa while cryptophytes dominate the upper slough (Nick Welschmeyer, personal communication). Concentrations of bacteria, dissolved organic matter (DOM), and turbidity are consistently greater in the upper slough as well (Figure 8). Phytoplankton species, as well as prevalent macroalgal species, such as *Ulva* Spp., and benthic denitrifying organisms, create a sink for nitrate carried up the main channel from OSR on the rising tide. Approximately 23% of incoming nitrate in the main channel of the slough is consumed (Plant et al, 2009).

Figure 7: Ariel "KiteCam" photo depicting the pulse of high-nitrate OSR water entering Elkhorn Slough on a rising tide (courtesy of Gary Thurmond, MBARI).

Figure 8: Chlorophyll (a), colored dissolved organic matter (CDOM) (b), turbidity (c) and phycocyanin (d) fluorescence gradients within the main channel of Elkhorn Slough. Phycocyanin is an accessory pigment found in cyanobacteria. Data collected September, 20 using a Turner CFINS fluorometry package.

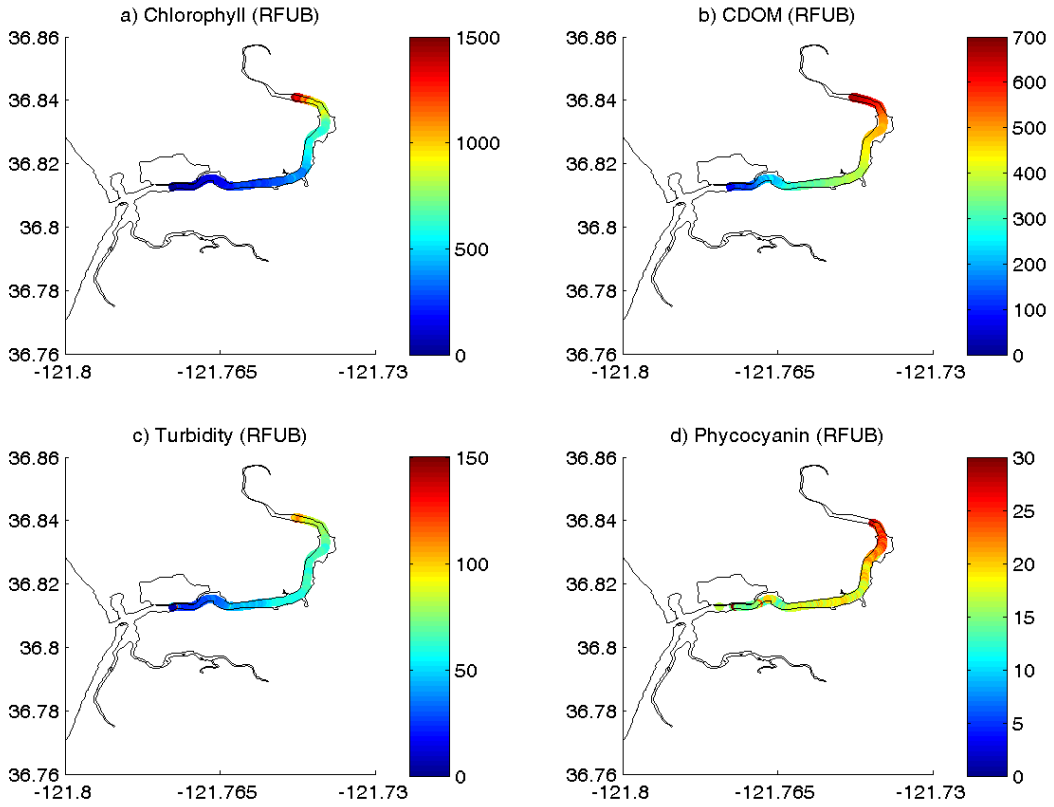

1.4 Bloom Dynamics in Monterey Bay and the Land-Sea Link

Changes in phytoplankton assemblages and rates of primary production in Monterey Bay are closely linked to the annual hydrographic cycles and associated nutrient regimes described in Section 1.2.1. In winter months, a deep mixed layer and low incident solar radiation suppress phytoplankton productivity at the surface. During

the subsequent upwelling period, the biological response to increased sunlight and nutrient delivery to the euphotic zone is distinct; surface production rates within the bay can reach 500 mg C $m^{-3}d^{-1}$ with maximum chlorophyll concentrations of 10-15 mg m^{-3} (Pennington & Chavez, 2000). Microalgal abundance during this time is dominated by rapidly-growing diatom species, such as *Chaetoceros spp*, that can readily exploit nutrient rich environments (Pennington & Chavez, 2000). During the oceanic period (summer - early fall), high surface irradiance and reduced upwelling leads to increased stratification and limited nutrient availability at the surface. Production during this time is frequently dominated by dinoflagellate species, whose motility provides the necessary niche to overcome water column stability. Chlorophyll concentrations are typically <5 mg m^{-3} at this time with production rates <300 mg C $m^{-3}d^{-1}$ on average (Pennington & Chavez, 2000). However, dense dinoflagellate blooms are not uncommon in Monterey Bay during this time, and extreme bloom events, exhibiting chlorophyll concentrations greater than 500 mg C m^{-3}, have been documented (Ryan et al, 2008).

Dense dynoflagellate blooms in Monterey Bay are of particular concern due to the increasing global occurrence of harmful algal blooms (HABs) in coastal ocean waters. Seventy-five percent of HAB species are dinoflagellates (Smayda, 1997), including *Alexandrium, Akashiwo, Cochlodinium,* and *Ceratium*, all species known to occur in Monterey Bay. Toxins produced by certain species can bioaccumulate through the food web, while high-biomass, non-toxic blooms can lead to anoxia and fish-kills. The occurrence and associated dynamics of extreme HABs in Monterey Bay has been the subject of many recent studies. In Oct-Nov, 2007, the largest-scale dinoflagellate bloom

ever observed in Monterey Bay developed within two weeks of the season's "first flush" rain event, suggesting that land-based nutrients from Elkhorn Slough might play a key role in triggering such blooms (Figure 9) (Ryan, 2009). This study aims to further investigate this link through the analysis of various nitrate supply mechanisms, both oceanographic (upwelling and internal waves) and terrestrial (Elkhorn Slough), along the inner-shelf of Monterey Bay.

Figure 9: Satellite image of November, 2007 harmful algal bloom in Monterey Bay (NOAA)

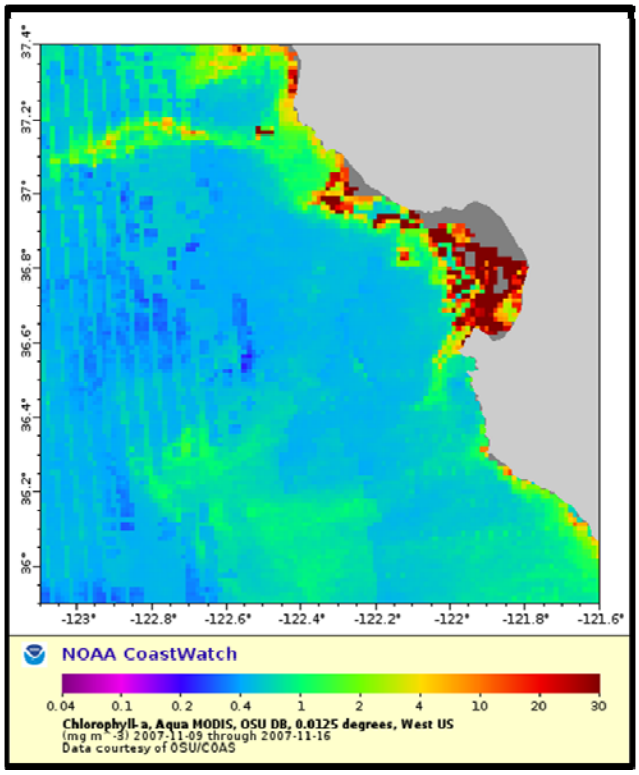

1.5 Scope of Project

This study will focus on the relative importance of nitrate transport out of the Elkhorn Slough system to coastal ocean productivity in nearshore Monterey Bay. Primary objectives are to quantify nitrate transport from Elkhorn Slough to the surface waters (< 20m) of the Monterey Bay inner-shelf and compare to transport estimates from upwelling and internal waves. The study period will span June, 2008 to May, 2010, with a focus on the transitional summer season (June – November) in order to examine the interplay among spring upwelling, increased summer stratification, maximum nitrate concentrations in OSR, and the onset of late fall/early winter rains. Research questions to be investigated include:

1) What is the average nitrate transport out of Elkhorn Slough to nearshore Monterey Bay during the summer season and how does this rate change with the onset winter conditions?
2) What is the average nitrate transport to nearshore Monterey Bay from coastal upwelling and internal waves during the summer season? How do these rates compare to terrestrial transport from Elkhorn Slough?
3) How does Elkhorn Slough influence nitrate variability observed along the inner-shelf at moorings L20 and L20-2?

2. METHODS

2.1 Datasets

2.1.1 Land-Ocean Biogeochemical Observatory

Hydrographic and nutrient data in Elkhorn Slough and nearshore Monterey Bay was examined using the Land-Ocean Biogeochemical Observatory (LOBO). This was the primary dataset used for this study. LOBO is a robust network of five moorings in Elkhorn Slough and nearshore Monterey Bay specifically designed for continuous, long-term monitoring of complex biogeochemical processes (Jannasch et al, 2008). Moorings L01 – L04 were positioned at distinct environments within ES, providing a robust platform for tracking hydrographic changes and chemical fluxes through the slough environment (Figure 10). Nearshore moorings L20 and L20-2 were recently incorporated into the LOBO network as key observational tools at the land-sea interface. Site locations for nearshore moorings were chosen with careful consideration of field logistics as well as scientific context. 1 km was chosen as an appropriate distance from shore for nearshore moorings in order to assess the impact of terrestrial processes. In other words, this distance was deemed an appropriate representation of the land-sea interface. L20 was deployed approximately 2.5 km north of the Moss Landing Harbor entrance at 20m depth on the inner-shelf of Monterey Bay from June - November, 2008. After recovery, this mooring was redeployed the following summer approximately 2.5 km south of the harbor (20m depth) as L20-2. L20-2 persisted through rough swell conditions, providing key observations of discrete winter storm events, including lag times associated with

land-to-sea transport, as well as information pertaining to hydrographic transitions between multiple oceanographic seasons.

Each mooring was equipped with a suite of in-situ sensors that sampled once per hour (Table 2, Figure 11). A key component of the LOBO mooring array is the In-Situ Ultraviolet Spectrophotometer (ISUS), developed by Ken Johnson and Luke Coletti at the Monterey Bay Aquarium Research Institute (MBARI) (Johnson & Coletti, 2002). The ISUS is a novel in-situ nutrient analyzer capable of acquiring long-term, high-resolution nitrate measurements under a variety of field conditions. ISUS technical components include a continuous wave deuterium light source (spectral range of 200 – 400 nm), a photodiode array spectrometer, and a low-power controller and datalogger (Johnson & Coletti, 2002). Nitrate concentrations are deconvolved from acquired spectra due to the unique absorption spectra of the nitrate ion, and the high spectral resolution (~1nm) and dynamic range of the ISUS.

All instruments were calibrated pre and post deployment by MBARI personnel and an integrated telemetry system provided automated data transmission in near real-time. Processing of all LOBO raw data was performed via a server application that parsed and logged incoming data files to a network file server (Jannasch et al, 2008). A set of programs set to operate once per hour converted raw data into meaningful units and stored the data as ASCII files that were available through the online LOBOViz program

Table 2: LOBO mooring specifications

Mooring	Location	Deployment Dates	Water Depth (m)	Sensor Depth (Sfc, Deep (m))	Surface Array	Deep Array
L01	ES Main Channel	2003 - present	9	0.6, 2.5	a, c, d, e, f	b
L02	Kirby Park	2004 - present	4	0.4, 1	a, c, d, e, f	b
L03	Old Salinas River	2004 - present	1.5	0.3, NA	a, c, d, f	NA
L04	Parson's Slough	2005 - present	5.5	0.4, 2.5	a, c, d, e, f	b
L20	Offshore North	Jun, 2008-Nov,2008	20	0.6, 16.5	a, c, d, e, f	b,c
L20-2	Offshore South	Jun, 2009-present	20	0.6, 16.5	a, c, d, e, f	b,c

a. Seabird 16plus CTD (conductivity, temperature, pressure)

b. Seabird 37 CTD (conductivity, temperature, pressure)

c. Seabird 50 (pressure)

d. MBARI/Satlantic In-situ Ultraviolet Spectrophotometer (ISUS, nitrate)

e. WETlabs FLNTU (fluorescence and backscatter)

f. Aanderaa 3930 Optode (oxygen)

interface (http://www.mbari.org/lobo/loboviz.htm). Data streams were continuously monitored for quality control during processing. Each data point was flagged as "good", "questionable", or "bad". For nitrate, the quality flag was based on the root mean square residual fit as well as other technical issues pertaining to periods of fouling or service.

Temperature, salinity and nitrate observations from moorings L01, L02 and L03 taken during the time period spanning the nearshore mooring deployments were the primary datasets analyzed for this study, although historical temperature and nitrate data from L03 (in Old Salinas River Channel) were also used to characterize background variability of nitrate loading within the Elkhorn Slough system. All LOBO data was retrieved online using the "good & questionable" data quality field. Outliers were removed, and data were interpolated to a common, hourly time grid using Mathworks' Matlab. Negative nitrate values within the data records were not removed. Instead, three-day means were calculated for each dataset containing negative values. The lowest negative mean for each dataset was then added to that record as an offset. This method was deemed appropriate as the ISUS reports estimates of concentrations, as opposed to actual concentrations. Offsets applied are listed in Table 3.

Table 3: LOBO nitrate data offsets

Mooring	**Nitrate Offset (µM)**
L01 surface	+3
L02 surface	+6
L20 surface	+1
L20-2 surface	+0.5

Figure 10: LOBO mooring locations.

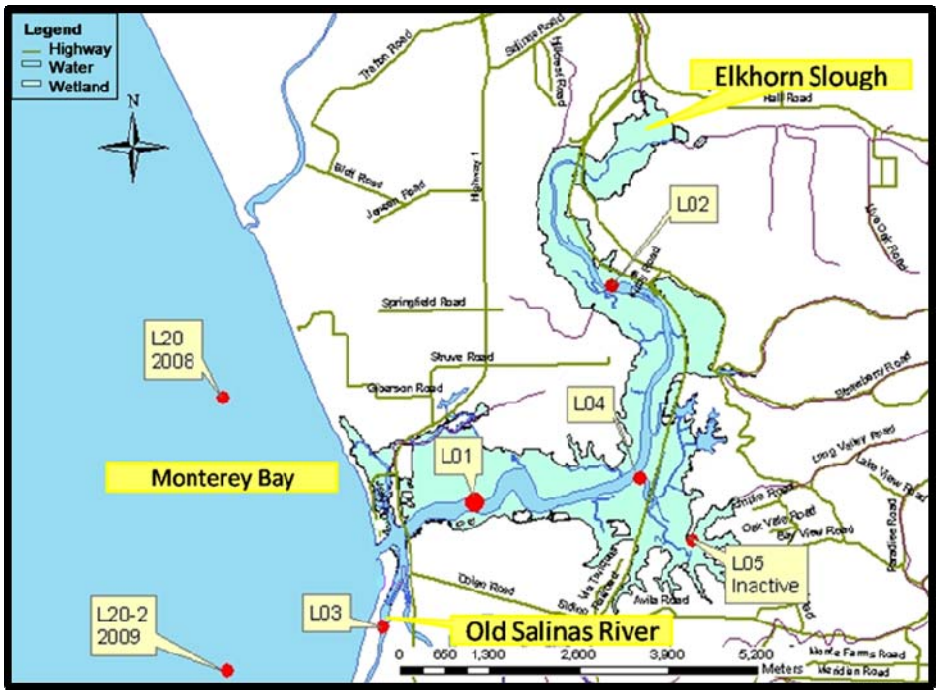

Figure 11: Typical LOBO mooring instrument configuration.

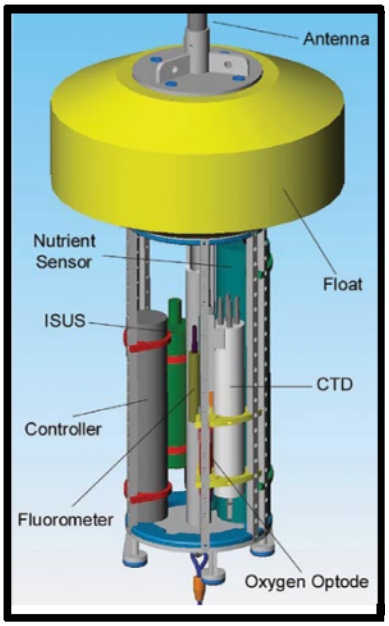

2.1.2 Hydrologic Data

A Sontek Argonaut Shallow Water current meter was deployed south of the tide-gates at the bottom of the OSR channel in January, 2007 (Figure 12). This instrument provided stream stage data and average current velocity data at 5 and 10 minute sample frequencies for summer, 2008, and summer, 2009, respectively. Data from this instrument, along with cross-channel bathymetry measurements, were used to calculate flow in order to characterize discharge variability associated with terrestrial runoff exiting OSR. Flow data was then averaged over the diurnal tidal cycle in order to account for effects from the tide-gates at Potrero Rd. Gaps in data were filled by applying a Model II, least-squares geometric mean regression between flow derived from the Argonaut current meter, and flow from United States Geological Survey (USGS) station 11152650 further upstream (Figure 13; Figure 14). Persistent irrigation runoff near Old Salinas River causes there to be a baseline flow in OSR, while flow at the USGS station is zero.

Daily freshwater nitrate concentrations (nitrate at salinity = 0) in OSR were estimated by applying a salinity-nitrate regression to data from LOBO surface mooring L03 over tidal periods. This provided an approximation of nitrate concentration for the freshwater end-member entering OSR.

Figure 12: Location of Old Salinas River tide gates and Sontek Argonaut current meter. (images: google maps, http://www.sontek.com/argonautsw.php)

Figure 13: Regression relationship between flow data from USGS station 11152650 and flow data derived from the Argonaut current meter.

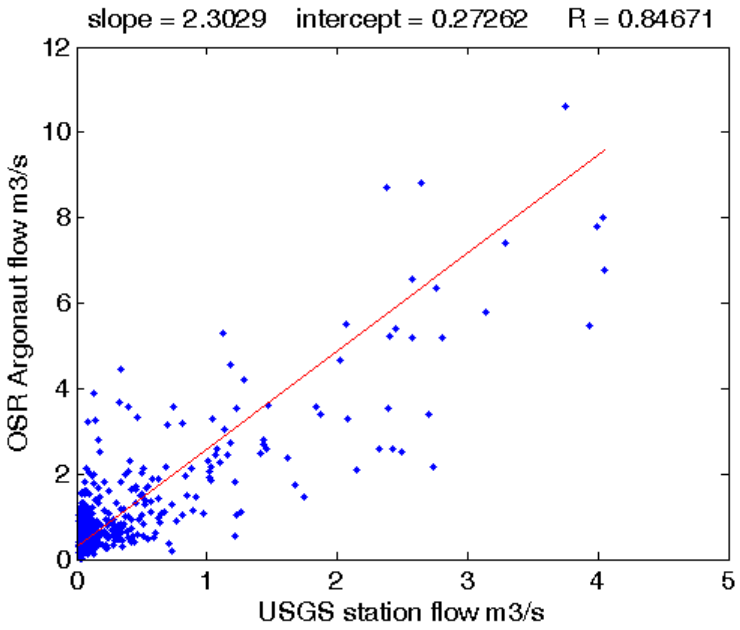

Figure 14: Map depicting channel classification in the Tembladero watershed and location of pertinent discharge stations (CCoWS, 2004)

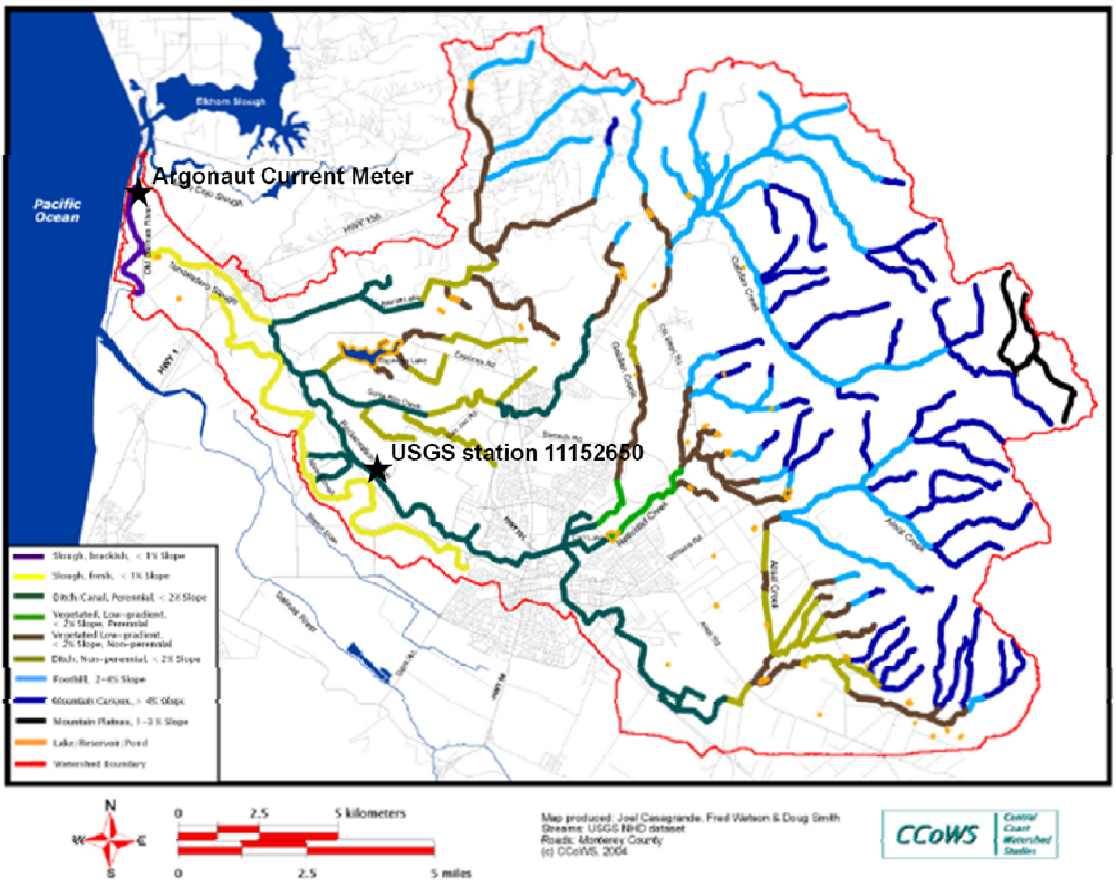

2.1.3 Meteorological Data

Precipitation data, sampled once per minute, from the MLML weather station was used to characterize rain events during the study period. Data and sensor descriptions for the MLML weather station can be found online at http://pubdata.mlml.calstate.edu/.

Hourly meteorological data (wind speed and direction) from MBARI mooring M1 in Monterey Bay (latitude 36.75, longitude -122.03) was used to describe general wind patterns and to compare dominant forcings apparent during the study period.

In addition to these datasets, the Pacific Fisheries Environmental Laboratory (PFEL) daily mean upwelling index at 36 °N 122 °W, a part of the National Oceanographic and Atmospheric Administration (NOAA), was used for estimates of volume transport to surface waters from upwelling. The PFEL upwelling index is based on Ekman transport theory, derived from local wind stress (see Equation 1, where *UI* is volumetric transport, *f* is the coriolis parameter, τ is alongshore wind-stress, and ρ is the density of seawater) (Bakun, 1973; Bakun, 1975). Units of UI are in m^3s^{-1} per 100 meters of coastline.

$$UI = \frac{\left(\left(\frac{1}{f}\right)\tau\right) \times 100}{\rho} \qquad \text{(Equation 1)}$$

All meteorological data was retrieved online and interpolated to a common, hourly time-grid using Mathworks' Matlab. The calendar year (January – December) is used when comparing annual meteorological conditions, as opposed to the hydrologic water year (October – September).

2.1.4 Portable Underway Data Acquisition System (UDAS)

The surface expression of nearshore ocean water was mapped on several occasions during the summer of 2009 using Moss Landing Marine Laboratories' high-frequency portable Underway Data Acquisition System (UDAS). Developed by Luke Beatman, this flow-through system integrates a suite of standard and novel hydrographic instrumentation, including Seabird's SBE 38 Digital Oceanographic Thermometer and SBE 45 Thermosalinograph, Scufa Fluorometer, Wet Labs C-Star 10cm Transmissometer, and the Satlantic ISUS nitrate analyzer. Water is pumped through an intake hose and then through a network of tubing which passes through each sensor. The system is easily deployed from a Boston Whaler and operational up to a speed of approximately 5 knots, with instruments typically set to sample every 4 seconds. The UDAS allows the user to map the surface expression of large areas over short time-scales. Such technology is ideal for sampling regions of water mass interaction, such as the discharge plume of Elkhorn Slough. Previous work has been done by Fischer (2009) utilizing UDAS to sample discharge from ES. Similar attempts were made on ebbing tides during the summer of 2009 in order to investigate the dynamics behind peaks in nitrate observed at the nearshore mooring location.

2.2 Data Summary

The date ranges for the multiple time-series used in this project are outlined in Figure 15. Many of the datasets covered multiple years, although the date ranges spanning LOBO nearshore mooring deployments have been chosen as the primary time periods of focus. Matlab was used in all data analysis.

Figure 15: Date ranges for time-series datasets used in this project.

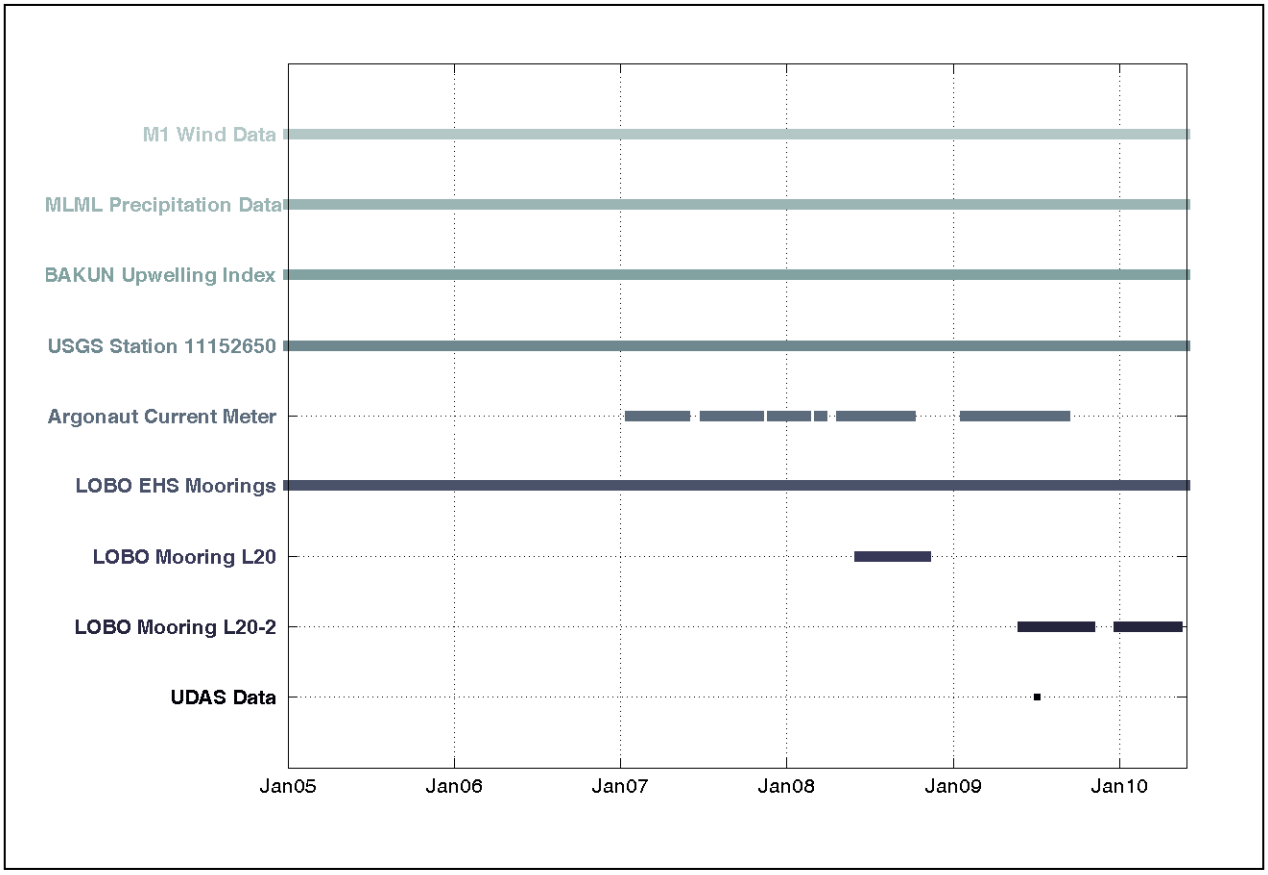

2.3 Nitrate Transport Calculations

Nitrate transport to inner-shelf surface waters of Monterey Bay was calculated for three distinct sources: (1) point-source discharge of terrestrial waters from Elkhorn

Slough, (2) coastal upwelling, and (3) internal waves during the summer seasons spanning the study period. Estimates of terrestrial nitrate transport out of Elkhorn Slough during the winter of 2009 are also presented for comparative purposes. Terrestrial transport is expressed as a molar load (moles per unit time) from the following equation:

$$L_t = Q_t C_t \quad \text{(Equation 2)}$$

where L is nitrate load at time, t, Q is volumetric transport or stream flow (m^3/s), and C is nitrate concentration (μmol/L) of source waters. Units of load were converted to kmol/d.

Calculating nitrate transport from coastal upwelling roughly followed Equation 2 as well, although two separate approaches were considered for characterizing Q and C. In the first approach, termed the "PFEL" approach, the NOAA PFEL upwelling index time series (for 36° N, 122° W) was used to characterize daily volume transport from upwelling (Bakun, 1973; Bakun, 1975). Units of m^3s^{-1} per 100 m coastline were scaled to the length of Monterey Bay in order to arrive at a total nitrate load entering Monterey Bay from coastal upwelling. 20 μM was used as a conservative estimate for the nitrate concentration of deep water.

The second approach, termed the "LOBO" approach, used data from deep (16m) LOBO nearshore mooring arrays to characterize nitrate concentrations. The NOAA PFEL upwelling index (for 36° N, 122° W) was also used in this approach to characterize average volume transport during active upwelling. However, due to the distance between the upwelling index node and the study site, it was important to find a way to identify specific days throughout the season where nearshore surface waters were influenced by upwelling. Therefore, for the second approach, thresholds were defined to characterize

nearshore "upwelling days" by using temperature data from nearshore moorings L20 and L20-2 (McPhee-Shaw et al, 2007). "Upwelling days" were defined as days having an average daily temperature at depth (16 m) below 12.5 °C, and a temperature difference between surface and deep less than 3.5 °C (weakly stratified). Nitrate flux to nearshore surface waters from upwelling was then calculated by multiplying average nitrate values at depth during upwelling days by average transport rates from the upwelling index during active upwelling.

Calculating nitrate transport to nearshore surface waters from internal waves followed a different method. Due to the lack of current measurements in this study, calculating nitrate transport from internal waves as the product of the advective velocity and local nitrate concentration was not possible. Instead, following McPhee-Shaw et al, 2007, transport from internal wave events was approximated as an average flux convergence ($d[NO_3]/dt$) calculated over a week of active internal wave motions. In order to calculate the total amount of nitrate transported to surface waters from internal waves over each season, each average exposure rate was then multiplied by the total number of days exhibiting internal wave activity throughout each season (McPhee-Shaw et al, 2007). Internal wave days were defined as having an average daily temperature variance at depth greater than 0.5 $°C^2$ within the 0.9 – 2.2 cpd frequency band. Because properties of surface waters within the top meter are subject to variability from local, high-frequency atmospheric effects, data from LOBO nearshore deep arrays was used for all internal wave-driven transport calculations.

2.4 Time Series Analysis

Spectral analysis was performed on temperature and nitrate time series from LOBO nearshore moorings L20 and L20-2 (surface and deep nodes) in order to assess the distribution of energy (variance) per unit frequency at each location, and to verify that the time scales associated with internal wave transport are relevant to the data in this study. The power spectral density (PSD) of each record was calculated using Welch's averaged, modified periodogram method. The Welch method divides the time series into segments of specified length (usually a power of 2 for fast computation) with 50% overlap, and then computes a periodogram for each segment. The spectra are then averaged, yielding a final PSD and associated frequency vector. A reasonable choice is to choose a window size that allows for 8 times the period of interest (L. Washburn, E. McPhee-Shaw, personal communication). For the hourly data in this study, a window size of 512 hours (12 days) was thu

s chosen (> 8x the diurnal period).

Temperature series were also bandpass filtered around the diurnal and semidiurnal tidal frequencies [0.9 2.2] cpd using a bandpass filter routine provided by William Shaw. This reduces amplitudes of "unwanted" frequencies, allowing for a more accurate assessment of the temporal variability of internal tide amplitudes at each location.

3. RESULTS

3.1 Terrestrial Nitrate Transport out of Elkhorn Slough

3.1.1 Seasonal Hydrology in Elkhorn Slough

Nitrate dynamics within Elkhorn Slough are closely linked to changes in seasonal hydrology. Figure 16 below presents a five-year precipitation record from the Moss Landing Marine Laboratories weather station (a), five years of stream flow in Old Salinas River (b), and a five-year nitrate time-series at LOBO moorings L03 (c), L01 and L02 (d). Average annual precipitation for 2005 - 2010 was 27.07 cm, with 77% of rainfall occurring between November and March. The largest amount of rainfall received in a single day from 2005 - 2010 was 7.11 cm, over twice the amount of precipitation recorded on any other day. This event occurred on October 13 during the 2009 El Nino year and was the first rain event, termed "first flush", of the season. Annual precipitation over the two-year study period was 24.00 cm in 2008 and 28.58 cm in 2009. 2008 received 51 days of measurable precipitation, while 2009 received 58 measurable days. Four days in 2008 received over 1.27 cm in a single day, versus 5 days in 2009. 95% and 68% of rainfall occurred between November and March for 2008 and 2009, respectively. Total precipitation from June - November was 0.74 cm in 2008 and 8.38 cm in 2009.

Seasonal stream flow patterns in Elkhorn Slough were closely correlated to precipitation. Peak flow occurred in the winter months, from November to March, and entered Elkhorn Slough at two locations: Carneros Creek at the head of the slough, and Old Salinas River near the mouth of the harbor. Winter flow in Carneros Creek can reach up to 3.8 m^3/s (Caffrey et al, 2007). Over the study period, winter flow in Old Salinas

River frequently exceeded 5 m^3/s, and reached values between 10-15 m^3/s during large storm events. During the summer and early fall (June – November), flow in Carneros Creek was negligible and Old Salinas River was the primary source of freshwater entering the slough. Summer flow in OSR over the study period remained between 0.5 and 1.5 m^3/s and was driven by irrigation runoff from surrounding agriculture.

Nitrate concentrations throughout Elkhorn Slough are largely influenced by changes in local precipitation and stream flow. For example, nitrate concentrations at moorings L01 and L02 were greatest during the winter months which is typical in most hydrologic systems (Figure 16d). This is because precipitation runoff from winter storms mobilizes nitrate that has collected on land surfaces, ultimately carrying it to nearby rivers and streams and increasing the total nitrate load carried by the system. This pattern was not apparent in Old Salinas River, whose channel hydrology is largely driven by agricultural runoff. The seasonal nitrate maximum at LOBO station L03 in Old Salinas River occurred in the summer, when precipitation was close to zero. Nitrate concentrations in OSR during this season were frequently between 2000-3000 μM, which is over two orders of magnitude greater than nitrate concentrations in the upper slough. Furthermore, annual nitrate maximums in this region of the slough show a steady increase (Figure 16c). From 2005 to 2009 the annual nitrate maximum in OSR increased by 50%. In winter, increases freshwater input from precipitation results in diluted nitrate concentrations within OSR.

Figure 16: Five-year precipitation record from Moss Landing Marine Laboratories weather station (a), stream flow in Old Salinas River (b), surface nitrate concentration at LOBO mooring L03 (in Old Salinas River) (c) and surface nitrate concentrations at LOBO moorings L01 (ES main channel) and L02 (Kirby Park) (d).

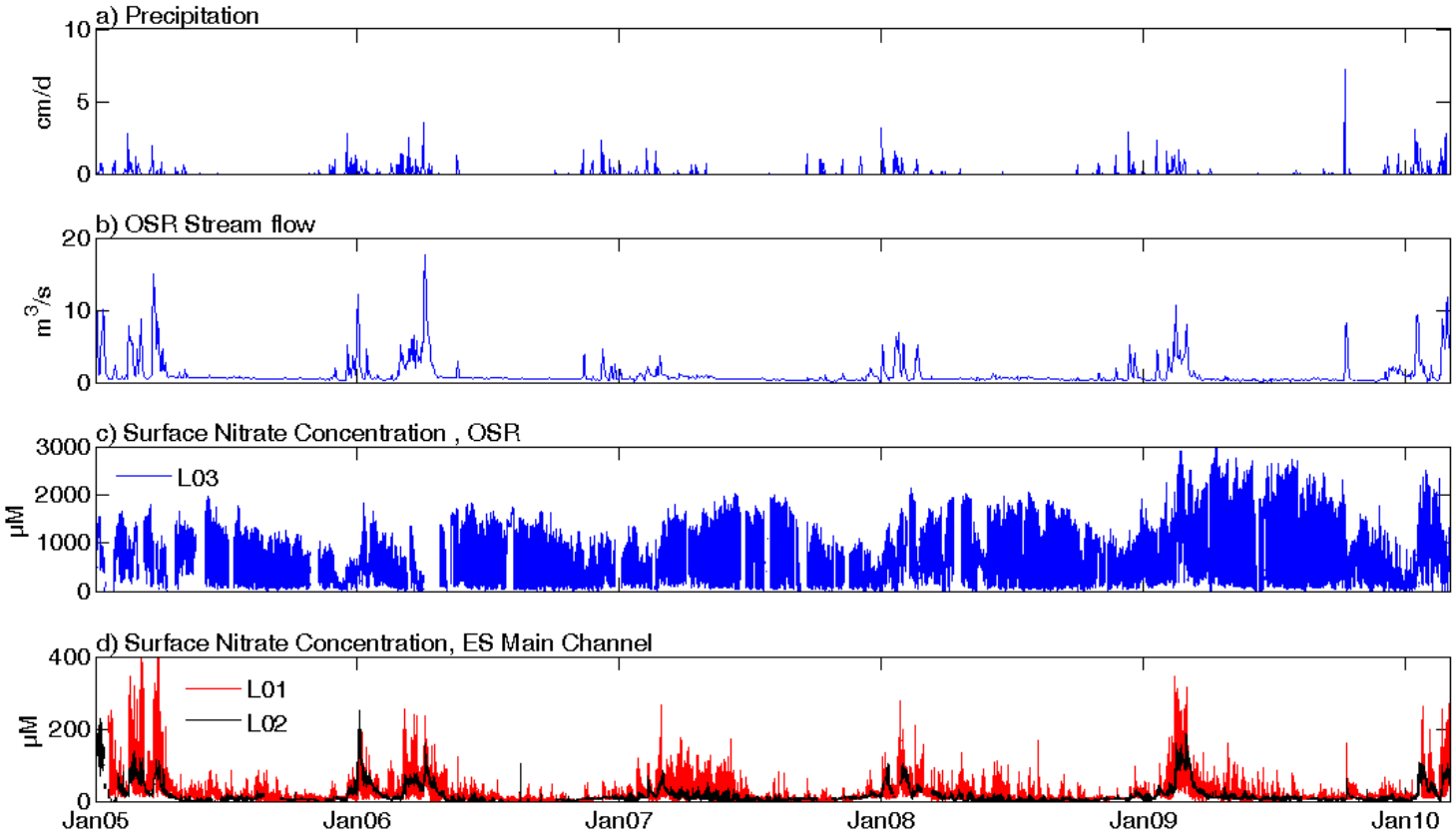

3.1.2 Summer Nitrate Loads from Elkhorn Slough

In the summer season Carneros Creek is typically dry, resulting in zero freshwater flow into the upper slough (Caffrey et al, 2007). Because the transport of chemical constituents through a hydrologic channel requires a suspending flow, Carneros Creek is not typically a source of nitrate to the slough during dry months. Surface low-tide nitrate concentrations at Kirby Park (LOBO station L02) nearest to Carneros Creek remained below 30 µM for each summer season (excluding a rain event in October, 2009, to be discussed later) (Figure 17).

Figure 17: Surface nitrate concentrations at LOBO mooring L02 in Kirby Park from June – November, 2008 and 2009, surface and deep.

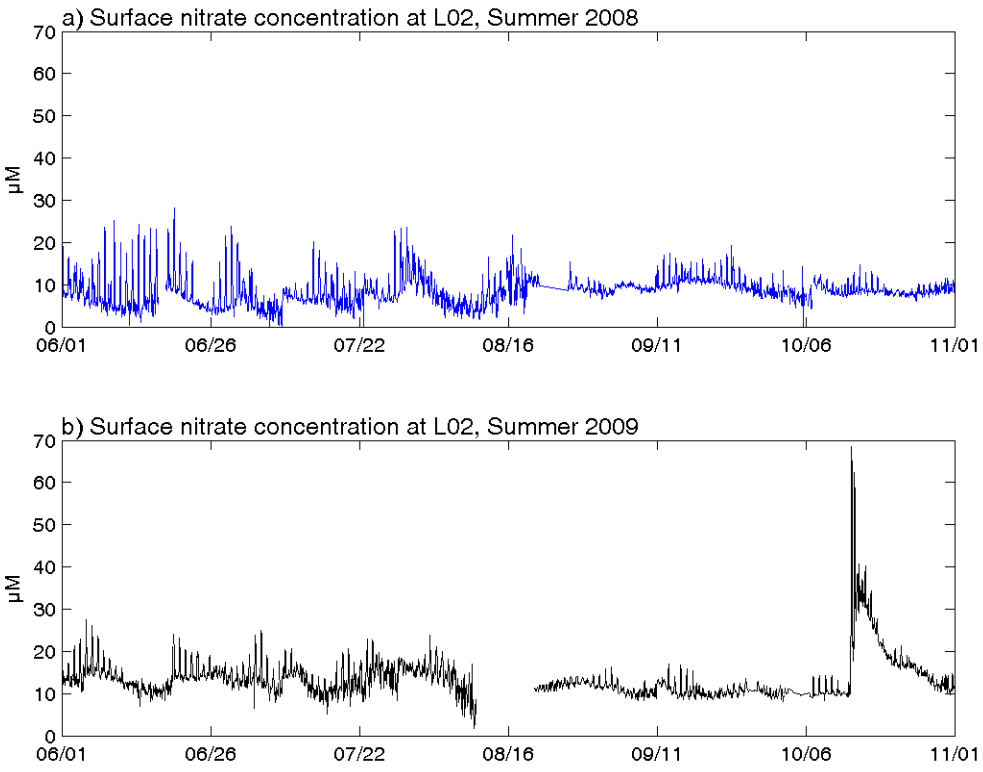

Although minimal, stream flow was measureable in OSR from June - November due to persistent irrigation runoff (Figure 18-a). Average stream flow values for 2008 and 2009 during this season were 0.488 and 0.545 m^3s^{-1}, respectively. Stream flow exceeded 1 m^3s^{-1} during zero days in 2008, and during six consecutive days in 2009. Maximum summer stream flow was 0.947 m^3s^{-1} in 2008 and 8.196 m^3s^{-1} in 2009. The 2009 maximum occurred during the year's first flush event. Maximum stream flow in 2009 excluding this event was 0.67 m^3s^{-1}.

The average daily freshwater nitrate concentration from June – November in OSR was 1976 μM in 2008 and 2481 μM in 2009. Daily freshwater nitrate concentrations ranged between 552 – 2953 μM during the summer of 2008 and from 164 – 3741 during the summer of 2009 with annual maximums occurring in June, 2008 and July, 2009. Freshwater nitrate concentration dropped below 1000 μM for only 7 and 6 days in the summers of 2008 and 2009, respectively.

As described in Section 2.3, the product of stream flow and nitrate concentration provides an estimate of total nitrate load. Average summer nitrate loads in OSR (excluding loads during the large storm event of October, 2009, to be discussed in Section 3.3.5) were 85.7 and 83.9 kmol/d for 2008 and 2009, respectively. Maximum daily loads for the 2008 and 2009 summer seasons were 204 and 643 kmol/d, respectively. Total integrated transport for each season was 11828 and 11885 kmol for 2008 and 2009, respectively.

Figure 18: Stream flow (m^3s^{-1}) (a), calculated freshwater nitrate concentration (µM) (b), and total nitrate load (kmol/d) (c) in Old Salinas River from June – November, 2008 (blue) and 2009 (black).

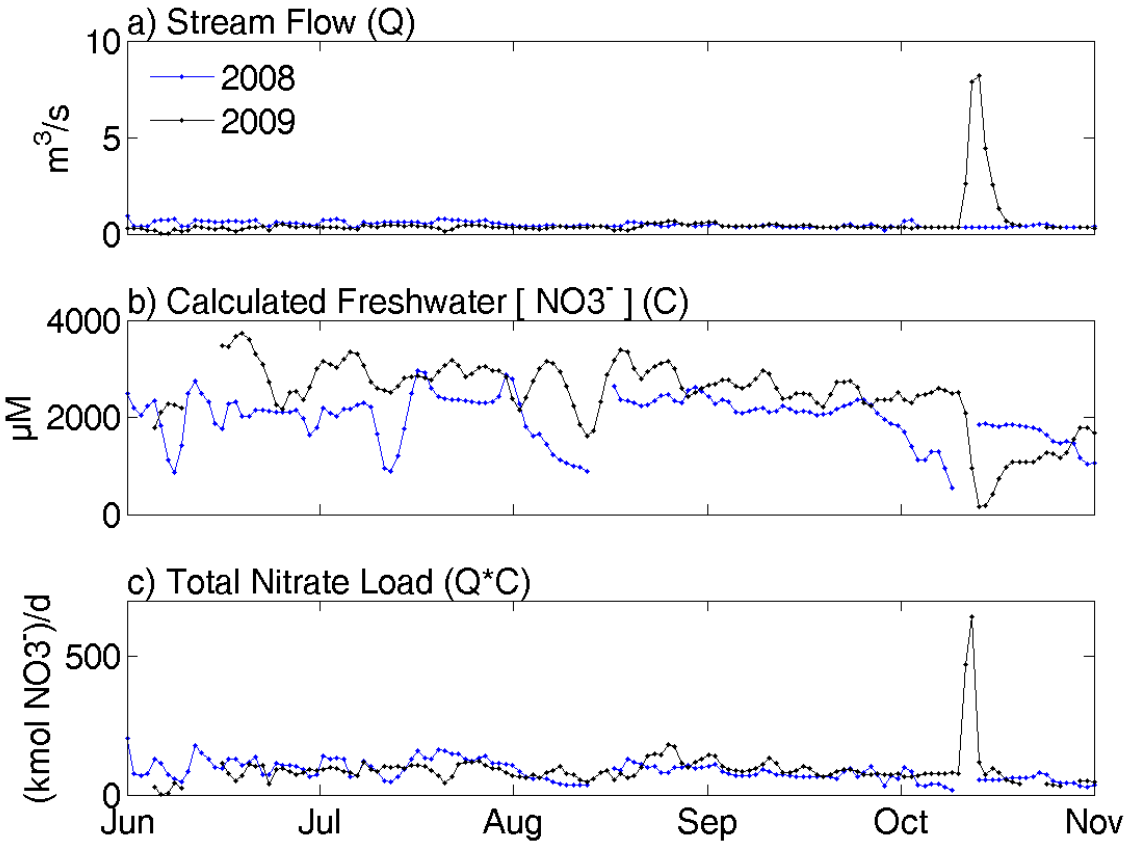

3.1.3 Winter Nitrate Loads from Elkhorn Slough

During the rainy season (November – March) Elkhorn Slough received freshwater input from both Carneros Creek and Old Salinas River. Pulses of runoff from precipitation events lead to significant increases in stream flow and subsequent nitrate loading at both locations. In Carneros Creek, winter stream flow can reach up to 3.8 m^3/s (Caffrey et al, 2007). In 2001 during the rainy season, 35 – 120 μM nitrate concentrations were observed 5 km upstream of Elkhorn Slough in Carneros Creek (Los Huertos, 2001). As a conservative upper-bound, such stream flow and concentration values would give a maximum loading of 39 kmol NO_3^-/d into the main channel of Elkhorn Slough, an expected source of nitrate export to Monterey Bay (Chapin et al, 2004). Nitrate concentrations in the upper slough near LOBO station L02 in Kirby Park track terrestrial runoff signals and can range between 20 - 200 μM during the rainy season.

While it is important not to exclude Carneros Creek as a possible source of nitrate to coastal Monterey Bay during the rainy season, export from Old Salinas River channel is of far greater significance. Figure 19 depicts stream flow (m^3/s), freshwater nitrate concentration (μM) and total nitrate transport (kmol/d) out of OSR from November, 2008 – March, 2009 (referred to hereafter as winter, 2008) and November, 2009 – March, 2010 (referred to as winter, 2009), respectively. Average winter stream flow was 1.4 m^3s^{-1} in 2008 and 1.5 m^3s^{-1} in 2009. Stream flow exceeded 1 m^3s^{-1} during

44 days in 2008 and 56 days in 2009. Maximum summer stream flow was 10.6 and 9.3 m^3s^{-1} in 2008 and 2009, respectively.

The average daily freshwater nitrate concentration from November - March in OSR was 1524 μM in 2008 and 1231 μM in 2009. Daily freshwater nitrate concentrations ranged from 629 – 2893 μM during winter, 2008 and from 146 – 3519 during winter, 2009. Freshwater nitrate concentrations dropped below 1000 μM for 16 and 61 days in the winters of 2008 and 2009, respectively.

Average winter nitrate loads were 192 and 116 kmol/d for 2008 and 2009, respectively. Maximum daily loads for the 2008 and 2009 winter seasons were 1065 and 775 kmol/d, respectively. Integrated transport for winter, 2008 was 22307 kmol and that for 2009 was 13994 kmol.

Figure 19: Stream flow (m3s-1) (a), calculated freshwater nitrate concentration (µM) (b), and total nitrate load (kmol/d) (c) in Old Salinas River from November – March, 2008 (blue) and 2009 (black).

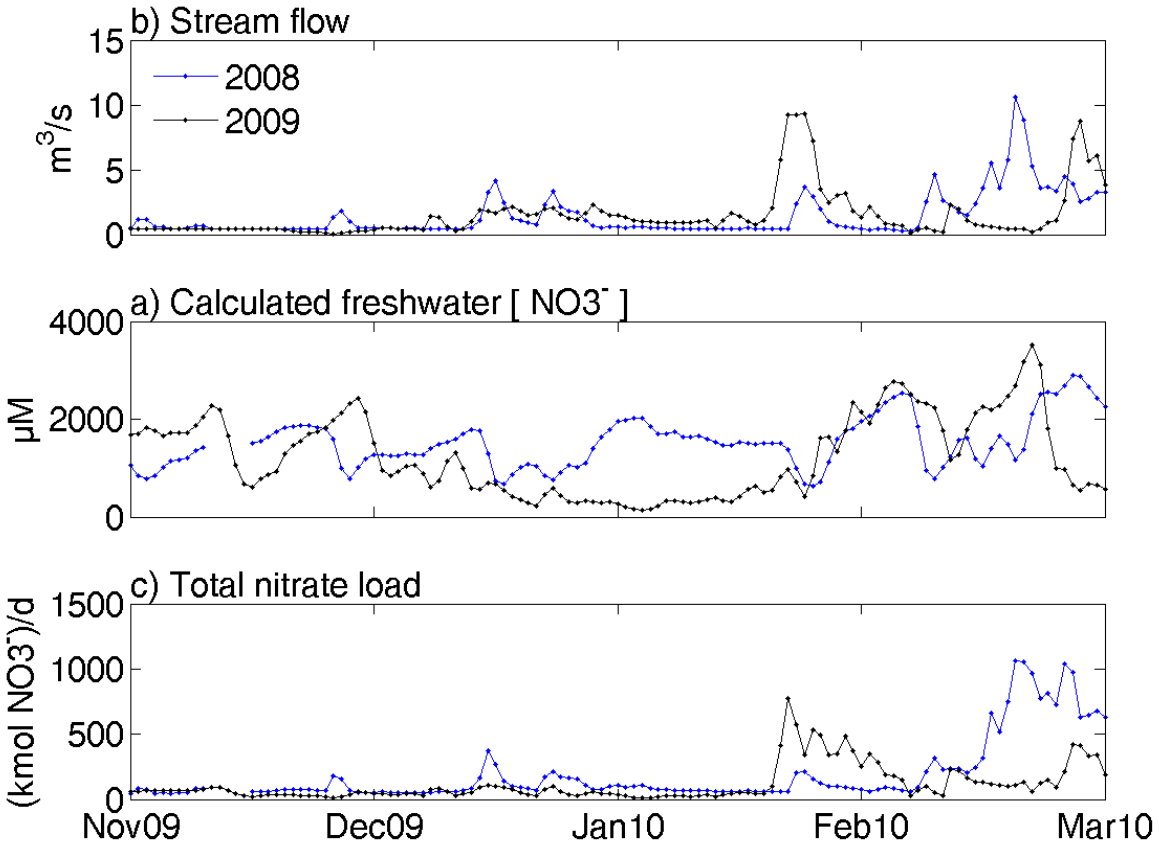

3.2 Coastal Nitrate Transport from Oceanographic Sources

3.2.1 Spectral Analysis

Results of spectral analysis, using summer data records from LOBO inner-shelf moorings L20 and L20-2, are presented in Figures 20 -21. Energetic variance is evident over a broad low-frequency band (0.07 – 0.3 cpd; roughly 3 – 14 day period). Distinct peaks at diurnal, semidiurnal, and numerous tidal harmonic frequencies are also apparent across deep records for both L20 (2008) and L20-2 (2009). Spectral signals for surface records are neither as strong nor distinct, although peaks are evident at diurnal and semidiurnal tidal frequencies for the L20-2 surface nitrate record and both surface temperature records.

Spectral energy is strongest at the semidiurnal frequency across all deep records and at the diurnal frequency across all surface records. Spectral energy is also greater at mooring L20-2 than at L20 in both temperature and nitrate time-series. This is most likely a spatial effect of mooring L20-2's proximity to the Monterey Submarine Canyon, a local hot-spot for internal wave generation (Kunze et al, 2001; Carroll, 2009).

Figure 20: Power spectral density of surface and deep (20m) temperature records at LOBO moorings L20 (left panel) and L20-2 (right panel). Bold black lines depict 95% confidence interval. Spectral peaks at diurnal (K1, left) and semidiurnal (M2, right) tidal frequencies are indicated.

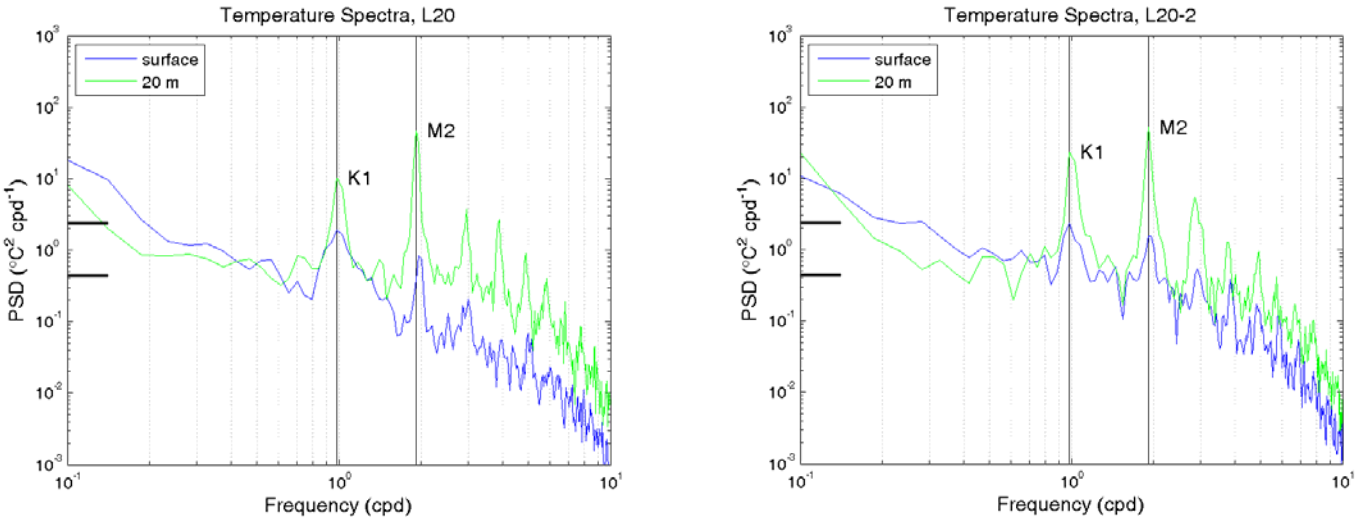

Figure 21: Power spectral density of surface and deep (20m) nitrate records at LOBO moorings L20 (left panel) and L20-2 (right panel). Bold black lines depict 95% confidence interval. Spectral peaks at diurnal (K1, left) and semidiurnal (M2, right) tidal frequencies are indicated.

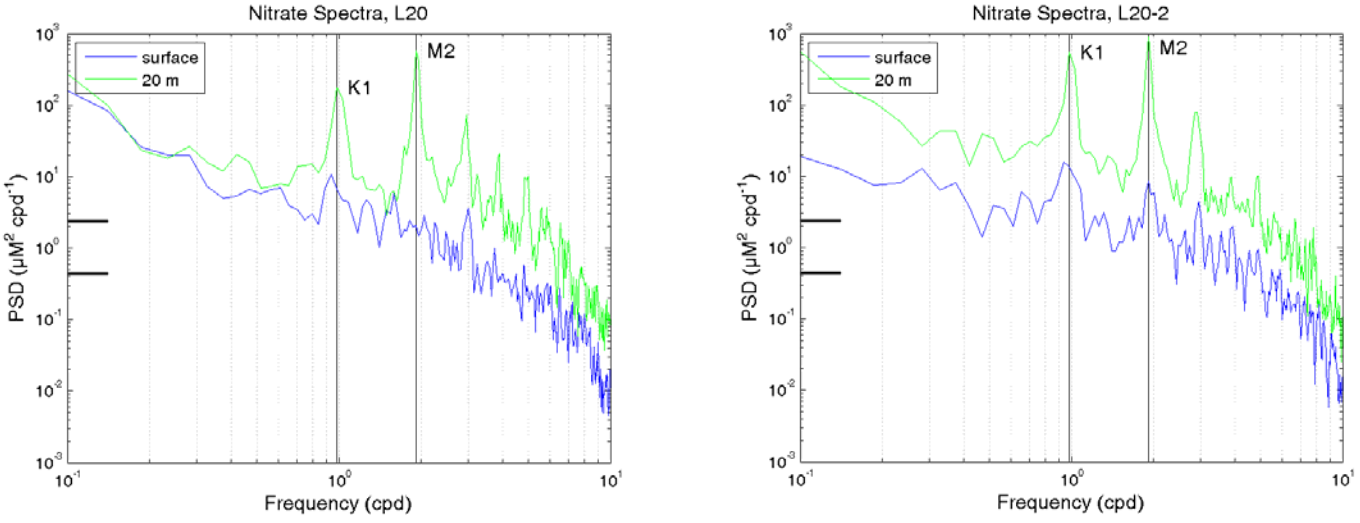

The results of spectral analysis show that tidal (semidiurnal and diurnal) and subtidal frequencies are relevant time scales for characterizing nitrate variability within this dataset. The following sections describe oceanographic nitrate transport mechanisms (coastal upwelling and internal waves) characteristic of such time-scales and their respective contributions to the nearshore nitrate supply over the study period.

3.2.2 Seasonal Upwelling Dynamics in Monterey Bay

The MBARI M1 mooring was chosen as a data-source for describing general upwelling conditions for regional Monterey Bay. Figure 22-a shows wind data at MBARI's M1 mooring from January, 2005 – January, 2010. U wind vectors are depicted in teal, v in blue. Northwesterly winds, conducive to coastal upwelling and defined here by a coordinate direction between 275 – 355 °, can be identified as positive u-vectors with negative v-vectors. Periods of persistent northwesterly winds were frequently observed from March to mid-June, lasting up to two weeks. Average wind speed for sustained northwesterly winds during this time (where northwest is the average daily wind direction for 3 or more consecutive days) was 4.0 – 10 m/s. As described in Section 1.2.1, such winds drive offshore surface Ekman transport and eventually lead to the upwelling of cold, nutrient rich, deep water to the surface. Figure 22-b shows NOAA's PFEL upwelling index (Bakun, 1973; Bakun, 1975), in m^3/s per 100 m coastline, from January, 2005 – January, 2010. The strongest periods of upwelling occurred in the spring season (March – June), and vertical volume transport frequently exceeded 250 m^3s^{-1} per

100 m coastline, and correlated with strong northwesterly winds. Average daily upwelling rates during the spring were 107 m^3s^{-1} per 100 m coastline from 2005 – 2009.

Daily averaged temperature and salinity data from January, 2005 – January, 2010 at the MBARI M1 mooring (surface and 20m depth) are presented in Figure 23. Seasonal fluctuations in temperature, driven by changes in upwelling intensity, are clearly evident and coincide with changes in salinity. Over the five year period, surface temperatures and salinities ranged from 8.9 – 16.5 °C and 31.6 to 34.0, respectively. Temperatures and salinities at 20m depth ranged from 8.9 – 15 °C and 32 – 34, respectively, over the same time period. Annual temperature minimums occurred in April or May from 2005 – 2009 and averaged 9.8 and 9.4 °C for surface and deep over this five year period. Annual temperature maximums occurred in August for 2005 – 2007, September in 2008, and June in 2009 and averaged 16.1 and 14.5 °C for surface and deep locations, respectively. The average difference in temperature from surface and 20m depth was 0.9 °C for this five year period. The average difference in salinity between the two depths was 0.08.

Figure 22: M1 winds (a), and NOAA PFEL upwelling index (b) from January, 2005 – January, 2010.

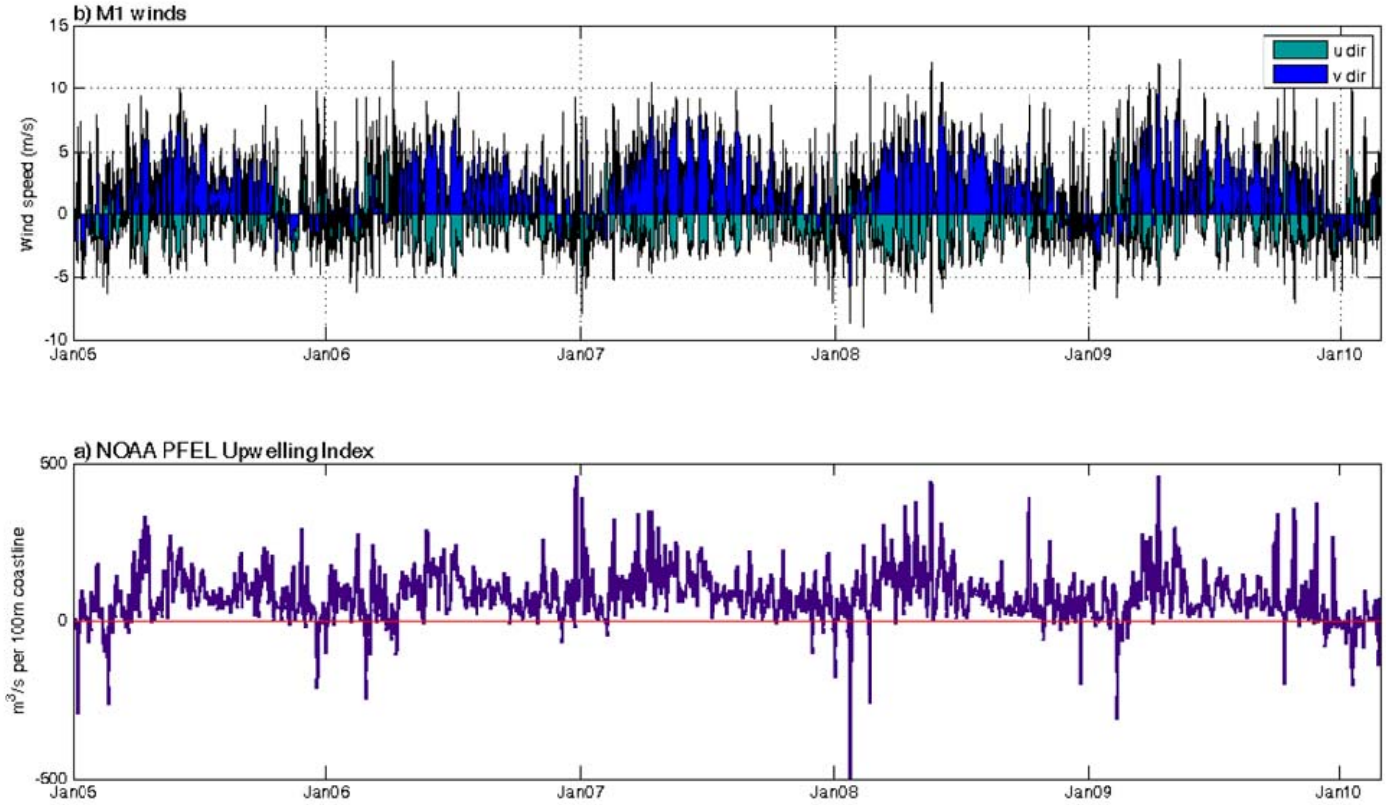

Figure 23: Daily average temperature (a), and salinity (b) data from the MBARI M1 mooring from January, 2005 – January, 2010.

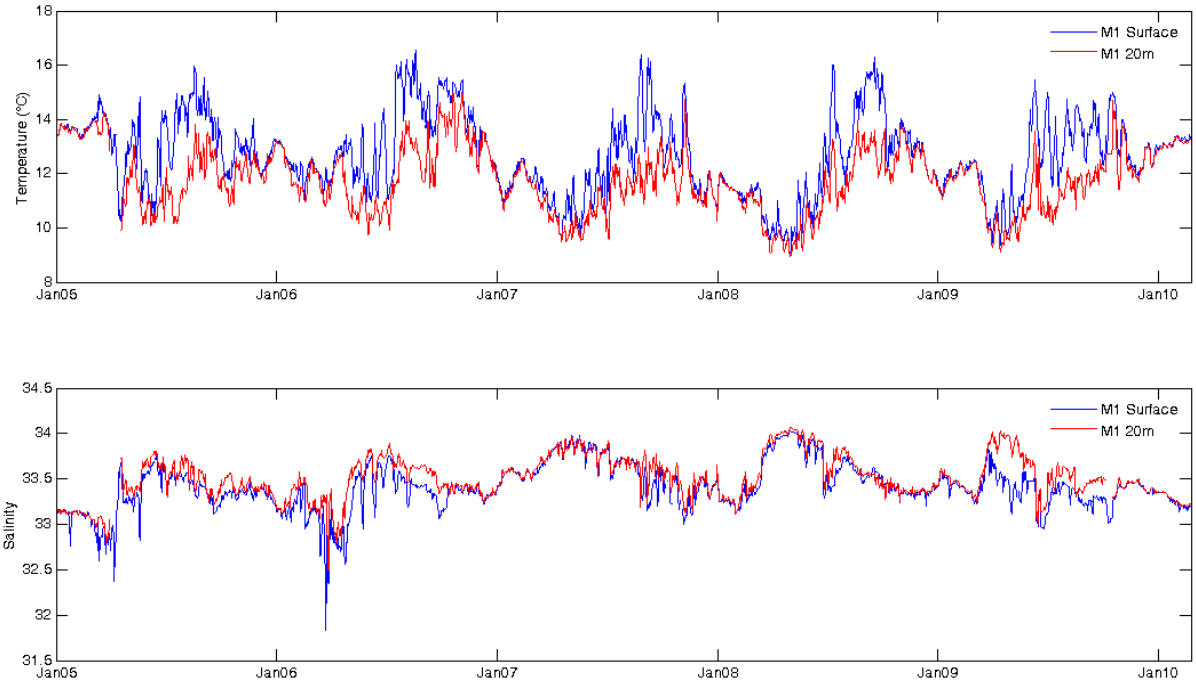

The above plots provide a general synopsis of seasonal meteorological and hydrographic trends typically observed within Monterey Bay, and characteristic of the California Current System. The following section focuses on upwelling dynamics and associated nitrate transport for the summer season during the two-year study period (2008 – 2009). Spring upwelling dynamics were not addressed in further detail because it is well known that oceanography dominates the nitrate signal during this time.

3.3.2 Coastal Upwelling Conditions during the Summer Study Period

The summer hydrographic season in Monterey Bay can be referred to as a transitional phase. This period, spanning June – November, typically exhibits variable winds and intermittent periods of upwelling between long relaxation events and associated increases in stratification (Breaker & Broenkow, 1994). The summer of 2008 experienced multiple strong upwelling events from June – August, as well as one in October (Figure 24). Average wind speed during sustained northwesterly winds was 5.5 – 6.6 m/s and average upwelling rates for the same periods were 90.2 m^3s^{-1} per 100 m coastline. The seasonal average wind direction, wind speed, and upwelling rate for 2008 was 256°, 5.213m/s, and 79.0 m^3s^{-1} per 100 m coastline, respectively.

During the summer of 2008, surface temperatures at M1 ranged from 9.8 °C (during upwelling events) to 17.2 °C. Average summer temperatures at M1 in 2008 were 13.5 and 11.9 °C for surface and deep (20m) sensors, respectively. Average salinities were 33.59 and 33.64 for surface and deep, respectively. Temperature differences between the surface and 20 m depth ranged from 4.2 °C during stratified conditions, to 0 °C at the height of an upwelling event.

The summer of 2009 experienced multiple upwelling periods as well (Figure 25). Average wind speed during northwesterly winds was 4.0 – 7.9 m/s and average upwelling rate for the same periods was 92.3 m^3s^{-1} per 100 m coastline. The seasonal average wind direction, wind speed, and upwelling rate for 2009 was 251°, 4.9 m/s, and 68.0 m^3s^{-1} per 100 m coastline, respectively.

During the summer of 2009, surface temperatures at M1 ranged from 11.2 °C (during upwelling events) to 16.9 °C. Average summer temperatures at M1 in 2009 were 13.5 and 11.7 °C for surface and deep (20m) sensors, respectively. Average salinities were 33.28 and 33.46 for surface and deep, respectively. Temperature differences between the surface and 20 m depth ranged from 5.1 °C during stratified conditions, to 0 °C at the height of an upwelling event. Average temperature difference between surface and deep water was 1.8 °C.

3.2.3 Nitrate Loads from Coastal Upwelling

As described in Section 2.3, two approaches (termed "PFEL" and "LOBO") were taken for calculating nitrate transport to Monterey Bay surface waters from coastal upwelling. Following threshold constraints for the LOBO approach defined in Section 2.3, 68 upwelling days were recorded during the summer of 2008 (Figure 26-d). Average nitrate concentrations in deep water during these periods ranged from 11.5 – 22.7 μM and averaged 18.02 μM. An average rate of 90.2 m^3/s per 100 m coastline was used to characterize vertical volume transport during active upwelling.

During the summer of 2009, 75 upwelling days were recorded (Figure 27-d). Average nitrate concentrations in deep water ranged from 9.8 – 22.0 μM and averaged 13.81 μM. An average rate of 92.3 m^3/s per 100 m coastline was used to characterize vertical volume transport during active upwelling.

Figure 24: M1 winds (a), NOAA PFEL upwelling index (b), M1 temperature (surface and deep) (c), and M1 salinity (surface and deep) (d) from June – November, 2008.

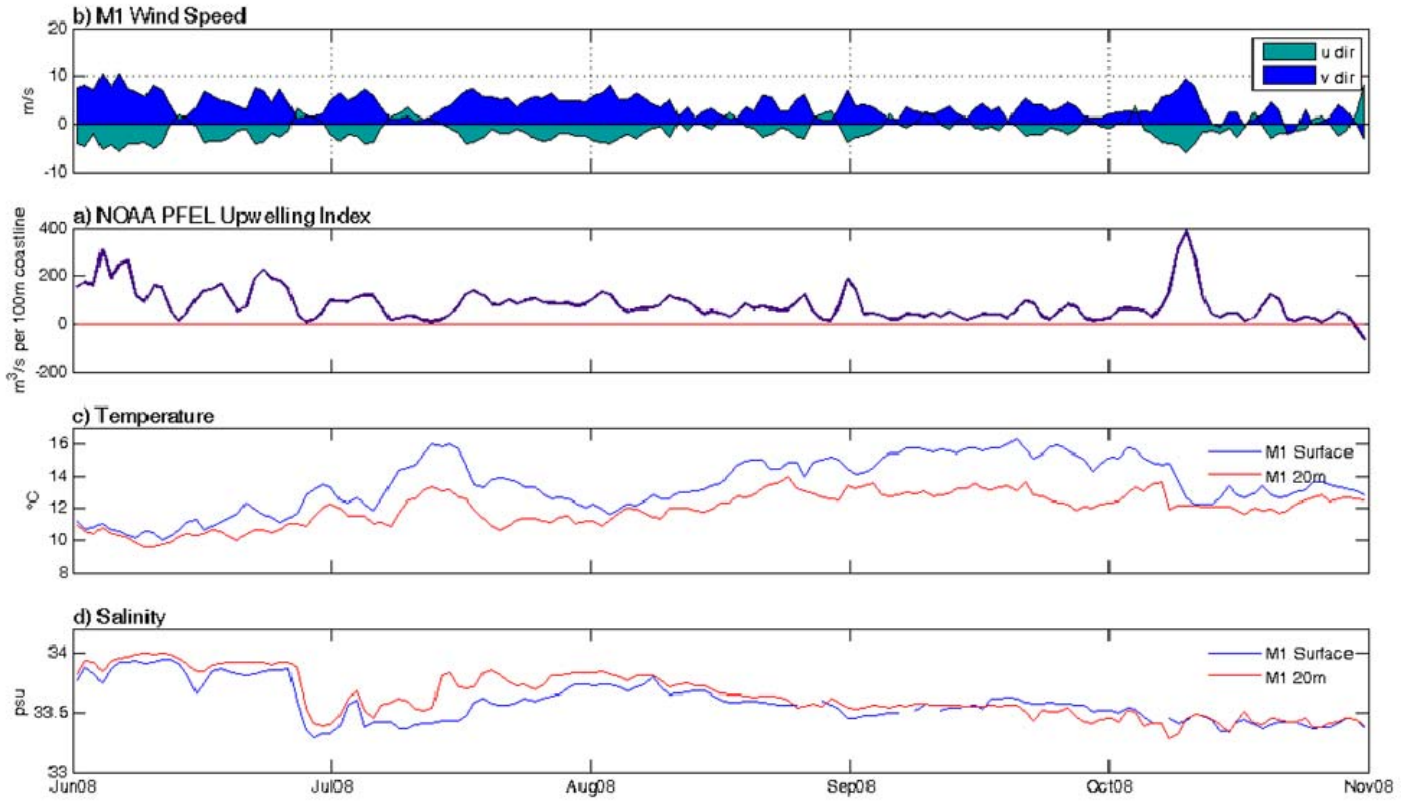

Figure 25: M1 winds (a), NOAA PFEL upwelling index (b), M1 temperature (surface and deep) (c), and M1 salinity (surface and deep) (d) from June – November, 2009.

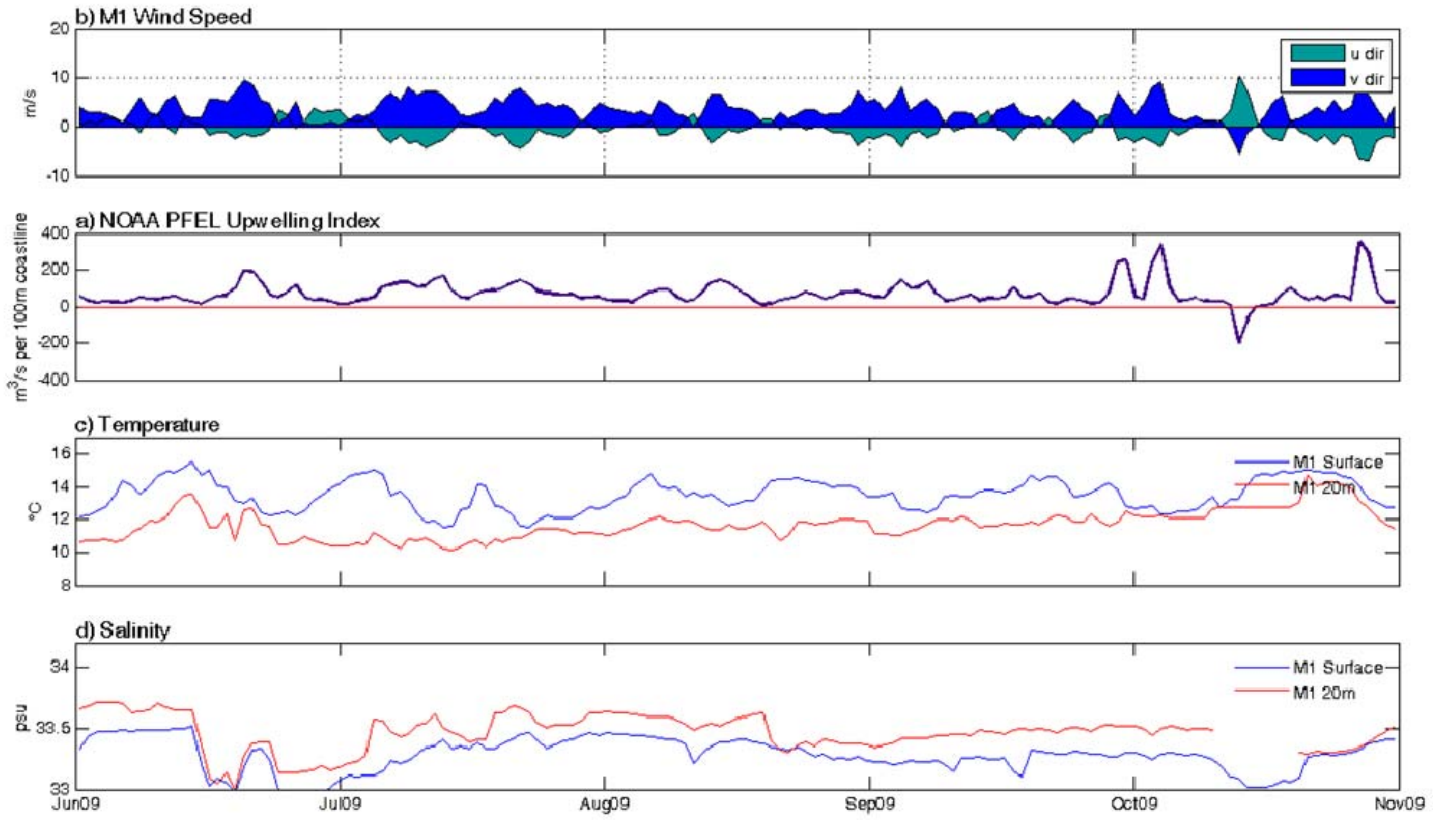

Figure 26: a) Summer temperature at mooring L20, surface and deep. b) Daily averaged temperature at mooring L20, surface and deep. Red line depicts temperature threshold for defining upwelling days. c) Vertical temperature difference between surface and deep nodes at mooring L20. Red line depicts threshold for defining upwelling days. d) Daily averaged nitrate concentration at depth, mooring L20. Red circles denote upwelling days, as defined by the two threshold conditions.

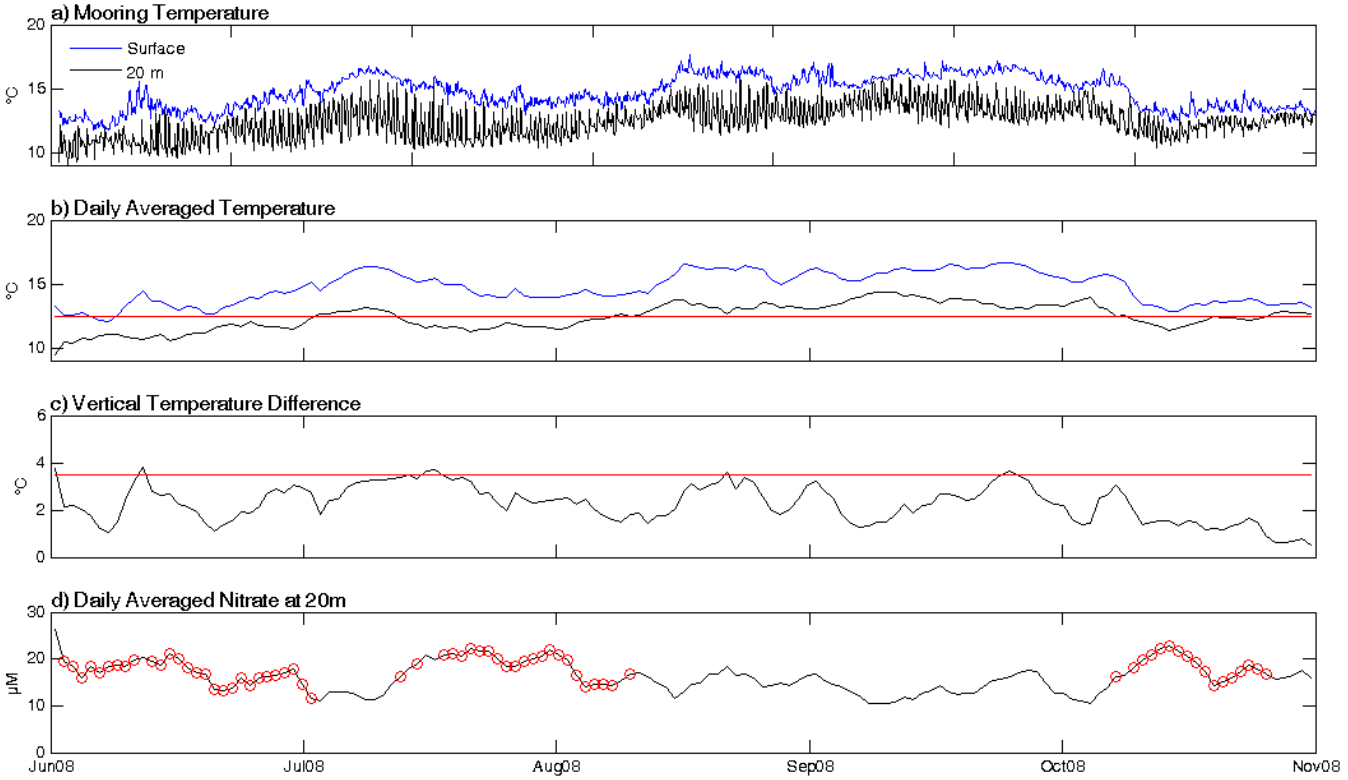

Figure 27: a) Summer temperature at mooring L20-2, surface and deep. b) Daily averaged temperature at mooring L20-2, surface and deep. Red line depicts temperature threshold for defining upwelling days. c) Vertical temperature difference between surface and deep nodes at mooring L20-2. Red line depicts threshold for defining upwelling days. d) Daily averaged nitrate concentration at depth, mooring L20-2. Red circles denote upwelling days, as defined by the two threshold conditions.

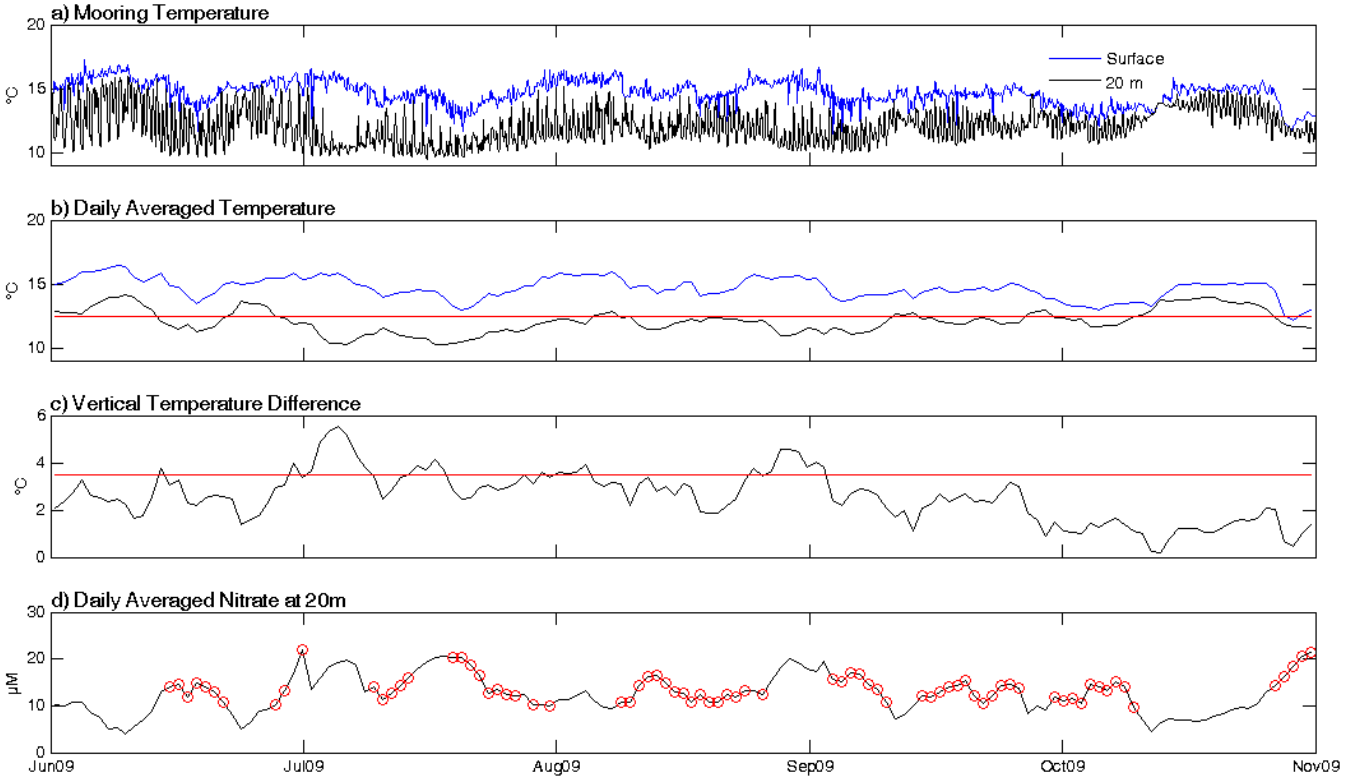

Loading results for both approaches are displayed in Figure 28. Average daily nitrate transport from upwelling using the PFEL method was 4.938×10^4 and 4.858×10^4 kmol/d for the summers of 2008 and 2009, respectively. Total integrated loads using this method were 7.061×10^6 and 6.946×10^6 kmol for the summers of 2008 and 2009, respectively. Using the LOBO method, nitrate transport during observed upwelling days averaged 5.609×10^4 and 4.425×10^4 kmol/d for the summers of 2008 and 2009, respectively. Total integrated nitrate load for the summer of 2008 and 2009 using this method were 3.820×10^6 and 3.306×10^6 kmol, respectively.

Figure 28: Nitrate transport to Monterey Bay from coastal upwelling during June - November, 2008 (top panel) and 2009 (bottom panel).

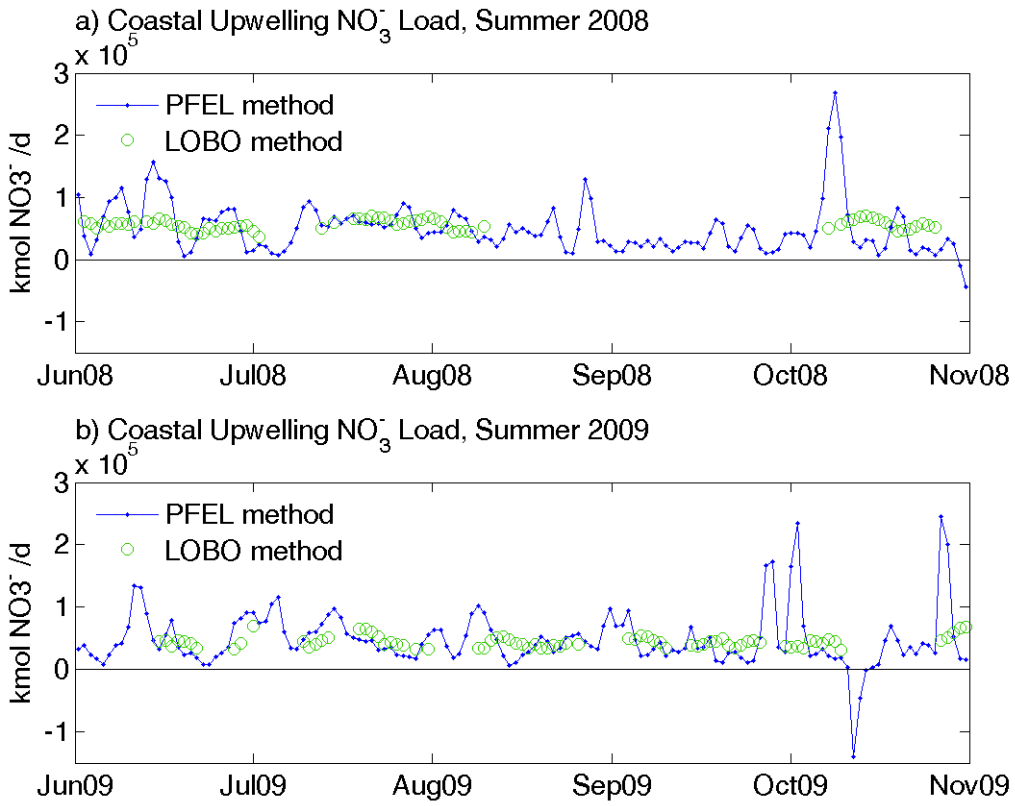

3.2.4 Nitrate Transport from Internal Waves

In addition to coastal upwelling, internal waves have been documented as an important mechanism for transporting nitrate from depth to inner-shelf surface waters along the California coast and Monterey Bay (Lucas et al, 2011; McPhee-Shaw et al, 2007; Carroll, 2009; Shea & Broenkow 1982). The high-frequency variability demonstrated by the spectral results in Section 3.3.1 is primarily due to internal wave events, driven by the internal tide, although wind-driven baroclinic motions can also contribute to such variability. Examples of coupled temperature – nitrate oscillations due to internal waves at moorings L20 and L20-2 are shown in Figures 29-30 for June 24 – July 1 of 2008 and August 2 - 9, 2009, respectively. Average flux convergences ($d[NO_3]/dt$) for each week (2008 and 2009) were 0.336 and 1.341 μM/d, respectively.

In order to calculate the total amount of nitrate transported to surface waters from internal waves over each season, each transport rate calculated above was multiplied by the total number of days exhibiting internal wave activity throughout each season. Internal wave days were defined as having an average daily temperature variance at depth greater than 0.5 °C within the 0.9 – 2.2 cpd frequency band (Figures 31-32). 62 "internal wave days" were observed during the 2008 summer season, versus 87 in the 2009 summer season. This leads to a total integrated transport of 2.08×10^{-8} kmol/L and 1.17×10^{-7} kmol/L nitrate from internal wave activity in 2008 and 2009 respectively.

Figure 29: Nitrate concentration (a) and temperature (b) at mooring L20, surface and deep, from June 24 – July 1, 2008.

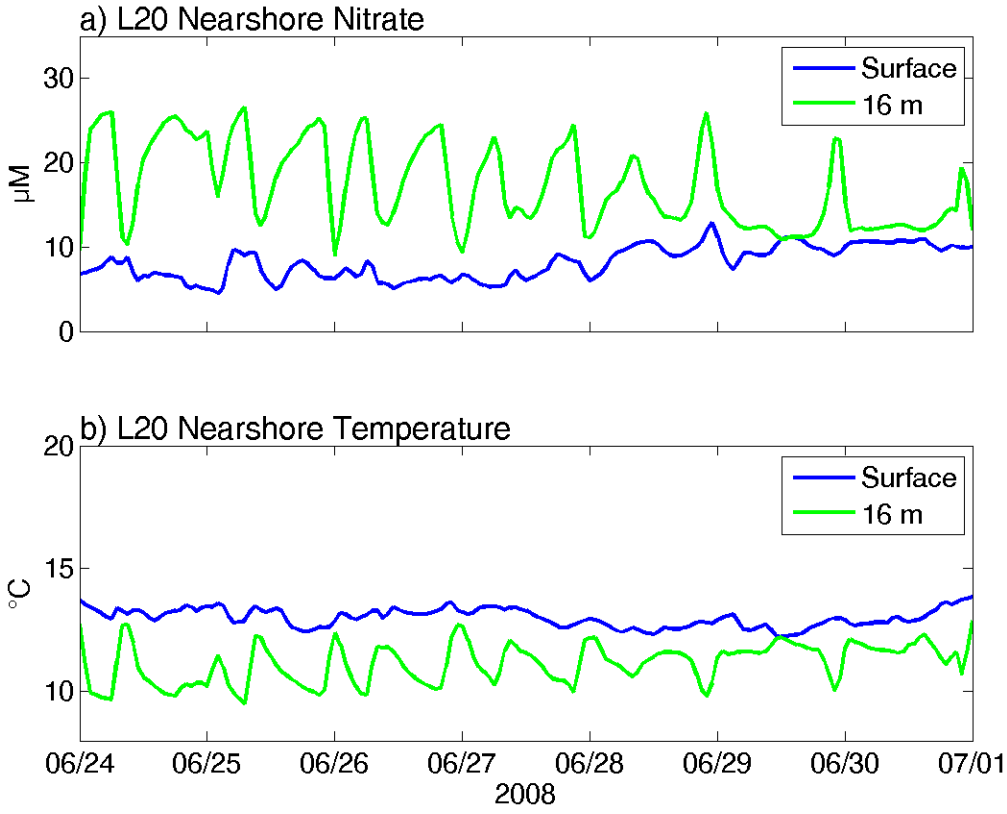

Figure 30: Nitrate concentration (a) and temperature (b) at mooring L20, surface and deep, from August 2 -9, 2009.

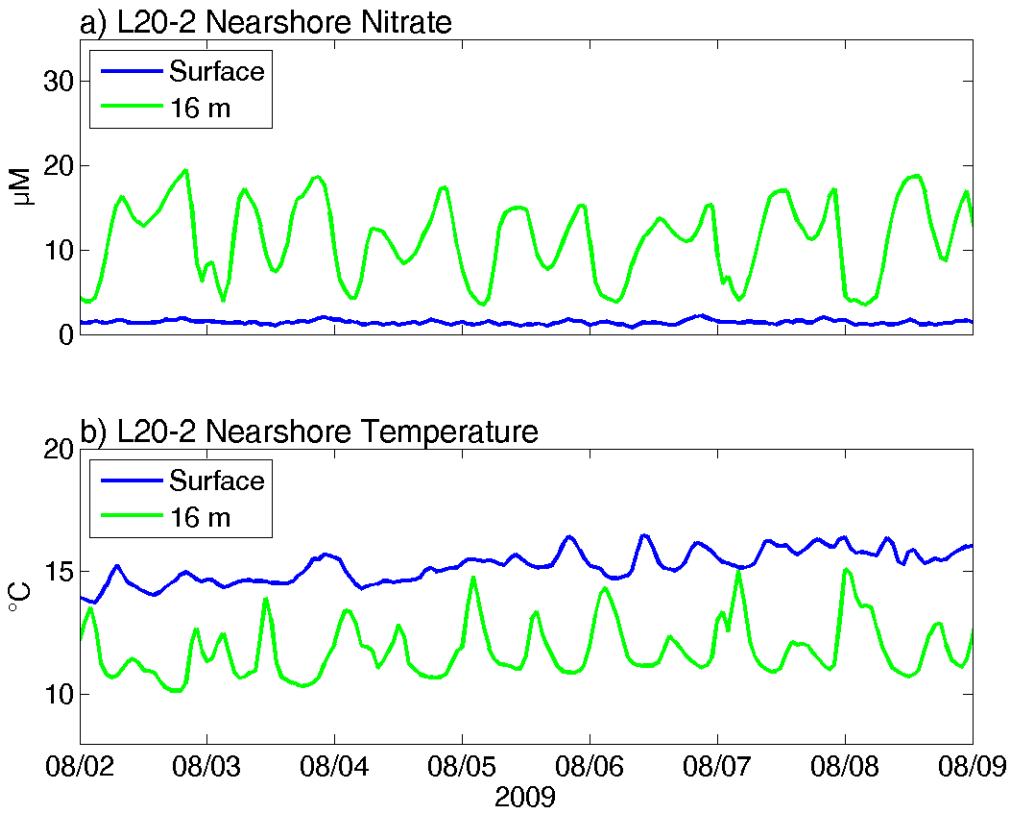

Figure 31: Unfiltered temperature data (a) and daily temperature variance within the 0.45 – 1.1 d frequency band (b) at mooring L20, deep node. Red line denotes threshold for defining internal wave days.

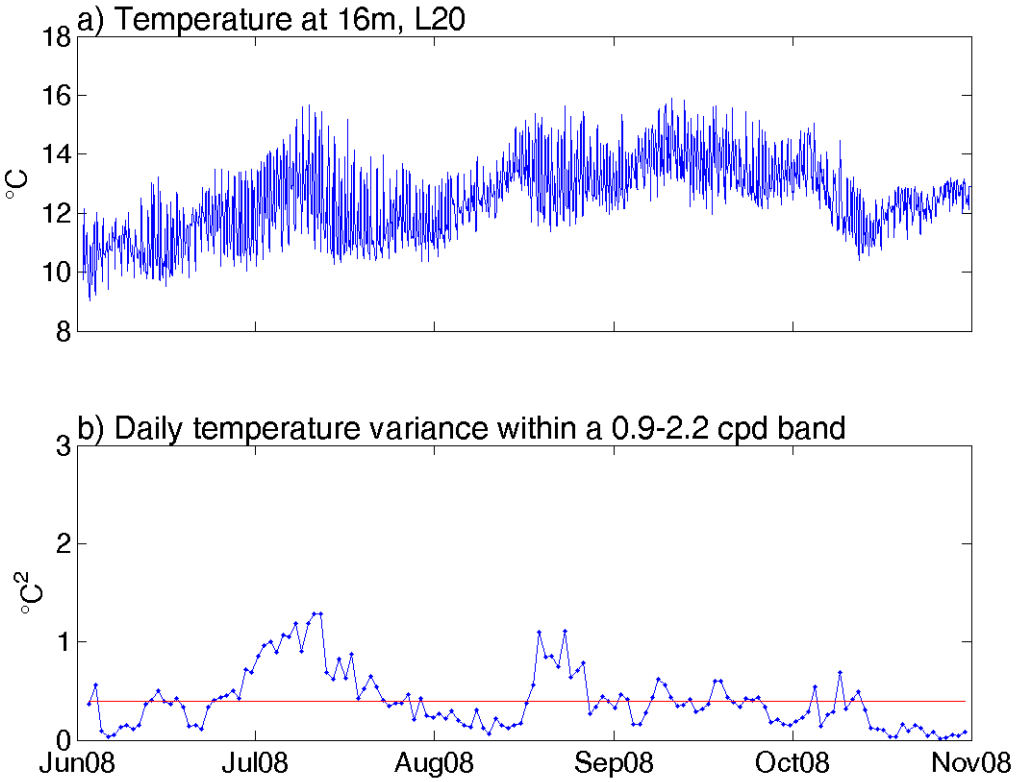

Figure 32: Unfiltered temperature data (a) and daily temperature variance within the 0.45 – 1.1 d frequency band (b) at mooring L20-2, deep node. Red line denotes threshold for defining internal wave days.

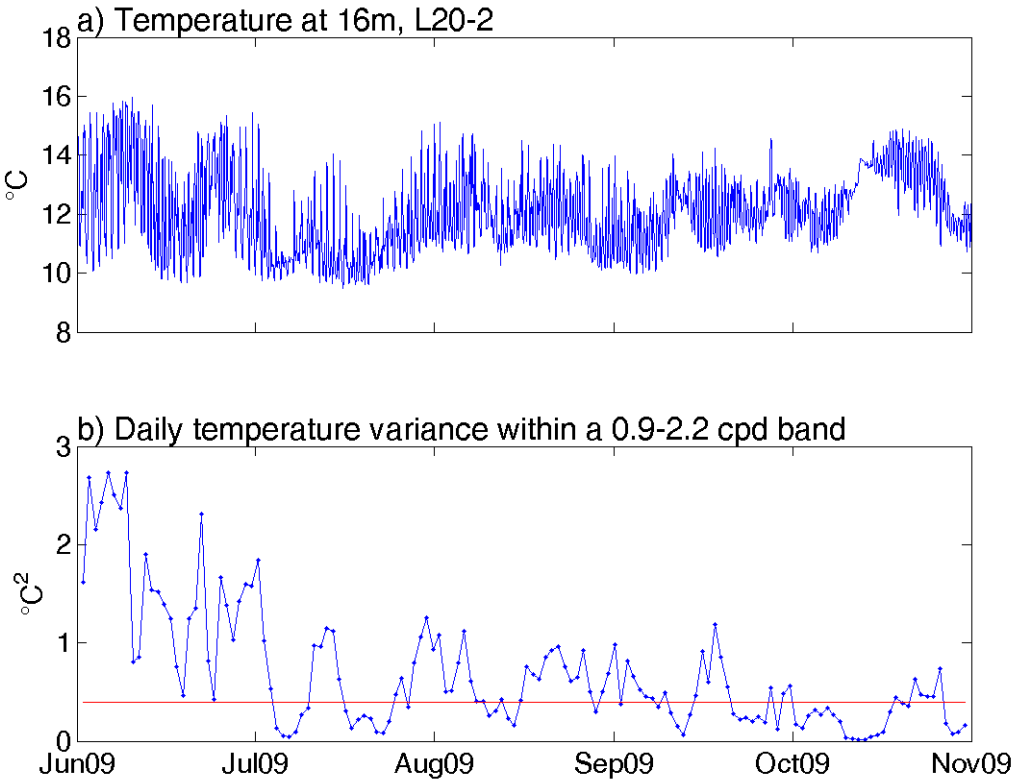

3.3 Nearshore Monterey Bay Surface Nitrate Variability

3.3.1 Nearshore Mixing Model

In the previous sections, terrestrial nitrate transport to Monterey Bay from Elkhorn Slough (ES), coastal upwelling and internal waves were estimated for two summers covering the study period. Nitrate transport from ES during the winter months was also examined for comparative purposes. However, in order to more carefully assess the relative impact of terrestrial nitrate loading from ES on nearshore surface waters, the nearshore region of impact must be more thoroughly constrained.

Thus, we may ask the following questions: (1) what is a reasonable mixing volume for nearshore surface waters in connection with the ES discharge plume? (2) Accounting for this volume, what is the maximum change in nitrate over time (dC/dt) possible due to discharge from ES? (3) Can this dC/dt be resolved by ISUS technology at nearshore LOBO moorings?

Since Elkhorn Slough is an estuarine lagoon, its discharge dynamics are largely governed by tidal pumping, as opposed to direct riverine flow. Therefore, some of the mixing occurring between stream load inputs and ocean water occurs inside the estuary. Without a comprehensive description or model of mixing processes occurring within ES (ie between the slough's main channel and Old Salinas River channel), loading and nearshore box-volume estimates can be used as a conservative approach to approximating changes in nearshore nitrate concentrations in response to interactions with ES discharge. According to Broenkow and Breaker, 2005, the amount of ocean water exchanged with ES over a single tidal cycle, the "tidal prism", is 6.2×10^6 m^3. This

value provides a good baseline, although the nearshore mixing volume may be further constrained by considering the physical characteristics of the tidal discharge plume.

In a 2009 study, Andrew Fischer used data from a surface underway mapping system (UMS), an automated underwater vehicle (AUV), drifters, moorings, and the Moderate Resolution Imaging Spectroradiometer (MODIS) to characterize the discharge plume of Elkhorn Slough. Fischer found that, generally, the ES discharge plume extends ~1km offshore to the southwest, with a width of approximately 1km and a depth of 5-10 m. The plume can be described as 'jet-like' in nature, advection-dominated and influenced primarily by inertial effects (Fischer, 2009). According to Warrick et al (2004), such jet-like structures "encourage rapid mixing with ambient coastal waters immediately upon discharge". It can thus be assumed that estuarine discharges from ES are mixed evenly in near shore coastal waters, with effects extending a distance beyond the dimensions of the discharge plume.

Figure 33 depicts three areal mixing scenarios for ES and near shore Monterey Bay surface waters, using LOBO moorings L20 and L20-2 locations for constraining maximum offshore distance: (1) plume influence is predominantly to the north, extending 2.5 km up the coast and 1.5 km offshore, (2) plume influence is predominantly to the south, with similar dimensions, (3) plume is evenly mixed north and south of the harbor. It is probable that the ES discharge plume excursion and mixing area exhibits variable behavior, with dimensions most likely falling somewhere in between the range encompassed above, that is, between 3 and 15 km^2. Mixing volumes become further constrained with depth estimates for vertical mixing. Here a vector of possible depths is

also most appropriate, which can be arrived at through consideration of different values for vertical eddy diffusivities. Using a lower bound of 10^{-5} m^2/s for open ocean eddy diffusivity (Munk, 1966), and an upper bound of 10^{-3} m^2/s for eddy diffusivity near the Monterey Submarine Canyon (Kunze et al, 2001), and assuming mixing occurs over a semidiurnal the tidal period, we get upper and lower mixing depth limits of [2.1 and 6.6] m. As a conservative measure, and considering the depth range of the discharge plume, a final depth vector of [2 5 10 20] m can be applied.

Using these dimension vectors, a final matrix of possible mixing volumes is considered (Table 4). Considering this range of possible mixing constraints, and assuming a 2μM/hr detection limit for ISUS technology, we can calculate a final matrix of minimum nitrate transport values necessary for detection at nearshore LOBO moorings (Table 5). Even with lower-bound estimates for mixing dimensions, Table 5 indicates that at least 288 kmol/d nitrate transport out of ES is necessary for detection at the mooring. As outlined in Section 3.1.2, daily rates of nitrate transport greater than 200 kmol/d are rarely observed during the summer season in the ES system.

Figure 33: Possible areal mixing scenarios for nearshore surface waters and the Elkhorn Slough discharge plume.

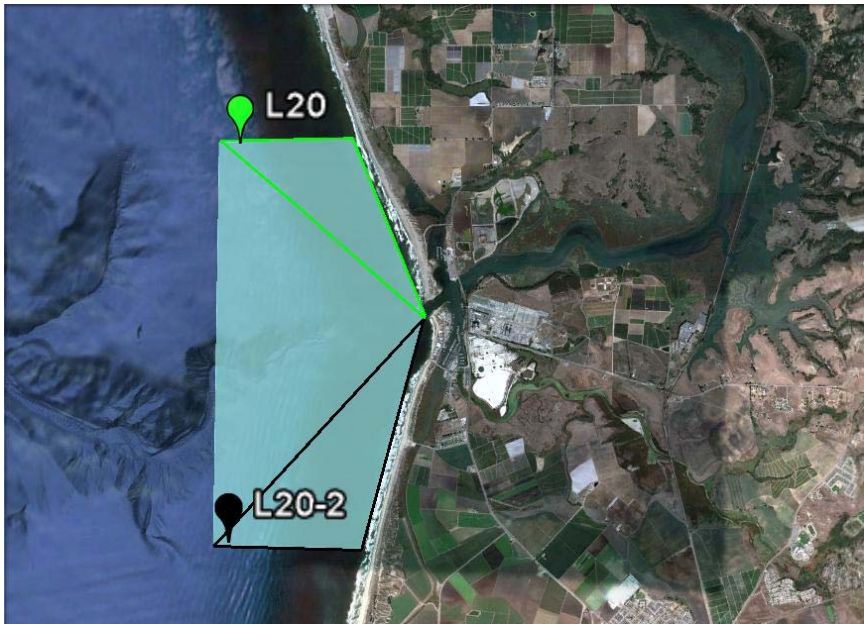

Table 4: Matrix of possible mixing volumes (in m3)

Possible Mixing Areas	Possible Mixing Depths			
	2 m	**5 m**	**10 m**	**20 m**
$3x10^6$ m^2	$6.0x10^6$ m^3	$1.5x10^7$ m^3	$3.0x10^7$ m^3	$6.0x10^7$ m^3
$8x10^6$ m^2	$1.6x10^7$ m^3	$4.0x10^7$ m^3	$8.0x10^7$ m^3	$1.6x10^8$ m^3
$15x10^6$ m^2	$3.0x10^7$ m^3	$7.5x10^7$ m^3	$1.5x10^8$ m^3	$3.0x10^8$ m^3

Table 5: Matrix of minimum daily transport required for detection at LOBO nearshore moorings, assuming 2μM/hr detection limit and possible mixing dimensions outlined above in Table 4. Units are in kmol/d.

Possible Mixing Depths

Possible Mixing Areas	2 m	5 m	10 m	20 m
$3x10^6$ m^2	288	720	1440	2880
$8x10^6$ m^2	768	1920	3840	7680
$15x10^6$ m^2	1440	3600	7200	14400

3.3.2 Nearshore Mooring Observations

Nearshore oceanographic observations from LOBO moorings L20 (surface and deep, June – November, 2008) and L20-2 (surface and deep, June – November, 2009) are presented in Figures 34 – 35. Surface hydrography and associated nitrate concentrations at each mooring exhibit high-frequency and low-frequency variability, a response to both internal wave and coastal upwelling transport mechanisms. Terrestrial nitrate transport can also potentially influence inner-shelf nitrate variability at tidal timescales (from tidal discharge plumes) and subtidal time scales (from episodic runoff events). However, as described in the previous section, low stream flow makes terrestrial transport during the summer season difficult to resolve, and requires a more in-depth analysis of hydrographic and nutrient mooring data.

Summary statistics for each mooring parameter are shown in Tables 6-9. Distinct differences are observable between the two mooring time-series, as is evident in the parameter statistics. Nitrate maximum and range at each depth were greater at mooring L20-2 (south of the harbor, 2009), while average nitrate values were greater at L20 (north of the harbor, 2008). Temperature and salinity ranges were also greater at L20-2, suggesting greater variance overall at mooring L20-2 than at L20.

Summary statistics outlined in Tables 6-9 provide a general synopsis of background coastal oceanographic conditions in Monterey Bay during each summer of 2008 and 2009. However, for insight into the dynamics of nitrate variability at these two locations, and in order to hone in on magnitude and frequency of different source inputs, a more in-depth analysis of this time-series is required.

Figure 34: Nitrate (a), temperature (b), and salinity(c) at LOBO nearshore mooring L20 (3km north of Moss Landing Harbor, and 1.5 km offshore), surface (blue) and 16 m depth (red).

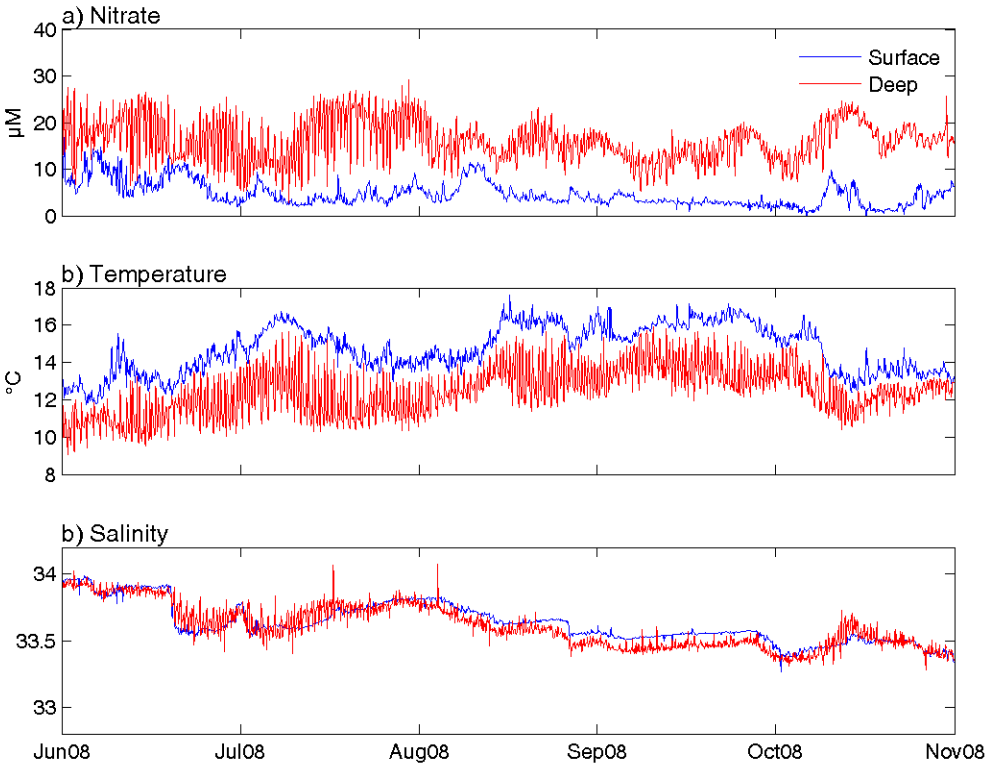

Figure 35: Nitrate (a), temperature (b), and salinity(c) at LOBO nearshore mooring L20-2 (3km south of Moss Landing Harbor, and 1.5 km offshore), surface (blue) and 16 m depth (red).

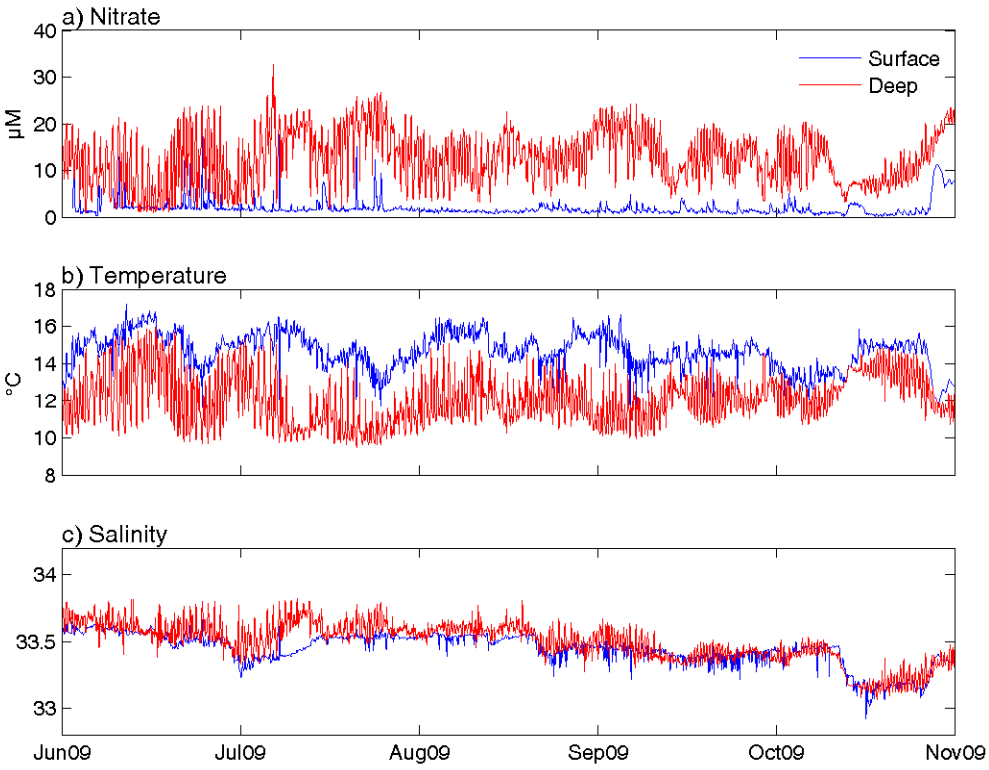

Table 6: Parameter statistics for nearshore mooring L20 (June – November, 2008), surface array.

	Min	Max	Mean	Std Dev	Range	Mean Highest 5%
Nitrate	0	16.8	4.7	2.6	17.4	11.5
Salinity	33.2	34.0	33.6	0.2	0.8	33.9
Temperature	11.8	17.6	14.7	1.3	5.9	16.7

Table 7: Parameter statistics for nearshore mooring L20-2 (June – November, 2009), surface array.

	Min	Max	Mean	Std Dev	Range	Mean Highest 5%
Nitrate	0	34.7	2.9	4.2	34.8	18.0
Salinity	29.3	33.7	33.1	0.5	4.3	33.6
Temperature	10.5	17.2	13.9	1.1	6.7	16.1

Table 8: Parameter statistics for nearshore mooring L20 (June – November, 2008), deep array.

	Min	Max	Mean	Std Dev	Range	Mean Highest 5%
Nitrate	0	16.9	4.7	2.6	17.5	11.5
Salinity	33.2	34.0	33.6	0.2	0.8	34.0
Temperature	11.8	17.6	14.7	1.3	5.9	16.7

Table 9: Parameter statistics for nearshore mooring L20-2 (June – November, 2009), deep array.

	Min	Max	Mean	Std Dev	Range	Mean Highest 5%
Nitrate	0	34.7	3.9	4.2	34.8	18.0
Salinity	29.3	33.7	33.1	0.5	4.3	33.6
Temperature	10.5	17.2	13.9	1.1	6.7	16.1

3.3.3 Identification of Terrestrial Signals

As outlined in Section 3.3.1, detection of terrestrial-sourced nitrate using high-frequency, in-situ nitrate sensors alone is limited by seasonally low transport values, large mixing volumes and subsequent dilution with coastal ocean waters. Thus, an additional approach was considered in the investigation of summertime nearshore water mass interaction between the Elkhorn Slough system and Monterey Bay. Property plots were used to map the temperature-salinity (T-S) signatures of slough and ocean waters. Because temperature and salinity are conservative properties, T-S diagrams can be useful tools for characterizing water mass interaction. Figure 36 maps summer temperature and salinity signatures for Elkhorn Slough and Monterey Bay waters. Inner-shelf moorings L20 (2008) and L20-2 (2009) exhibit surface temperature and salinity characteristics within ranges observed at MBARI surface mooring M1, exemplifying the influence of offshore Monterey Bay waters. Deep mooring locations have colder temperatures, while Old Salinas River water exhibits a fresher signature, a result of summer freshwater irrigation runoff. The influence of both OSR and coastal ocean water on ES's main channel is also apparent in these plots, a result of tidal forcing. High salinities observed in ES are a result of interaction with hypersaline waters in the upper slough, a typical summer condition due to lack of flow and long residence times in that region.

The summer salinity anomaly in upper ES, as well as the large region of overlap between ES, coastal Monterey Bay and offshore Monterey Bay ocean water in these plots, makes it difficult to identify nearshore terrestrial signals with this method.

Summer discharge volumes from Old Salinas River are not large enough to significantly affect the hydrographic signature of nearshore coastal waters.

Figure 36: Temperature-salinity plot for select moorings in Elkhorn Slough and Monterey Bay from June - November, 2008 (a) and 2009 (b).

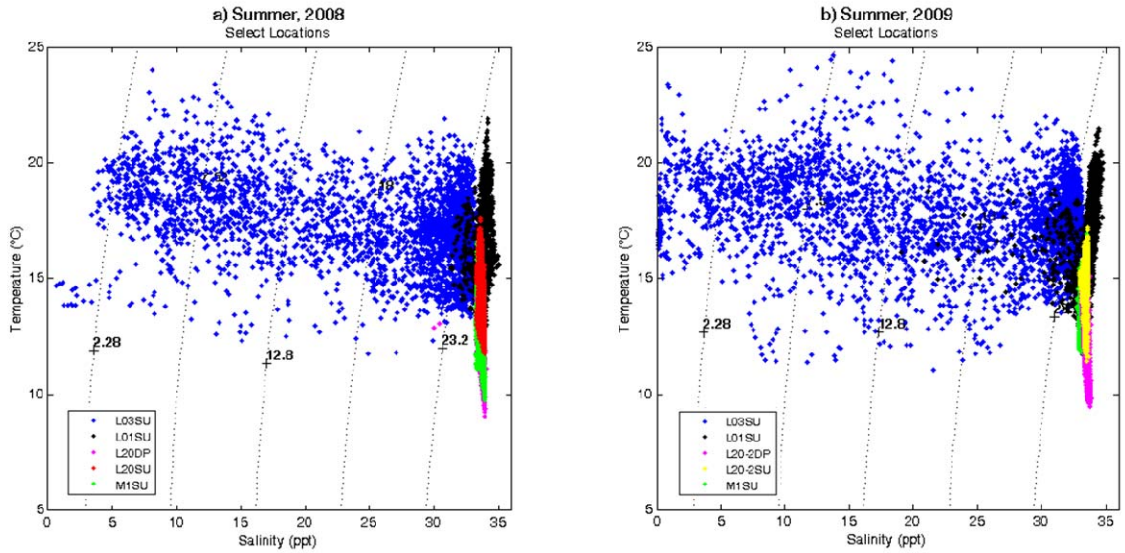

For comparison to summer conditions, Figure 37 shows temperature-salinity characteristics for the same water masses during the winter of 2009 (data from winter, 2008 not available). Temperatures for all water masses are, on average, 5 degrees colder than during the summer seasons. It is interesting to note that while M1 surface and L20 deep water masses exhibit salinities similar to summer conditions, surface waters in ES (L01) and coastal Monterey Bay (L20-2) are significantly more fresh, exhibiting salinity values < 30 at times. This can be attributed to increased precipitation and associated volumes of freshwater discharge. The effect on nearshore nitrate concentrations is apparent as well. Figure 38 depicts time-progressive property plots for temperature-

salinity, and salinity-nitrate at LOBO surface mooring L20-2 from June, 2009 to May, 2010. Increases in nitrate coincide with drops in salinity beginning in late December through March. Again, during the summer months (blue) salinity remains within a narrow range, dropping below 33 for a short time in October, a possible freshwater signal. Nitrate and temperature exhibit a large range during this time (also outlined in Table 7), which is a response to internal wave forcing.

Figure 37: Temperature-salinity plot for select moorings in Elkhorn Slough and Monterey Bay from November, 2009 - March, 2010.

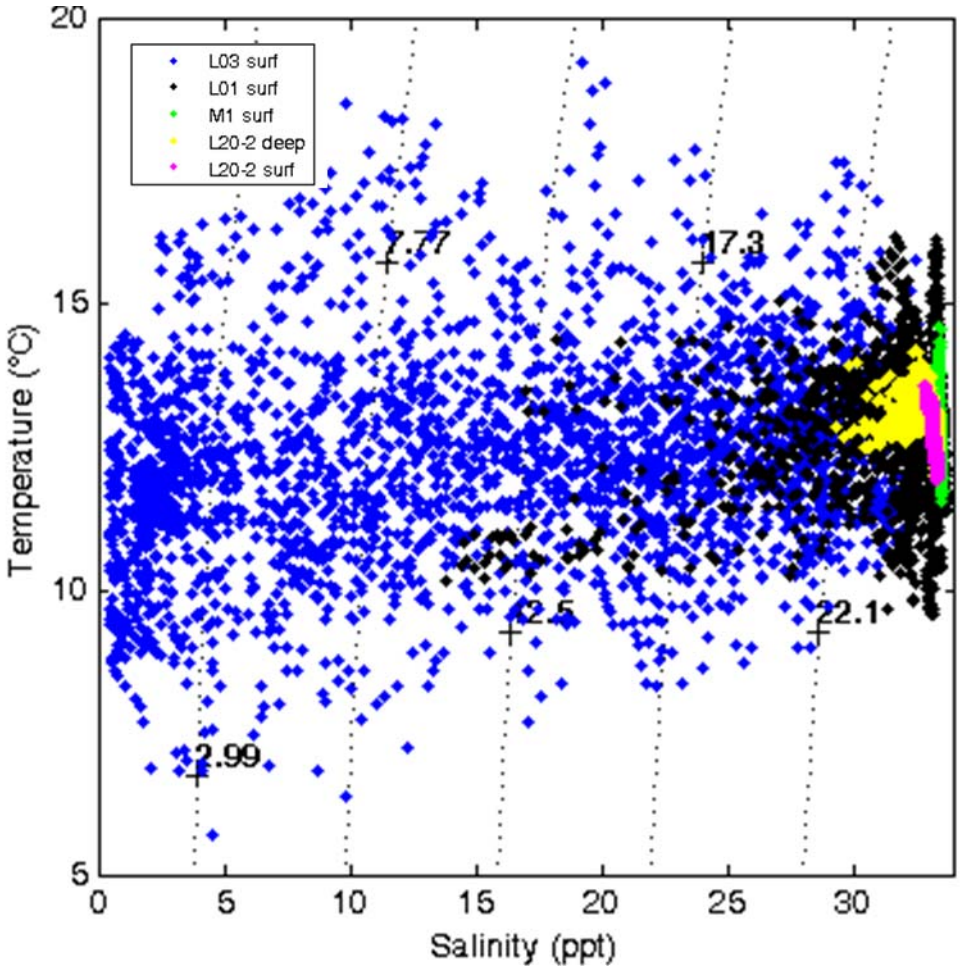

Figure 38: Temperature-salinity (a) and salinity-nitrate (b) time-progressive scatter plots for LOBO surface mooring L20-2 (June, 2009 – May, 2010).

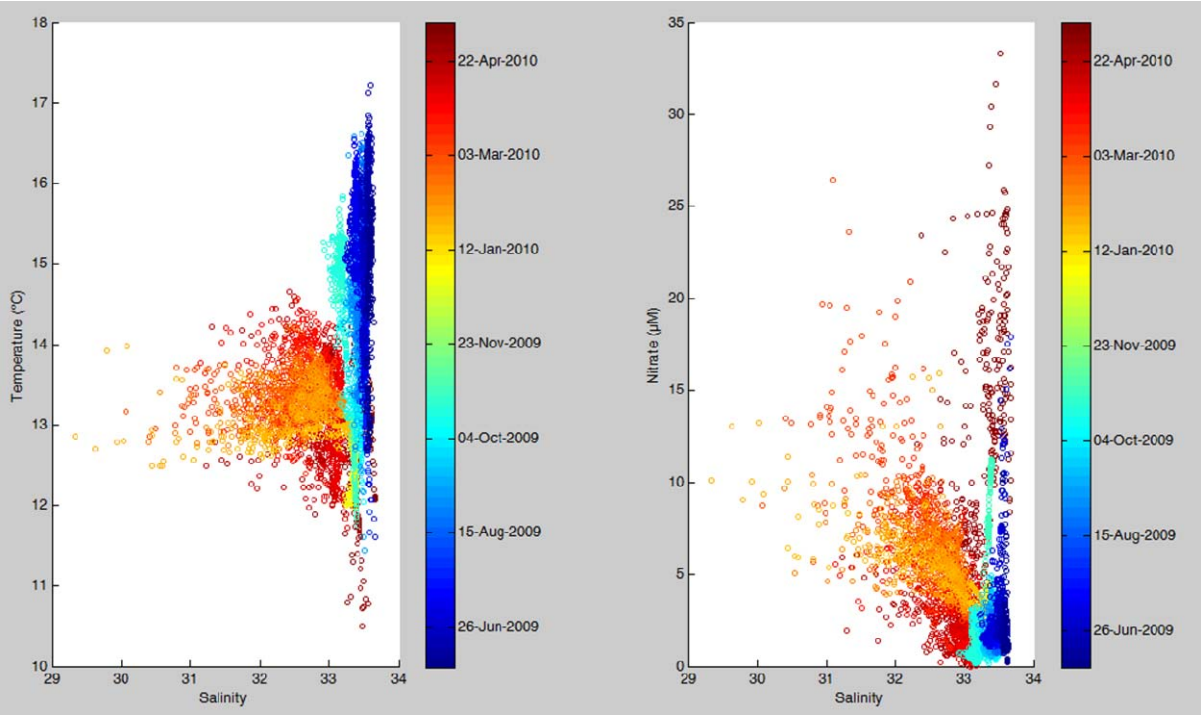

3.3.4 Surface Mapping of the Elkhorn Slough Summer Discharge Plume

Real-time monitoring during the first weeks of mooring L20-2 deployment revealed high frequency surface nitrate-pulses in the nearshore. The timing of the nitrate pulses observed at the mooring was coincident with low tides, suggesting a possible influence from the ebbing Elkhorn Slough discharge plume (Figure 39). Thus, investigation of the spatial expression of the surface nitrate peaks at mooring L20-2 was undertaken using MLML's portable underway data acquisition system (UDAS) in an attempt to derive any relationship between the observed high-frequency nitrate pulses and tidal discharge from nearby Elkhorn Slough.

Figure 39: Surface nitrate at mooring L20-2 (a) and Moss Landing tidal stage (b) during the early summer, 2009.

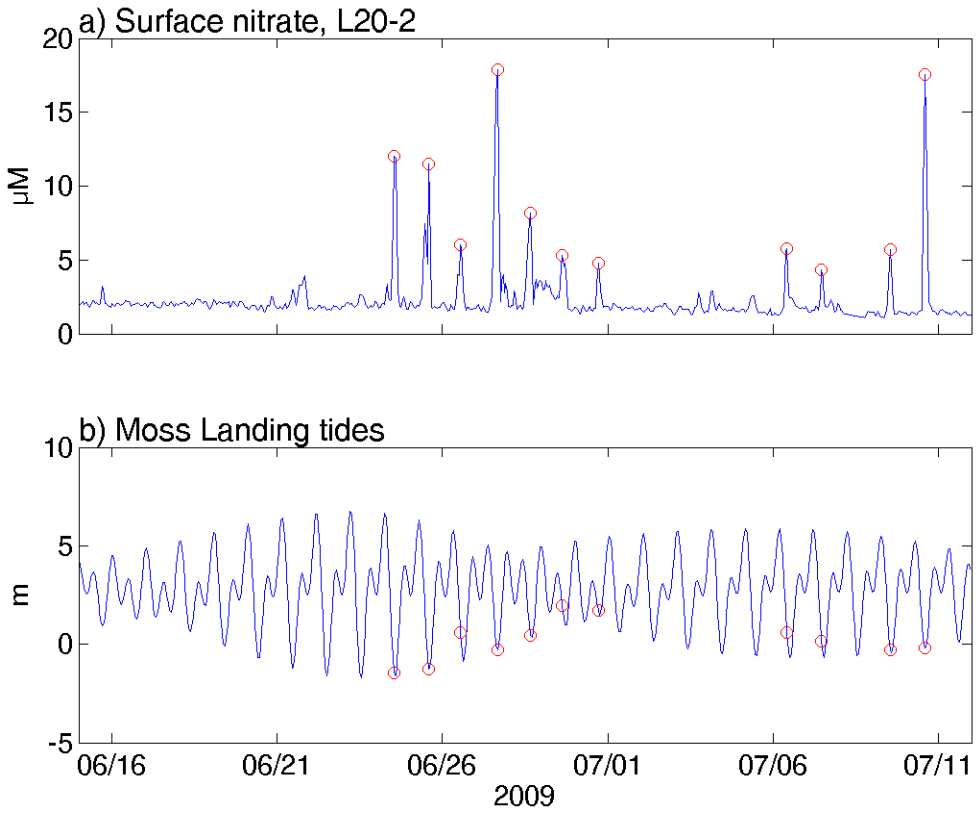

Several attempts were made to map the summer discharge plume from the harbor mouth toward LOBO mooring L20-2 during ebbing tides. The field program was designed in an attempt to distinguish the ES discharge plume: a turbid, high temperature, low salinity, high nitrate water mass, distinct from characteristics of surrounding ocean water. Figure 40 shows surface data acquired from the UDAS system on July 27, 2009, 05:29 – 07:57 PST. The tide reached 1.0 ft mean-lower-low water (MLLW) at 07:57 PST. Data from the UDAS sampling track shows the presence of a distinct water mass, although its hydrographic properties indicate cold, clear, high-salinity, high-nitrate water,

a possible deep water signature contrary to characteristics of the ES discharge plume. The underway system circled mooring L20-2 from 07:40 – 07:46 PST. Unfortunately, the hourly sample period of the mooring did not produce concurrent measurements with those taken by the UDAS. However, interpolated values for temperature and salinity at the L20-2 mooring were within one standard deviation of average measurements taken from the UDAS at the mooring location. Interpolated nitrate values were within two standard deviations. Despite the differences in measurement accuracy between the two instrumentation packages, the presence of the "plume-like" water mass detected by the UDAS coincides with the period of increasing nitrate at the mooring (Figure 41).

Figure 42 maps different water masses in the slough and nearshore environment using temperature-salinity (left) and temperature-nitrate (right) plots. LOBO mooring data represents measurements taken two weeks prior, as well as during, UDAS deployment. Data from the UDAS sample track is most representative of deep water, suggestive of possible canyon-head dynamics.

Figure 40: Fluorescence (a), turbidity (b), transmission (c), salinity (d), temperature (e), and nitrate (f) measurements taken during the July 27, 2009 UDAS field program. Strepresents the location of mooring L20-2.

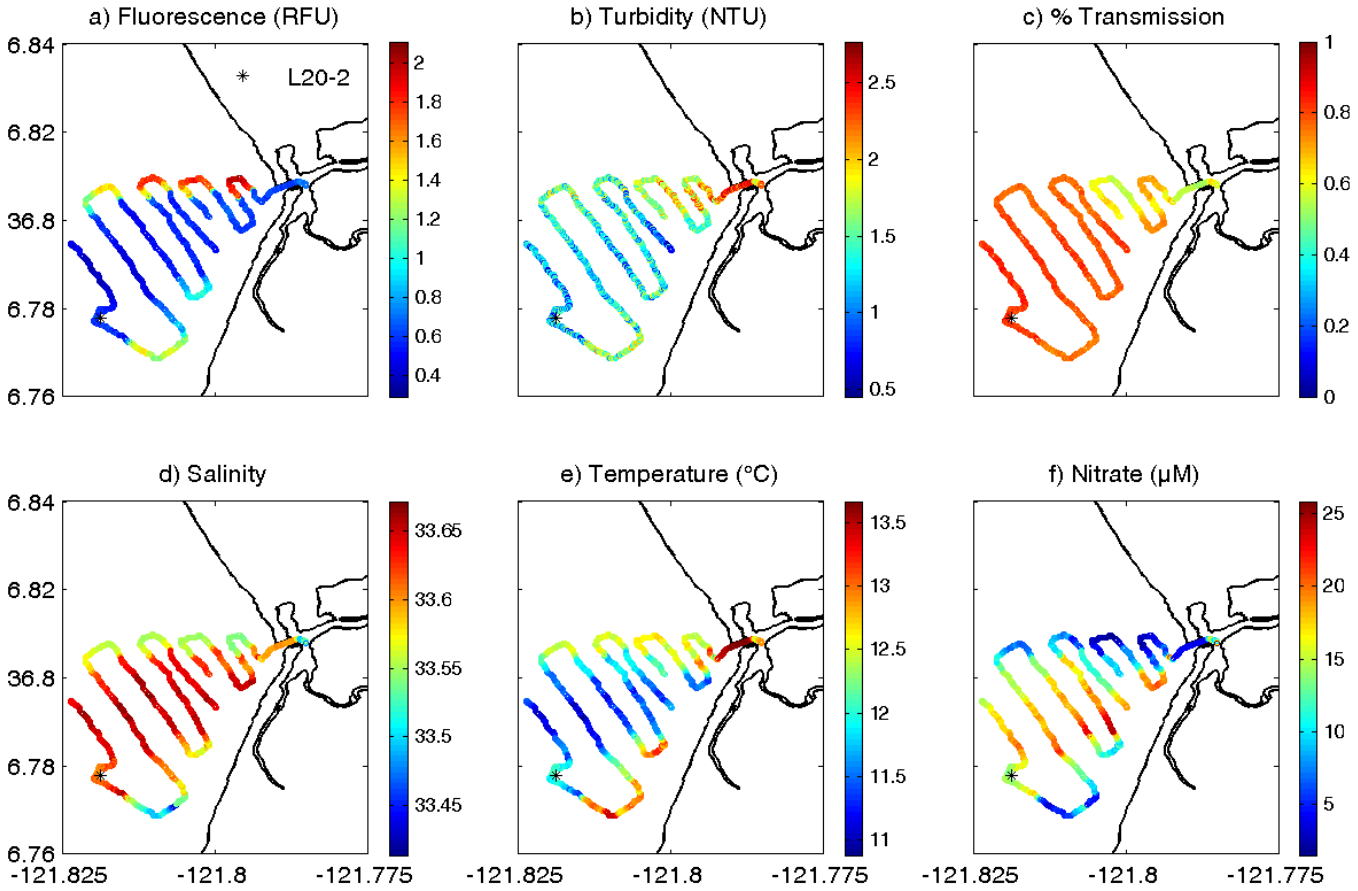

Figure 41: Nitrate (a), salinity (b), temperature (c), and chlorophyll (d) at mooring L20-2 from July 26 – July 29, 2009. Red fill denotes period of UDAS deployment. Times are in GMT.

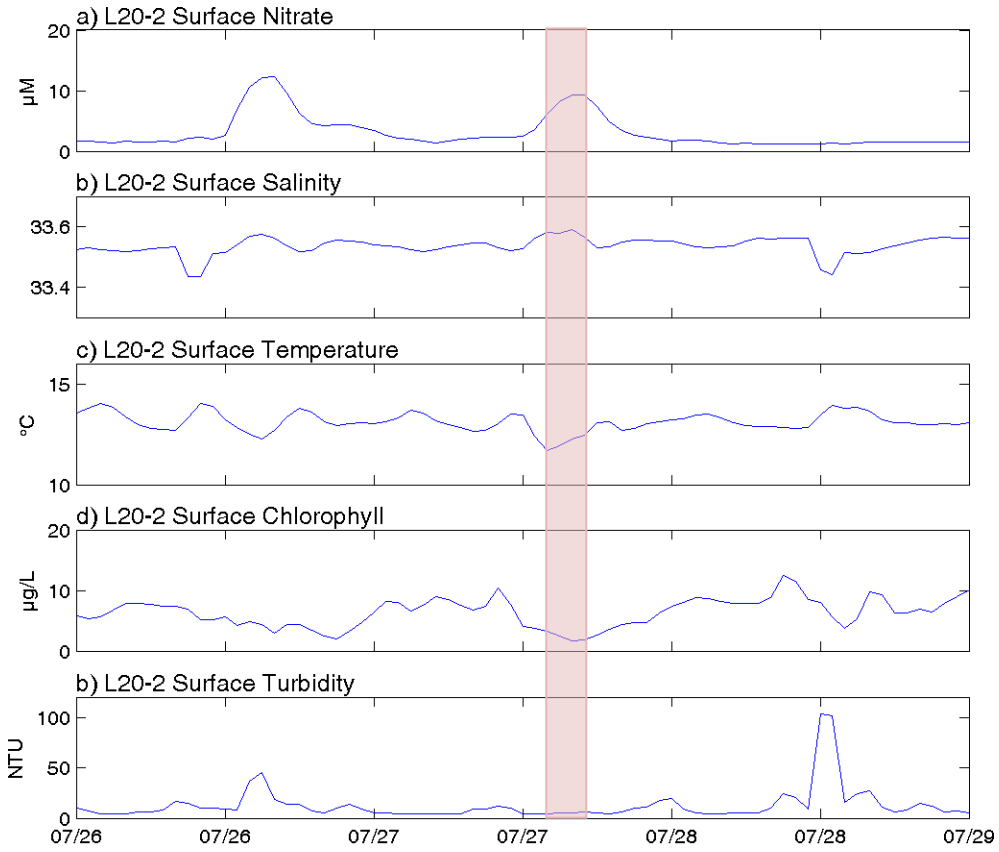

Figure 42: Temperature-salinity (left) and temperature-nitrate (right) property plots for water masses within ES and coastal Monterey bay (SU stands for surface, DP, deep). Yellow dots represent measurements taken during the UDAS deployment.

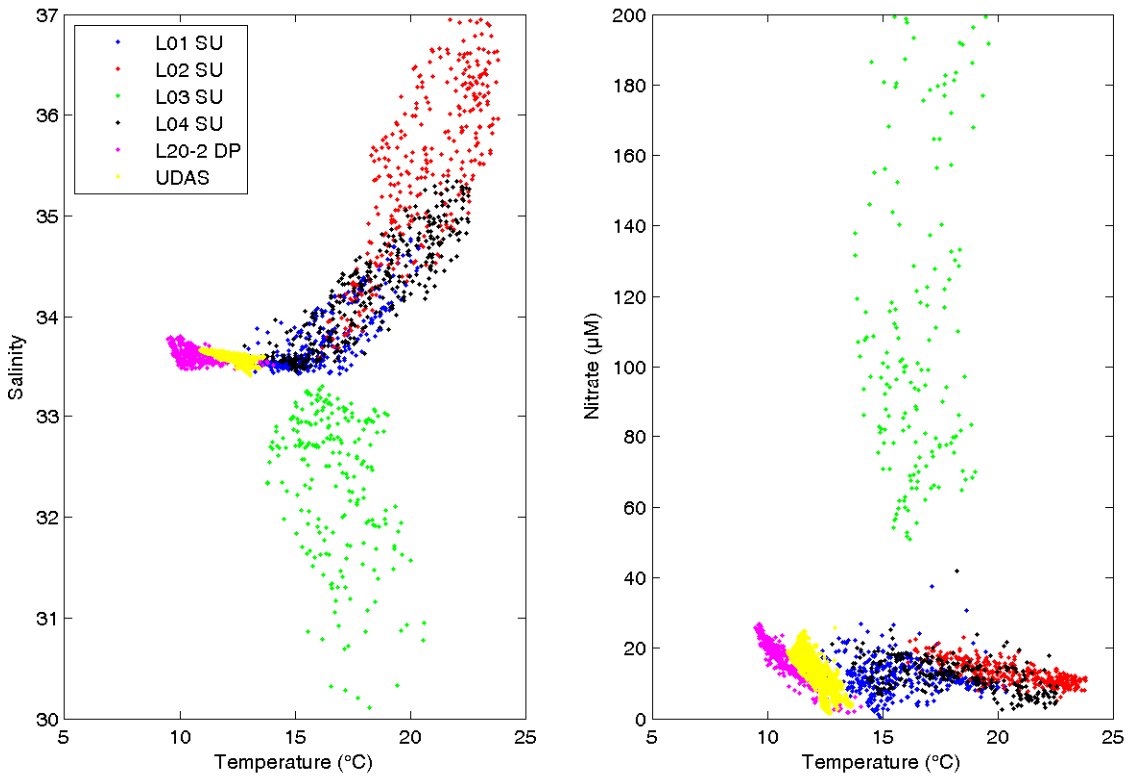

3.3.5 Terrestrial Runoff Event – "First flush, 2009"

The property plots in Section 3.3.3 reinforce the idea that the use of high-frequency in-situ instrumentation to detect terrestrial nitrate signals along the inner-shelf is dependent on magnitudes of freshwater discharge, despite high nitrate concentrations in nearby watersheds. Thus, the first rain event of the 2009 season, which occurred in early October, was chosen for an in-depth analysis of the nearshore response to an episode of elevated terrestrial loading. This was the largest precipitation event on record over the study period. 7.11 cm of rain fell on October 13, 2009 in Moss Landing (Figure 43-a), producing large volumes of runoff in surrounding watersheds leading to elevated stream flow and loading in Elkhorn Slough and Old Salinas River over the next two days. Stream flow in Old Salinas River increased by 7.9 m^3s^{-1} (a 24-fold increase), with a maximum of 8.23 m^3s^{-1} occurring on October 15 (Figure 43-b). Despite the mobilization of land-based nitrate by runoff, freshwater nitrate concentrations in OSR actually decreased due to the large volumes of freshwater entering the channel (Figure 43-c). However, the increase in stream flow was enough to cause transport in the channel to increase by 550 kmol/d (a 9-fold increase). Maximum nitrate transport occurred on October 14, halfway between the onset of precipitation and maximum (minimum) stream flow (freshwater nitrate concentration) (Figure 43-d).

Figure 43: Daily precipitation (a), and stream flow (b), nitrate concentration (c), and nitrate load (d) in OSR.

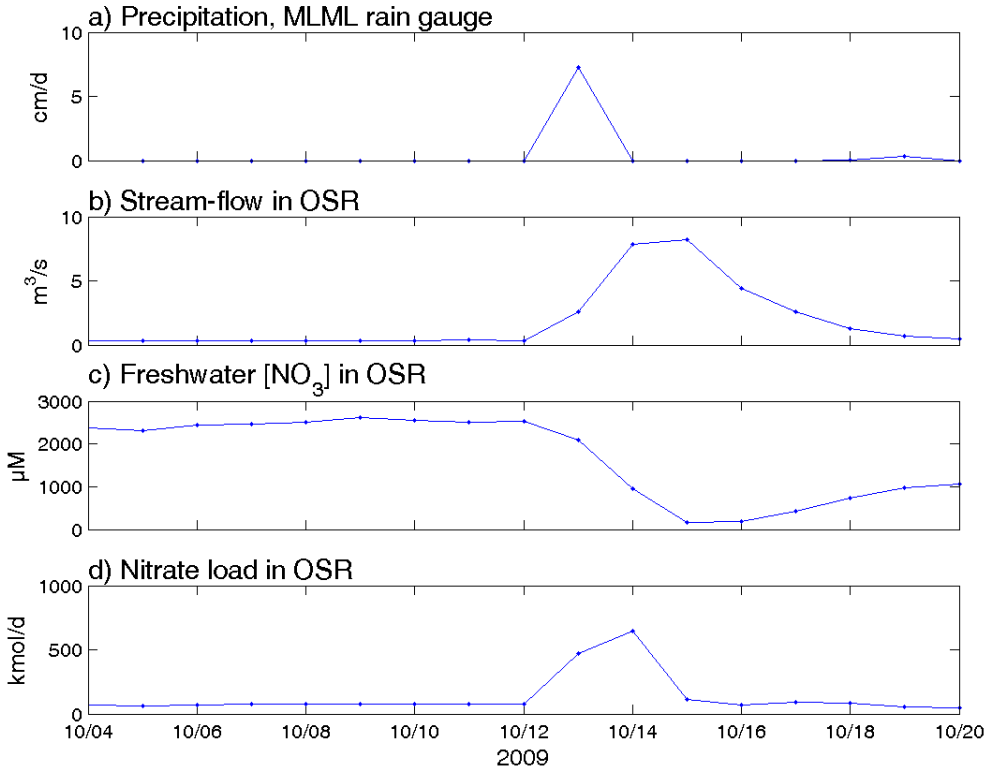

According to mixing model arguments outlined in Section 3.3.1, elevated volumes of stream flow and associated terrestrial nitrate transport out of OSR have the potential to affect surface nitrate variability along the inner-shelf. Figure 44 depicts hydrographic and nitrate conditions at LOBO inner-shelf mooring L20-2 (surface and 16m) from October 4 – 20, 2009 (the period surrounding the precipitation event). Gray fill denotes the period of precipitation. There are numerous things to note in this plot. Firstly, there was an approximate 2 µM increase in surface nitrate concentration following the precipitation event. Maximum surface nitrate concentration reached 3.1 µM two days after the storm (Figure 44-c). This time lag suggests that the signal was primarily due to terrestrial runoff. This is because land infiltration occurs

Figure 44: Temperature (a), salinity (b), nitrate concentration (c), and calculated density (d) at LOBO inner-shelf mooring L20-2 surface and deep (20m) during the period surrounding the 2009 "first-flush" precipitation event. Gray fill denotes period of precipitation.

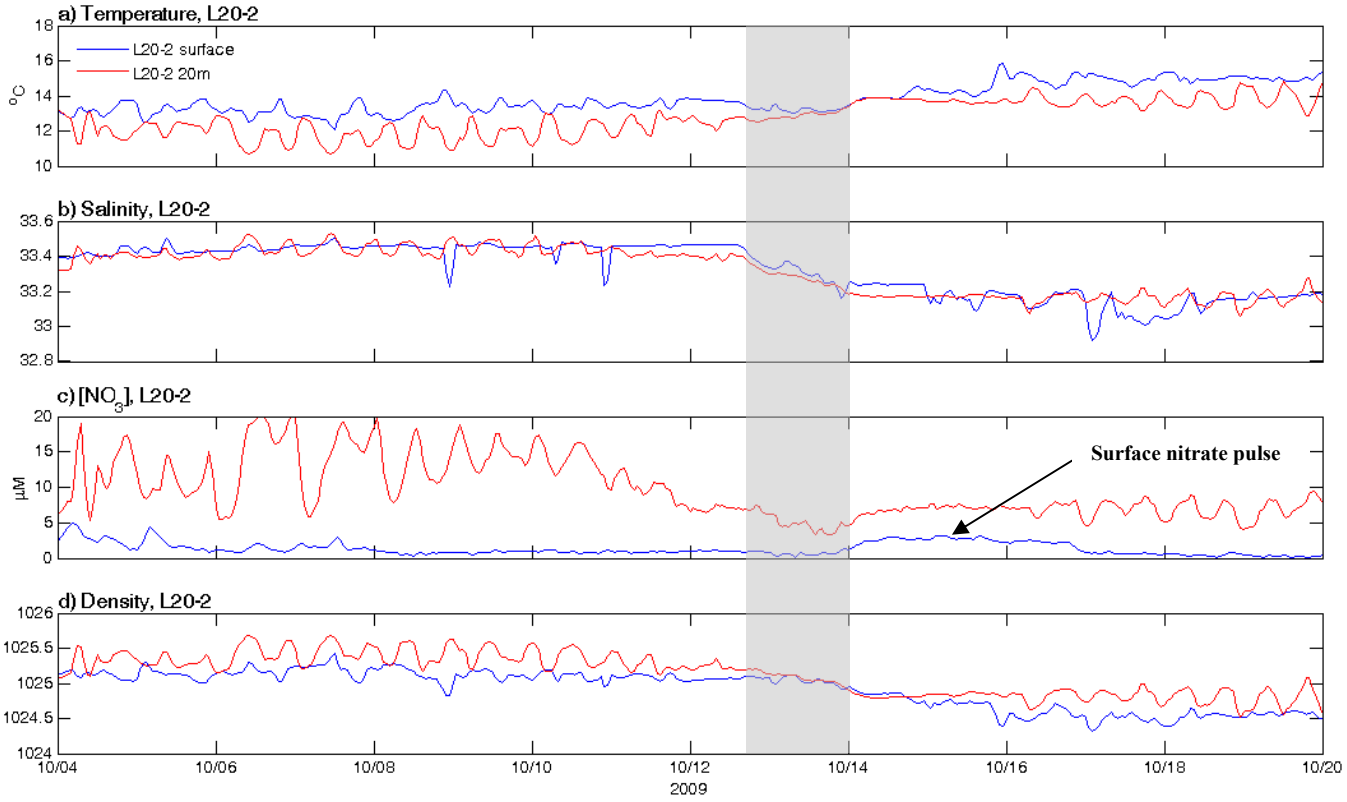

during the initial hours of a storm event, and there is a subsequent lag between rain and runoff, and an extension of the duration of high stream flow and loading relative to the rainfall event. A similar lag time was also apparent in the salinity time series. Figure 45-a shows the salinity anomaly, which is the salinity difference (in practical salinity units) relative to the mean salinity for the two weeks preceding the storm, for L20-2 surface and deep. From this, the hourly "freshwater fraction" (FF) was calculated (Figure 45-b), as defined by Equation 3 where S is salinity (McPhee-Shaw et al, 2007). The maximum FF was about 1.2%, occurring 5 days after the onset of the storm.

$$FF = (S_{max} - S_t)/S_{max} \qquad \text{(Equation 3)}$$

Figure 45: Salinity difference from pre-storm at L20-2 (a), and hourly freshwater fraction relative to pre-storm at L20-2 (b) from October 4 –20, 2009.

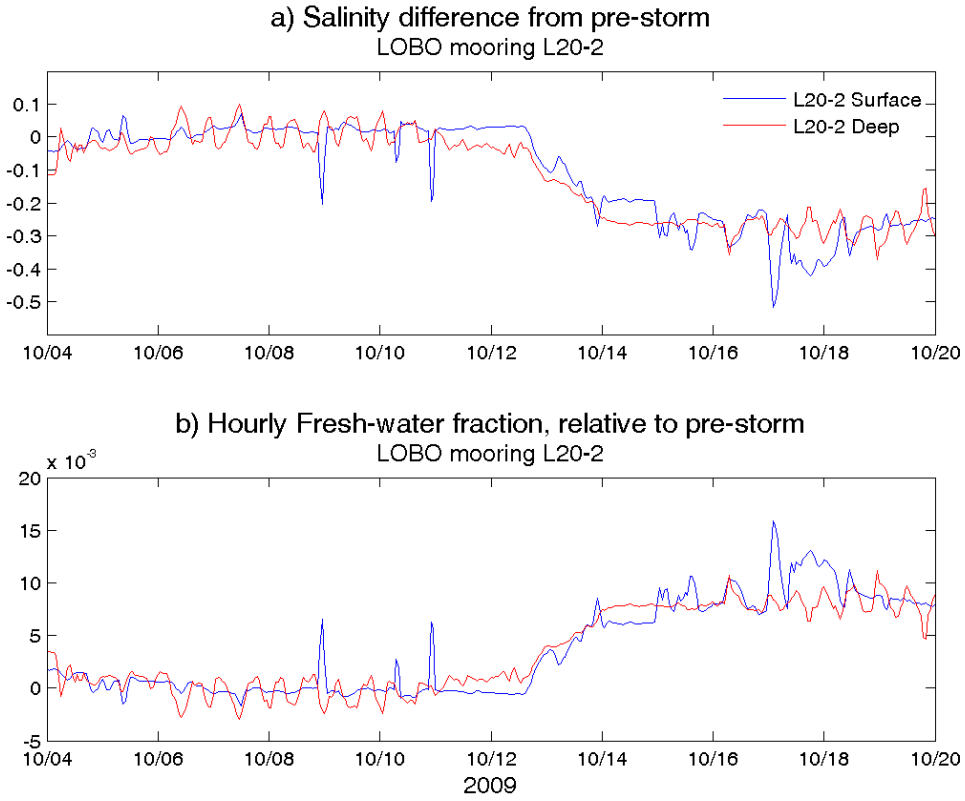

Assuming that the freshwater pulse seen at the mooring was completely caused by runoff from the local ES system, expected nitrate concentration at the nearshore mooring was modeled based on a simple, two end-member mixing model. This model can be described by Equation 4, where N represents nitrate concentration and FF represents the hourly freshwater fraction, as described above. The two end-members considered were a water mass typical of ocean waters and a water mass typifying terrestrial runoff from the ES system. Pre-storm surface nitrate concentration at mooring L20-2 was used to characterize ocean water. Instead of using just one value for terrestrial nitrate concentration, we chose a range of values [50 100 500 1000 2000] uM based on the calculated range of freshwater nitrate concentrations in OSR for the period surrounding the storm. The results of this model are presented in Figure 46. The black line denotes actual surface nitrate concentrations observed at L20-2.

$$N_{predicted} = \left[(FF)\left(N_{runoff}\right)\right] + \left[(1 - FF)(N_{ocean})\right] \quad \text{(Equation 4)}$$

Figure 46: Predicted and observed (black) surface nitrate concentration at LOBO mooring L20-2, based on terrestrial freshwater fraction.

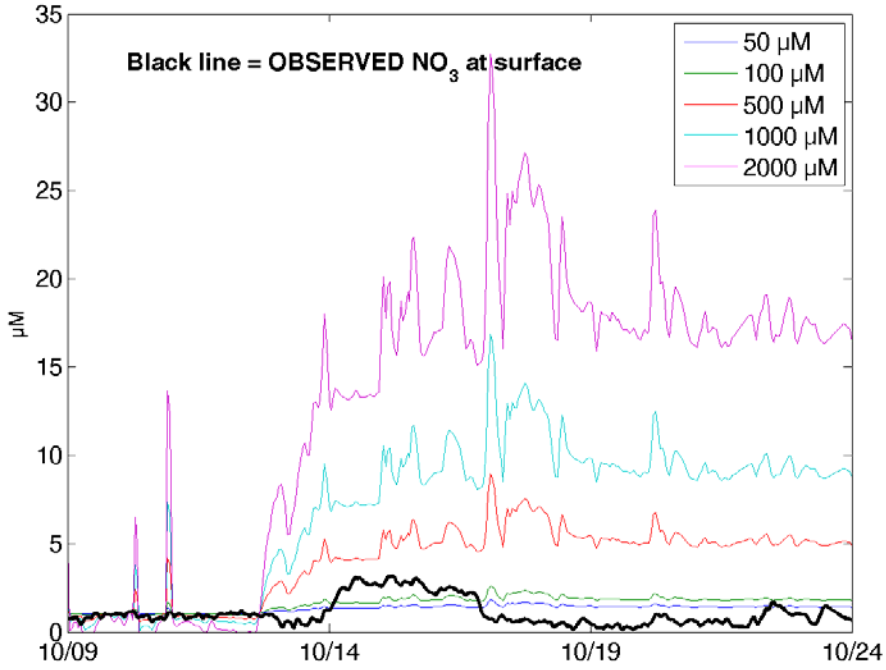

The model does fairly well at estimating the magnitude of ocean nitrate concentration post-storm when lower values of nitrate, between 100 and 500 uM, are used to characterize the terrestrial freshwater end-member. These are somewhat reasonable values; nitrate concentration in OSR reached a minimum of 180 µM two days after the storm, although values were in excess of 900 µM on October 14, one day after the storm.

There is, however, a noticeable discrepancy in timing between the predicted and observed nitrate pulse. The nitrate increase at the mooring occurred 1.3 days later than the predicted nitrate increase based on freshwater fraction observed in the ocean. A probable explanation is that the ocean salinity was affected by direct rainfall on the ocean surface. 7.11 cm of rain fell during the storm. Mixing this volume of rainwater into a

water column 20 m deep, we estimated that the freshwater fraction due to rainfall would be approximately 0.0036, which falls right into the range of observed values (Figure 45), and is over 50% of the freshwater fraction seen on October 13, the day of the predicted nitrate increase.

A secondary explanation is apparent when we consider the potential coastal ocean mechanisms at play during storms. For example, waves are often high during storm events which results in substantial mixing of the water column, as well as erosion of the seafloor and introduction of suspended sediment to shelf waters. Strong winds are responsible for stronger along-shelf currents and, importantly, cause intense vertical mixing of the water column. Data from mooring L20-2 showed evidence of intense vertical mixing. Waters at 16 m depth became nearly the same density as water at the surface (Figure 44-d). Since nitrate measured at depth is usually substantially higher than nitrate at the surface, vertical mixing of the water column could potentially contribute to the elevation of surface nitrate observed at L20-2. Average daily nitrate at the L20-2 deep sensor dropped from 15 μM before the storm, to 4.5 μM on the day of the storm, further indicating potential interaction with low-nitrate surface water (Figure 44-c)

Property plots were used to further investigate the interaction between surface and deep nearshore water masses during the storm event. Figure 47 depicts salinity-temperature (a), nitrate-temperature (b), salinity-nitrate (c) and density-nitrate (d) characteristics for surface and deep waters preceding the storm (October 8 –12), during the storm (October 13 – midday October 14), and after the storm (October 14 midday – October 17).

Before the storm, the two water masses were primarily separated by temperature and nitrate, with the surface waters spanning a temperature range of roughly 12.5 - 14 degrees while the deep waters ranged in temperature between 10.5 and 13 degrees. Most of the variability in these parameters at the deep sensor before the storm was due to internal waves. Salinity at both depths primarily ranged between 33.37 and 33.47, with some perturbation to higher salinity at the deep sensor, again due to onshore transport of deeper waters by internal waves.

The temperature, salinity, and nitrate characteristics of both surface and deep waters shifted dramatically during the storm. Importantly, the nitrate and temperature of both water masses collapsed into a smaller range than pre-storm for either depth, and into a temperature range that was the same for both surface and deep (12.5 to13.5 degrees) (Figure 47-a). This indicates that the water column was vertically well mixed, at least with respect to temperature. During the storm salinity was a bit higher in the surface waters than in the deep, although this seems to be compensated for by the same waters being slightly warmer. The range of densities was the same for both surface and deep during the storm as well (Figure 47-d).

After the storm, nitrate concentrations once again diverged, although maintained a range narrower than pre-storm conditions. The water column stratified in temperature after the storm, but was continuously pulled toward lower salinity. The surface waters got much warmer than at depth, reaching 16 °C. Although warm temperatures could indicate influence by terrestrial waters, they could also be attributed to a downwelling response bringing warmer offshore waters closer to shore. Figure 48 depicts offshore

conditions at MBARI mooring M1 during the period surrounding the storm. Downwelling-favorable winds, approaching 10 m/s, were observed starting October 13 and lasting until October 16 (Figure 48-a). An associated increase in temperature (reaching 15.7 °C) and decrease in salinity (reaching 32.9) was also observed on the days following the storm. Surface nitrate variability remained within a range apparent in the few days prior to the storm event.

Figure 47: Salinity-temperature (a), nitrate-temperature (b), salinity-nitrate (c) and density-nitrate (d) characteristics for surface and deep waters preceding the storm (October 8 – October 12), during the storm (October 13 – midday October 14), and after the storm (October 14 midday – October 17).

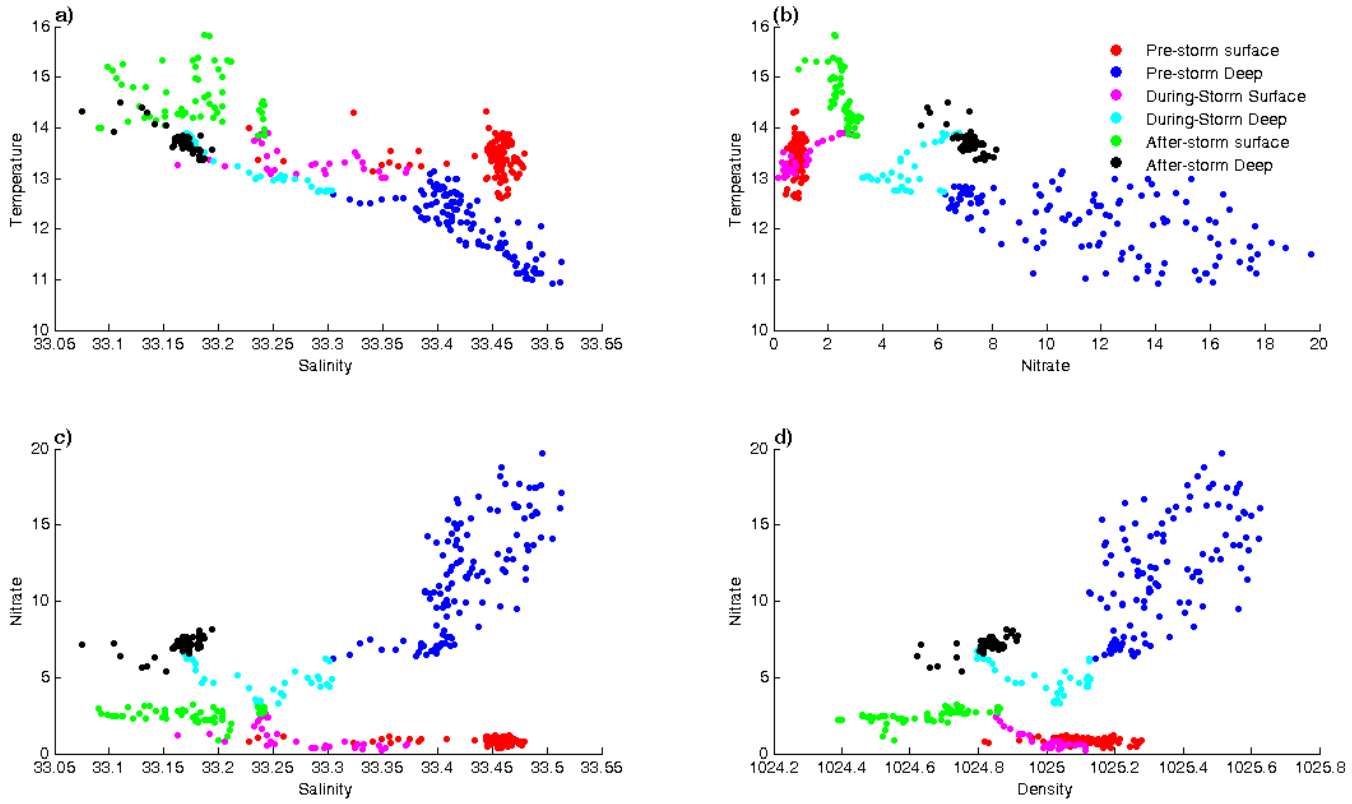

Figure 48: Equatorward winds (a), temperature (b), salinity (c), nitrate concentration (d), and calculated density (e) at MBARI offshore mooring M1, surface and deep (20m, when available) during the period surrounding the 2009 "first-flush" precipitation event. Positive wind vectors denote downwelling-favorable conditions. Gray fill denotes period of precipitation.

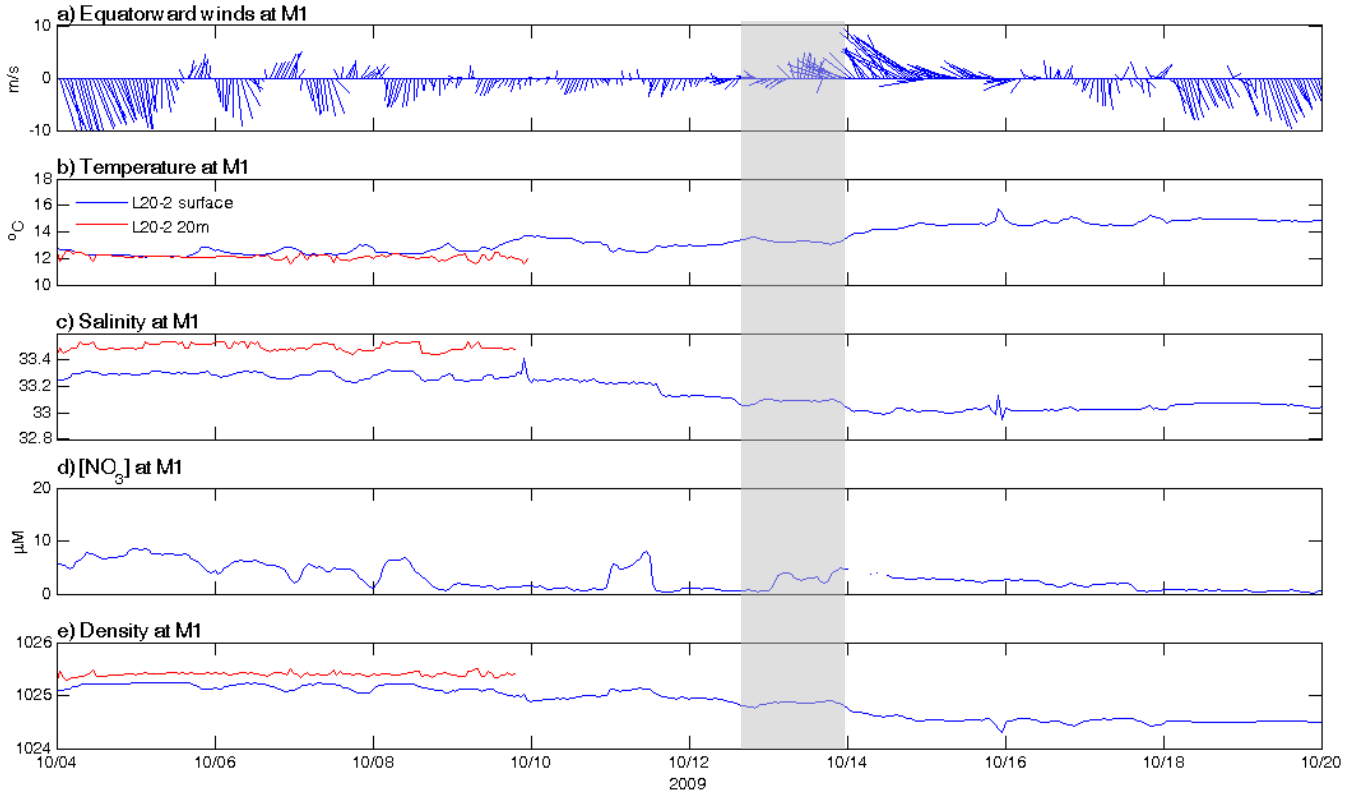

4. DISCUSSION & CONCLUSION

4.1 Characterization of Coastal Ocean Surface Nitrate Variability

The purpose of this study was to better characterize the role of nitrate transport out of Elkhorn Slough in the nitrate budget of Monterey Bay surface waters during the summer season. When assessing temporal changes in surface nitrate concentrations, both physical and biological processes affecting nitrate availability must be accounted for. Such independent processes are typically broken down into various source terms, the sum of which represents total change in nitrate over time at a particular location. In general, total temporal nitrate variability (dN/dt) can be described by the following equation:

$$\frac{dN}{dt} = \boldsymbol{B} + k_x\left(\frac{d\left(\frac{dN}{dx}\right)}{dx}\right) + k_y\left(\frac{d\left(\frac{dN}{dy}\right)}{dy}\right) + k_z\left(\frac{d\left(\frac{dN}{dz}\right)}{dz}\right) + \boldsymbol{u}\left(\frac{dN}{dx}\right) + v\left(\frac{dN}{dy}\right) + w\left(\frac{dN}{dz}\right)$$

(Equation 5)

where B represents net biological effects, kx, ky, and kz represent turbulent diffusion in the x, y, and z directions, u, v, and w represent advection in the x, y, and z directions, and N represents nitrate concentration of source water.

In the coastal surface waters of Monterey Bay, the largest rates of change in nitrate are typically the result of the physical advection of a nutrient-rich water mass. Although current velocities are greater in the horizontal direction, horizontal nitrate gradients are typically magnitudes smaller than those in the vertical, due to the sinking of organic matter and subsequent decomposition. However, horizontal nutrient gradients at the land-sea interface and within eutrophic coastal watersheds create potential exceptions.

This study was a comparison of advection terms, focused on the importance of the land-sea connection between the Elkhorn Slough system and the coastal waters of Monterey Bay. The following sections summarize and discuss the results of this study.

4.2 The Significance of Nitrate Loads in Elkhorn Slough

4.2.1 Biological Uptake in Elkhorn Slough

When assessing the relative significance of nitrate transport out of Elkhorn Slough to nearshore Monterey Bay, it is important to remember that loading estimates followed a conservative approach. The unique ability of estuarine systems to act as "buffer zones" between land and sea could result in a net transport out of ES being a fraction of the total calculated in this study. Nitrate transport out of the slough was quantified as the total nitrate load entering Old Salinas River and did not account for potential removal through biological uptake and denitrification. The Elkhorn Slough system is a highly productive, hypereutrophic environment, and home to an abundance of denitrifying bacteria (McKell, 2010). Old Salinas River water acts as a source of nitrate to biological organisms throughout the slough (Chapin et al., 2004). During maximum ebbing tide, high-nitrate, low-salinity water is drawn through the tide gates at Potrero Rd. into Old Salinas River Channel. A proportion of the water remaining in the harbor at mean lower-low water (MLLW) is then carried up the main channel of the slough by the flooding tidal current (Figure 49). During the summer months, the main channel of Elkhorn Slough acts as a large sink for nitrate (Chapin et al, 2004). Plant (2009) compared calculated terrestrial nitrate input into Elkhorn Slough with total nitrate

transport past LOBO mooring L01 and concluded that approximately 60% of nitrate transported up Elkhorn Slough's main channel is of terrestrial origin.

Figure 49: Water depth (m) (a), nitrate concentration (µM) (b), and salinity (c) at LOBO mooring L03 (left panel) and L01 (right panel).

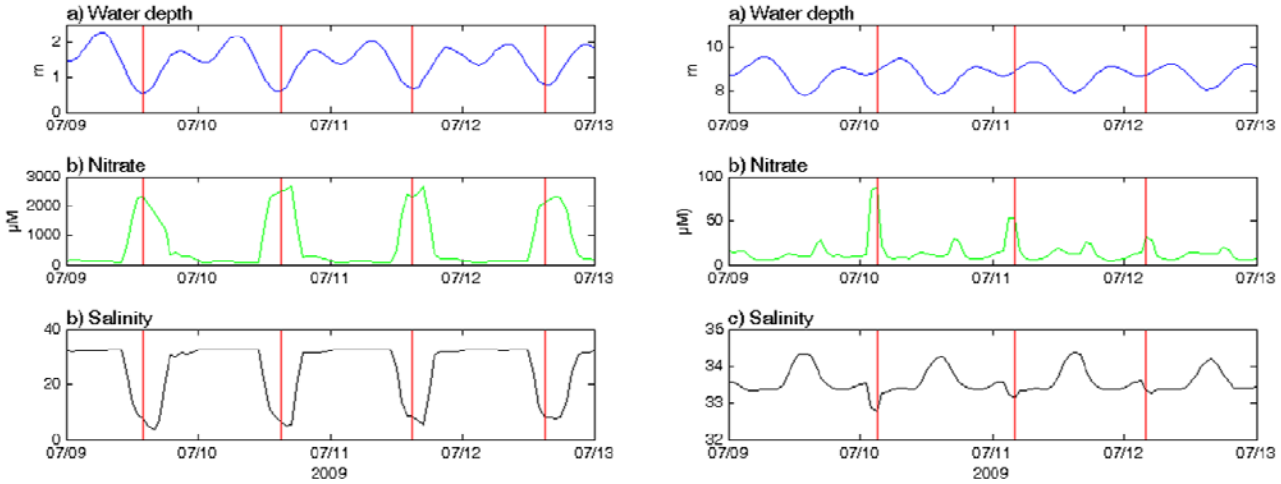

Assuming all of this nitrate is from OSR and is completely consumed or transformed by biological organisms, we can use the results of summer loading calculations in Section 3.1.2 to arrive at a lower bound estimate for net nitrate transport out of the ES system. This results in approximately 51 kmol/d nitrate transported out of the ES system during the summer season.

In the following sections, results of nitrate transport calculations are discussed. The initial approach presented in Section 3.1.2 for ES is used for all comparisons, but it is important to remember that these are conservative estimates.

4.2.2 Seasonal Context

This study focused on the summer, transitional season for calculating nitrate transport from three mechanisms: Elkhorn Slough, coastal upwelling and internal waves. The seasonal focus was designed to investigate the dynamic interaction among the multiple drivers of nitrate variability present during the summer months. For example, throughout the early summer, upwelling remains active and as temperatures warm, increases in stratification support internal wave activity. Toward the end of the summer, and into the early fall, the first rains of the season ensue. Throughout the extent of this time, maximum nitrate concentrations are observed in Old Salinas River (OSR), the southern channel of the Elkhorn Slough system.

As outlined in Sections 3.1.2 – 3.1.3, seasonal nitrate concentrations in OSR are over 500 μM greater during the summer than during the winter season. This trend is a direct result of the heavily loaded irrigation runoff that enters OSR through the Tembladero watershed. However, volumetric flow rate, in addition to nitrate concentration, is a necessary parameter for calculating total nitrate load carried by a system. Flow also varies seasonally in the ES system, with maximum flow rates coinciding with winter rain events. Thus, both summer and winter nitrate transport were calculated for Elkhorn Slough in order to better understand the relationship between nitrate concentration, flow rate, and total nitrate load in this system.

Results of loading calculations from Sections 3.1.2 and 3.1.3 are summarized in Table 10 below. Nitrate loads out of the Elkhorn Slough system for the winter seasons (2008 and 2009) were approximately 40 – 125% greater than during the summer seasons.

In 2008, the maximum daily nitrate load during the summer season was less than 20% that of the winter. In 2009, the maximum daily nitrate load for the summer season coincided with the largest precipitation event in five years, resulting in a nitrate load more comparable to winter conditions.

These results underscore the importance of flow rate versus nitrate concentration and suggest that, despite disproportionate nitrate concentrations in OSR during the summer season, flow rate is a more significant driver of nitrate loading within the Elkhorn Slough system.

Table 10: Comparison of summer (left column) and winter (right column) Nitrate Loads out of Elkhorn Slough.

	June – November		**November - March**	
	2008	**2009**	**2008**	**2009**
Average Daily Load (kmol/d)	86	84	192	116
Maximum Daily Load (kmol/d)	204	643	1065	775
Total Integrated Load (kmol)	11828	11885	22307	13994

4.3 Comparing Terrestrial (ES) and Oceanographic Source Inputs

The importance of land-based nitrate contributions and associated coastal eutrophication in non-upwelling coastal ecosystems has been well documented globally (Beman et al, 2005; Billen & Garnier, 2007; Bricker et al, 2007; Howarth et al, 2000; Howarth, 2008; Justic et al, 1995; Ludwig et al, 2009; Turner & Rabalais, 1994). The significance of nitrate supply from terrestrial transport systems along coastal upwelling

zones is less explicit, as it is generally accepted that nitrate supply in these regions is dominated by coastal upwelling. Nonetheless, comparisons of nitrate transport between terrestrial transport systems and oceanographic mechanisms have been made for select regions within the California Current System. For example, load comparisons over seasonal and annual timescales were performed along the Santa Barbara Channel (Warrick et al, 2005) and Columbia River region (Hickey & Banas, 2008). These studies found nitrate transport from coastal upwelling to be over 2 orders of magnitude greater than that from nearby freshwater systems, consistent with the general idea that coastal upwelling dominates the nitrate supply within the California Current system.

However, these studies suggest that terrestrial sources may become important over shorter time-scales, as during periods of relaxed upwelling. Our study provided the opportunity to investigate this idea by comparing local rates of terrestrial nitrate transport out of ES to nitrate transport from upwelling and internal waves using high-resolution (hourly) time series data. Table 11 summarizes calculated nitrate transport rates to the Monterey Bay surface waters for each mechanism over the multi-season study period.

Table 11: Comparative summary of nitrate transport results for terrestrial, upwelling and internal wave supply mechanisms. Units of average daily flux and integrated flux are kmol/d and kmol, respectively, unless otherwise indicated.

	June – November, 2008		**June – November, 2009**	
	Average flux	**Integrated flux**	**Average flux**	**Integrated flux**
Terrestrial (ES)	85.7	1.2×10^{4}	83.9	1.2×10^{4}
Upwelling (PFEL)	4.9×10^{4}	7.1×10^{6}	4.9×10^{4}	6.9×10^{6}
Upwelling (LOBO)	5.6×10^{4}	3.8×10^{6}	4.4×10^{4}	3.3×10^{6}
Internal Waves	0.3×10^{-9} kM/d	2.1×10^{-8} kM/d	1.1×10^{-9} kmol/L	1.2×10^{-7} kmol/L

Average daily nitrate transport out of Elkhorn Slough over the summer season was approximately two orders of magnitude smaller than that from upwelling. Internal waves proved a significant source of nitrate to the inner-shelf as well. The 2008 internal wave transport rate was consistent with rates calculated for the Santa Barbara Channel (McPhee-Shaw et al, 2007). The 2009 internal wave transport rate was three-fold greater than that of 2008, however, the proximity of mooring L20-2 to the head of the Monterey Canyon, a region of high internal wave activity, explains this discrepancy.

As is evident in Table 11, it is difficult to compare transport rates from internal waves (gray fill) to that of the other mechanisms due to inconsistent units. This is because the alternative method used to calculate internal wave transport resulted in units of kmol $L^{-1}d^{-1}$ as opposed to kmol d^{-1}. In order to account for this, nitrate transport by each mechanism was normalized to 1 kilometer of coastline. This not only provides consistent units, but also allows for a more localized comparison in the nearshore as opposed to regional Monterey Bay. For ES we assumed that total calculated transport was confined to a kilometer of coastline surrounding the harbor entrance, a reasonable assumption according to mixing arguments outlined in Section 3.3.1. For upwelling, volumetric transport rates from the PFEL index were scaled to 1 kilometer coastline. Lastly, internal wave transport rates were multiplied by a square kilometer, assuming that similar internal wave dynamics occur over this area near the canyon head. This results in final units of kmol $d^{-1}km^{-1}$ for each mechanism.

When normalized to 1 km coastline in the nearshore, average daily nitrate transport from ES is still an order of magnitude smaller than that of upwelling, and 4 to 13-fold smaller than that of internal waves (Table 12).

Calculated average internal wave transport was highly variable in this study, a possible spatial effect of each mooring's proximity to the Monterey Bay Canyon head. However, these rates are fairly reasonable. In a 1983 study, Shea and Broenkow estimated vertical volume transport from internal waves driven by the Monterey Bay Canyon to be approximately 10^9 m^3/d ($520x10^6 m^{-3}$/cycle). Assuming a 20 μM nitrate concentration for deep water and a 40 km length scale for Monterey Bay, this is equivalent to 500 kmol/d nitrate transported to Monterey Bay surface waters along 1 km coastline. This value is right within the range calculated using our methods for this study.

Table 12: Comparative summary of nitrate transport results for terrestrial, upwelling and internal wave supply mechanisms. Units of average daily flux and integrated flux are kmol $d^{-1}km^{-1}$ and kmol/km, respectively.

	June – November, 2008		**June – November, 2009**	
	Average flux	**Integrated flux**	**Average flux**	**Integrated flux**
Terrestrial (ES)	85.7	$1.2x10^4$	83.9	$1.2x10^4$
Upwelling (PFEL)	$1.2x10^3$	$1.8x10^5$	$1.2x10^3$	$1.7x10^5$
Upwelling (LOBO)	$1.4x10^3$	$9.8x10^4$	$1.3x10^3$	$8.5x10^4$
Internal Waves	$3.4x10^2$	$2.1x10^4$	$1.1x10^3$	$9.6x10^4$

Normalized comparisons can also be assessed in terms of percentage of total nitrate supply to the nearshore (using integrated totals). Figure 50 shows that total

integrated transport over the 2008 and 2009 summer seasons were 7 and 5%, respectively, of the total nitrate supply among the three mechanisms. Transport by internal waves was variable and significantly more active during the 2009 season, a possible effect of mooring L20-2's proximity to the Monterey Bay Submarine Canyon head.

Figure 50: Percentage of total integrated nitrate suply to the nearshore from Elkhorn Slough (ES), upwelling and internal waves (IW). Upwelling represents an average of the two approaches used for calculating transport from upwelling.

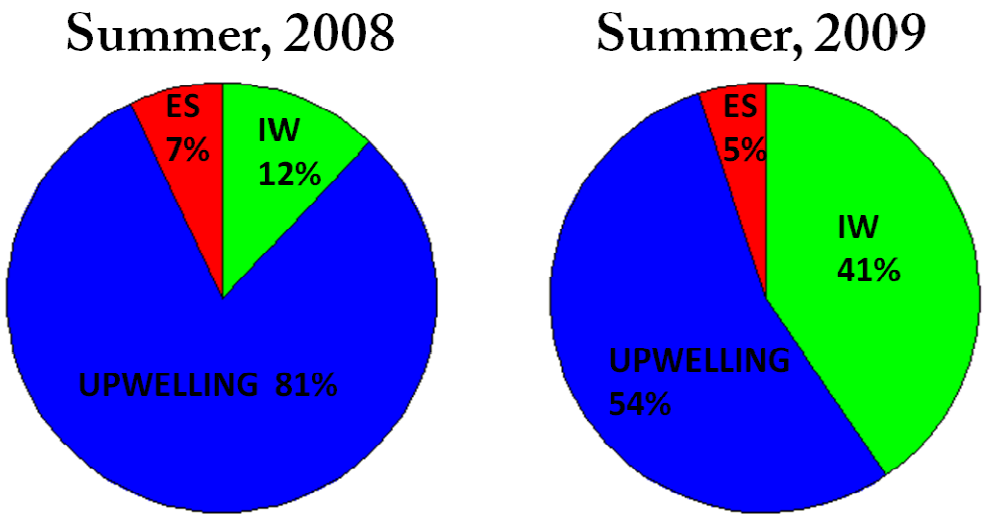

Additional comparative studies of nitrate transport mechanisms along the California coast have been made at high temporal resolution. For example, McPhee-Shaw et al, 2007 used hourly mooring data within the Santa Barbara Channel to diagnose major transport mechanisms responsible for supplying nitrate to the inner-shelf of this region. While reaffirming that upwelling supplies the majority of nitrate to inner-shelf

waters over an annual basis, this study highlighted the importance of temporality versus magnitude in such comparisons, demonstrating that internal waves are a key alternate method of nutrient delivery, as they occur during summer conditions when upwelling and terrestrial transport were minimal.

In a more recent study, Lane compared annual, monthly, and daily nitrate loading to Monterey Bay from rivers and wind-driven upwelling over a ten-year period (Lane, 2011 in review). Lane found that over annual and monthly timescales, her study "affirm[ed] the classification of Monterey Bay as an upwelling-dominated region (the minimum differences between nitrate input from rivers and from upwelling were 2 orders of magnitude for annual and monthly timescales), but also affirm[ed] this classification as a generality." Nitrate transport by rivers exceeded that of upwelling for 28% of estimates during the study period when conducted over daily timescales (Lane, 2011 in review).

Our results can be compared on a daily time-scale as well. Despite consistent summer loading out of ES, nitrate transport from ES exceeded that of upwelling and internal waves for only 3 days (1%) of the study period (Figure 50). This is a far less significant portion of the study period than found by Lane, 2011. Furthermore, percent results of temporal comparisons in both studies could be even lower when accounting for ocean mixing, a common driver of surface nitrate increases during winter storms. The 3-day period when ES transport exceeds upwelling transport in our study occurred in response to the largest precipitation event in over five years, "first flush 2009". As outlined in Section 3.3.5, ocean mixing played a large role in the nearshore nitrate response during this time.

Figure 51: Nitrate transport from Elkhorn Slough, upwelling (PFEL and LOBO methods) and internal waves over the two-summer study period. Circles represent days where each supply mechanism was active, as defined by threshold conditions for those methods.

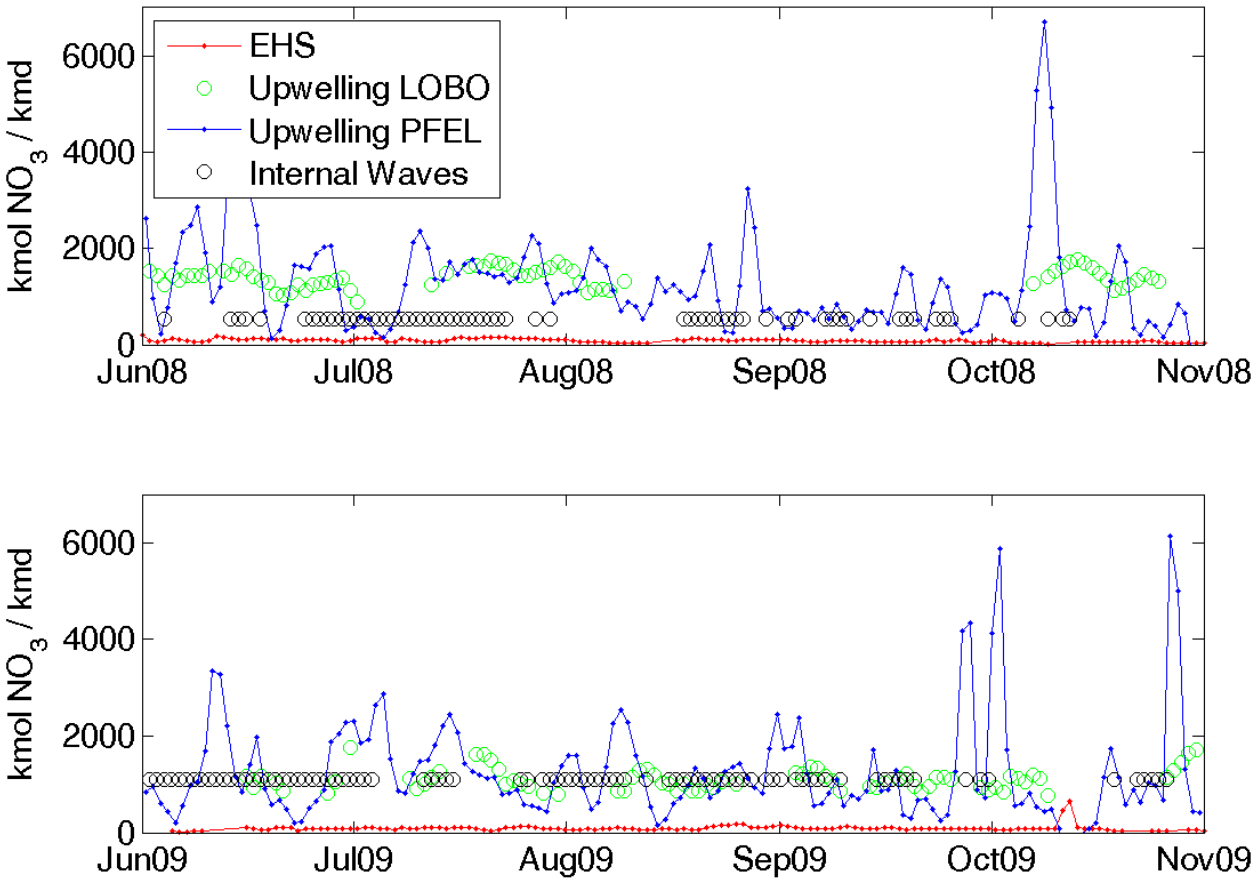

4.5 Detection of Terrestrial (ES) Nitrate Signals in Nearshore Monterey Bay

The mixing argument outlined in Section 3.3.1 demonstrated that detection of nearshore terrestrial nitrate signals from Elkhorn Slough using moored high-frequency in-situ instrumentation is potentially limited by relative magnitudes of nitrate transport out of the slough system. Further analysis of LOBO nearshore and slough data using temperature-salinity diagrams and time-progressive property plots confirmed this. Results of Section 3.3.3 suggested ES nitrate discharge may be discernable in the nearshore only during the winter season, when heightened flow rates lead to increases in total mass loads exiting the ES system. However, in-depth analysis of the largest storm and runoff event in five years ("first flush", 2009) in Section 3.3.5 showed that ocean mixing, between surface and high-nitrate deep water, played a large role in the surface nitrate response.

It is possible that our inability to detect a nearshore terrestrial nitrate signal from ES during our two-year study period was due to the limited spatial resolution in our experimental design. Oceanographic moorings, such as the nearshore moorings deployed for this study, are of Eulerian specification. LOBO moorings L20 and L20-2 remained at fixed positions, 1 kilometer off the coast. Subsequently, the moorings could have routinely missed the ES signature due to variability in the spatial extent of the ES discharge plume. Yet even an intensive field program involving high resolution surface mapping of the nearshore from Moss Landing Harbor out to 1 km (Section 3.3.4) failed to detect the ES discharge plume, and once again identified the influence of deep water.

The lack of influence detected from ES on nearshore Monterey Bay during our two-year study period supports the general assumption that deep water processes dominate the nearshore nitrate signature of coastal Monterey Bay.

4.6 Harmful Algal Blooms in Monterey Bay and the Land-Sea Link

As described in Ryan et al., 2008, "because the [Monterey Bay] extreme bloom season overlaps with the rainy season, fluxes of nutrients and freshwater (stratification) from land drainage may at times be important to bloom dynamics". Our research has shown that, despite high nitrate concentrations within the ES system from nearby agricultural loading, the nitrate supply of nearshore Monterey Bay was dominated by oceanographic mechanisms during the "extreme bloom" (summer to early fall) seasons of 2008 and 2009. When scaled to the nearshore, average daily nitrate transport out of ES was more than an order of magnitude less than nitrate transport from coastal upwelling, and 4 to 13-fold less than nitrate transport from internal waves. Nitrate transport out of ES reached magnitudes more comparable to oceanographic mechanisms only in response to heightened flow conditions during winter storms. However, ocean mixing often plays a large role in the surface nitrate response during storm events. This was exemplified through our in-depth analysis of the October, 2009 "first flush" storm event. Although diffuse, the role of mixing processes in surface nitrate variability should not be overlooked.

In addition to the nearshore nitrate supply, other nutritional factors and physical processes should be considered when investigating the relationship between ES and extreme algal blooms in coastal Monterey Bay. This study was limited to nitrate

quantification and did not provide insight into transport rates of other forms of nitrogen, such as urea or ammonium, throughout the ES system. For example, urea has been shown to be important in sustaining harmful algal blooms in Monterey Bay (Kudela et al, 2008).

Furthermore, complex circulation patterns also affect the probability of bloom inception. Retentive circulation stemming from the unique geography of coastal bays has been shown to concentrate phytoplankton, leading to increased local recruitment and bloom intensification (Roughan et al, 2005; Ryan et al, 2008). And lastly, biological response to environmental conditions varies among species, also dependent upon life stage and nutritional history. Thus, extreme algal blooms can be classified as transient events, highly variable in space and time, and controlled by oceanographic conditions. An understanding of nutrient conditions (including the coastal nitrate supply) may provide a framework for understanding such events, although future monitoring and prediction of extreme algal blooms in Monterey Bay will require extensive, novel technology as well as continued collaboration among scientific disciplines.

REFERENCES

Bakun, A. 1973. Coastal upwelling indices, west coast of North America, 1946-71. U.S. Dept. of Commerce, NOAA Tech. Rep., NMFS SSRF-671, 103p.

Bakun, A. 1975. Daily and weekly upwelling indices, west coast of North America, 1967-73. U.S. Dept. of Commerce, NOAA Tech. Rep., NMFS SSRF-693, 114p.

Beman, M. J., K. R. Arrigo, and P. A. Matson. 2005. Agricultural runoff fuels large phytoplankton blooms in vulnerable areas of the ocean. *Nature*. 434: 211-214.

Bigelow, H. B. and M. Leslie. 1930. Reconnaissance of the waters and plankton of Monterey Bay. *Bulletin of the Museum of Comparative Zoology at Harvard College*. 70: 427-581.

Billen, G., and J. Garnier. 2007. River basin nutrient delivery to the coastal sea: Assessing its potential to sustain new production of non-siliceous algae. *Marine Chemistry,* 106: 148-160.

Bolin, R. L. and D. P. Abbott. 1963. Studies on the marine climate and phytoplankton of the central coastal area of California, 1954-1960. *California Cooperative Fisheries Investigations.* 9: 23-45.

Breaker, L.C., W.W. Broenkow. 1994. The circulation of Monterey Bay and related processes. *Oceanography and Marine Biology: An Annual Review.* 32: 1-64.

Breaker, L.C., W.W. Broenkow, W.E. Watson, and Y-H Jo. 2008. Tidal and non-tidal oscillations in Elkhorn Slough, California. *Estuaries and Coasts.* 31(2): 238-257.

Bricker, S. B. **,** B. Longstaff**,** W. Dennison**,** A. Jones**,** K. Boicourt**,** C. Wicks**,** J. Woerner 2007. Effects of nutrient enrichment in the nation's estuaries: a decade of change. *Harmful Algae* 8.

Broenkow, W. W., and L. C. Breaker. 2005. A 30-year history of tide and current measurements in Elkhorn Slough, California. Scripps Instituion of Oceanography Library, November 18. http://repositories.cdlib.org/sio/lib/8.

Caffrey, J. 2002. J. M. Caffrey, M. Brown, W. B. Tyler, and M. Silberstein, editors. In: Changes in a California Estuary: A Profile of Elkhorn Slough. Elkhorn Slough Foundation. Moss Landing, California. Pages 215-236.

Caffrey, J., T. P. Chapin, H. W. Jannasch, J. C. Haskins. 2007. High nutrient pulses, tidal mixing and biological response in a small California estuary: Variability in nutrient concentrations from decadal to hourly time scales. *Estuarine, Coastal and Shelf Science* 71: 368-380.

Carroll, D. 2009. Carmel Bay: Oceanographic dynamics and nutrient transport in a small embayment of the California coast. Master's thesis. Moss Landing Marine Laboratories.

Central Coast Watershed Studies (CCoWS), 2004. Final Report: Reclamation Ditch Watershed Assessment and Management Strategy. Prepared for the Monterey County Water Resources Agency (MCWRA) board of directors. Chapter 4: Hydrology and Channel Conditions Assessment. http://www.mcwra.co.monterey.ca.us/Agency_data/RecDitchFinal/Ch04_Hydro_ChannelCond.pdf

Chapin, T.P., J.M. Caffrey, H.W. Jannasch, L.J. Coletti, J.C. Haskins, & K.S. Johnson. 2004. Nitrate sources and sinks in Elkhorn Slough, California: Results from long-term continuous in-situ nitrate analyzers. *Estuaries* 27, no. 5: 882-894.

Elkhorn Slough Tidal Wetland Project Team (ESTWPT). 2007. Elkhorn Slough Tidal Wetland Strategic Plan. A report describing Elkhorn Slough's estuarine habitats, main impacts, and broad conservation and restoration recommendations. 100 pp.

Fischer, A. 2009. An Estuarine Plume and Coastal Ocean Variability: Discerning a Land-Sea Linkage in Monterey Bay, California. PhD dissertation, Cornell University.

Greneli & Turner. The Ecology of Harmful Algae. Springer, 2001.

Howarth, R. W. 2008. Coastal nitrogen pollution: A review of sources and trends globally and regionally. *Harmful Algae* 8: 14-20.

Howarth, R. W., D. Anderson, J. Cloern, C. Elfring, C. Hopkinson, B. Lapointe, T. Malone, N. Marcus, K. McGlathery, A. Sharpley, D. Walker. 2000. Nutrient pollution of coastal rivers, bays, and seas. *Issues in Ecology* 7:1-15.

Hickey, B. M., and N. S. Banas. 2008. Why is the Northern End of the California Current System So Productive? Oceanography 21: 90-107.

Hughes, B. 2009. Synthesis for management of eutrophication issues in Elkhorn Slough. Elkhorn Slough Technical Report Series 2009:1.

Jannasch, H. W., L. J. Coletti, K. S. Johnson, S. E. Fitzwater, J. A. Needoba, and J. N. Plant. 2008. The Land/Ocean Biogeochemical Observatory: A robust networked mooring system for continuously monitoring complex biogeochemical cycles in estuaries. *Limnology and Oceanography: Methods.* 6: 263-276.

Johnson, K.S. & L.J. Coletti. 2002. In-situ ultraviolet spectrophotometry for high resolution and long-term monitoring of nitrate, bromide and bisulfide in the ocean. *Deep-Sea Research I*. 49:1291- 1305.

Justic, D., N. N. Rabalais, and R. E. Turner. 1995a. Stoichiometric Nutrient Balance and Origin of Coastal Eutrophication. *Mar Pollut Bull* 30: 41-46.

Justic, D., N. N. Rabalais, R. E. Turner, and Q. Dortch. 1995b. Changes in Nutrient Structure of River-Dominated Coastal Waters - Stoichiometric Nutrient Balance and Its Consequences. *Estuar Coast Shelf* 40: 339-356.

Kudela, R., R. Dugdale. 2000. Nutrient regulation of phytoplankton productivity in Monterey Bay, California. *Deep-Sea Research II*. 47, 1023–1053.

Kudela, R. M., J. Q. Lane, and W. P. Cochlan. 2008a. The potential role of anthropogenically derived nitrogen in the growth of harmful algae in California, USA *Harmful Algae 8*: 103-110.

Kunze, E., L. K. Rosenfeld., G. S. Carter and M. C. Gregg. 2001. Internal waves in Monterey submarine canyon. *Journal of Physical Oceanography.* 32: 1890-1913.
Lane, J. 2011. In review: Assessment of river discharge as a source of nitrate-nitrogen to Monterey Bay, California. *Limnology and Oceanography.*

Largier, J.L., S.V. Smith and J.T. Hollibaugh, 1997. Seasonally hypersaline estuaries in Mediterranean climate regions. *Estuarine Coastal and Shelf Science*. 4: 789-797.

Leichter, J.J, et al. 2003. Episodic nutrient transport to Florida coastal reefs. *Limnology & Oceanography.* 48:4.

Los Huertos, M., L. E. Gentry, and C. Shennan. 2001. Land use and stream nitrogen concentrations in agricultural watersheds along the central coast of California. *Scientific World Journal* 1 Suppl 2: 899 615-622.

Lucas, A., P. Franks, C. Dupont. 2011. Horizontal internal-tide fluxes support elevated phytoplankton productivity overthe inner continental shelf. *Limnology and Oceanography.* 56–74

Ludwig, W., E. Dumont, M. Meybeck, and S. Heussner. 2009. River discharges of water and nutrients to the Mediterranean and Black Sea: Major drivers for ecosystem changes during past and future decades? *Prog Oceanogr* 80: 199-217.

McKell, E. 2010. Diversity and abundance of the nirS-denitrifying bacterial community in the Elkhorn Slough – Salinas River ecosystem. Master's thesis. Moss Landing Marine Laboratories.

McPhee-Shaw, E.E., D.A. Siegel, L. Washburn , M.A. Brzezinski, J.L. Jones, A. Leydecker and J.M. Melack. 2007. Mechanisms for nutrient delivery to the inner-shelf: Observations from the Santa Barbara Channel. *Limnology and Oceanography.* 52(5): 1748-1766.

Monterey County Water Resources Agency (MCWRA). 2008. Reclamation Ditch Watershed Assessment and Management Strategy; Part A: Watershed Assessment. 277 pp.

Munk, W. 1966. Abyssal Recipes. *Deep Sea Research*. Vol 13,4 (707-730).

Pennington, J. T., and P. Chavez. (2000). Seasonal fluctuations of temperature, salinity, nitrate, chlorophyll and primary production at station H3/M1 over 1989–1996 in Monterey Bay, California. *Deep-Sea Research II*. 42: 947–973.

Plant, J. N., J. A. Needoba, S. E. Fitzwater, L. J. Coletti, H. W. Jannasch, T. R. Martz, N. J., Nidzieko, and K. S. Johnson. 2009. Linking agriculture, nitrogen inputs and ecosystem metabolism in Elkhorn Slough on time scales of hours to years. Coastal and Estuarine Research Federation: Estuaries and coasts in a changing world. Portland, Oregon.

Rabalais, N., R. E. Turner, B. K. Sengupta, D. F. Boesch, P. Chapman, and M. C. Murrell. 2007 Hypoxia in the Northern Gulf of Mexico: Does the Science Support the Plan to Reduce, Mitigate, and Control Hypoxia? *Estuaries and Coasts*. 30, No. 5, p. 753–772.

Rosenfeld, L. K., F. B. Schwing, N. Garfield, and D. E. Tracy. 1994. Bifurcated flow from an upwelling center: a cold water source for Monterey Bay. *Continental Shelf Research.* 14(9): 931-964.

Ryan, J. P., J. F. R. Gower, S. A. King, W. P. Bissett, A. M. Fischer, R. M. Kudela, Z. Kolber, F. Mazzillo, E. V. Rienecker, and F. P. Chavez. 2008. A coastal ocean extreme bloom incubator. *Geophysical Research Letters* 35: L12602, doi:10.1029/2008GL034081.

Ryan, J. P., A. M. Fischer, R. M. Kudela, J. F. R. Gower, S. A. King, R. Marin III, F. P. Chavez. 2009. Influences of upwelling and downwelling winds on red tide bloom dynamics in Monterey Bay, California. *Continental Shelf Research.* 29: 785-795.

Ryan, J. P., 2009. New insights on red tides and harmful algal blooms in Monterey Bay Flash player video. http://www.mbari.org/news/homepage/2009/ryan-blooms/ryan-blooms.html.

Shea, R.E. and W.W Broenkow. 1982. The role of internal tides in the nutrient enrichment of Monterey Bay, California. *Estuarine, Coastal, and Shelf Science.* 15: 57-66.

Shepard, R. P. 1973. *Submarine Geology,* 3rd edition, Harper and Row, New York, 517 pp.

Skogsberg, T., A. Phelps. 1946. Hydrography of Monterey Bay, California. Thermal conditions, Part II,1934-1937. *Proceedings of the American Philosophical Society.* 90: 350-386.

Smayda, T. J. (1997), Harmful algal blooms: Their ecophysiology and general relevance to phytoplankton blooms in the sea, *Limnology and Oceanography*. 42, 1137–1153.

Storlazzi C.D., M. A. McManus, J. D. Figurski. 2003. Long-term, high-frequency current and temperature measurements along central California: insights into upwelling/relaxation and internal waves on the inner-shelf. *Continental Shelf Research*. 23(9): 901-918.

Turner, R. E. and N. N. Rabalais. 1994. Coastal eutrophication near the Mississippi river delta. *Nature.* 368: 619-621.

Wankel, S. D., C. Kendall, J. T. Pennington, F. P. Chavez, and A. Paytan (2007), Nitrification in the euphotic zone as evidenced by nitrate dual isotopic composition: Observations from Monterey Bay, California, *Global Biogeochem. Cycles, 21,* GB2009, doi:10.1029/2006GB002723.

Warrick, J.A., L.A.K. Mertes, L. Washburn, and D.A. Siegel. 2004b. Dispersal forcing of southern California river plumes, based on field and remote sensing observations. Geo-Marine Letters 24: 46-52
.
Warrick, J. A., L. Washburn, M. A. Brzezinski, and D. 981 A. Siegel. 2005. Nutrient contributions to the Santa Barbara Channel, California, from the ephemeral Santa Clara River. Estuarine, Coastal and Shelf Science 62: 559-574.

Vitousek, P., J. Aber, R. Howarth, G. Likens, P. Matson, D. Schindler, W. Schlesinger, and D. Tilman. 1997. Human alteration of the global nitrogen cycle: sources and consequences. *Ecological Applications.* 7: 737–750.